

DILUTE AND CONCENTRATED MIXED VALENCE SYSTEMS—SOME SIMPLE MODELS

A Thesis Submitted
In Partial Fulfilment of the Requirements
for the Degree of

DOCTOR OF PHILOSOPHY

by

KEYA SUR

TH
Phy/1978/0
Su.78 d

to the

DEPARTMENT OF PHYSICS
INDIAN INSTITUTE OF TECHNOLOGY KANPUR
SEPTEMBER, 1978

ORIGINAL LIBRARY
A 65971

15 MAY 1981

PHY-1970-D-SUR-D12

CERTIFICATE

Certified that the work presented in this thesis entitled, "Dilute and Concentrated Mixed Valence Systems: Some Simple Models" by Ms. Keya Sur has been carried out under my supervision and that this has not been submitted elsewhere for a degree.

T.V. Ramakrishnan.

(T.V. Ramakrishnan)
Professor
Department of Physics
Indian Institute of Technology
Kanpur-16, India

September, 1978

ACKNOWLEDGEMENTS

It is difficult to express how deeply indebted I am to Professor T. V. Ramakrishnan for what I have learnt from him as a student. I am grateful to him for suggesting the present investigation, his constant encouragement and patience shown throughout the course of this work.

I am grateful to Mr. Bhaskar Sur, Mr. Subodh Shukla, Mr. G. S. Vishweshwaran and Ms. Basabi Bhowmick for help in carrying out the numerical calculations.

I am thankful to Dr. S. G. Mishra, Dr. S. N. Gadekar, Dr. S. Ray for many useful discussions.

I am greatly indebted to Dr. Pankaj Sharan and Dr. A. K. Kapoor for invaluable help with the manuscript. It is a pleasure to acknowledge the help received from my friends and colleagues, particularly from Ms. Vasundhara Choudhry, Ms. Shobha Madan, Ms. Elizabeth A. Chackachery, Dr. P. N. Shukla, Mr. Bhaskar Sur for doing a thorough work of checking the manuscript.

My thanks are due to Mr. D. B. D. Bhargava of Allahabad University for excellent typing, to Mr. Nihal Ahmad and Mr. S. K. Tewari for filling in the mathematical symbols, to Mr. S. Kar for tracing the figures, and to Mr. Prashant Panda for cyclostyling the thesis.

Last but not the least, I am grateful to the 'Gangotri Four', for the pleasant sojourn at IITK.

30th September 1978

Keya Sur

CONTENTS

	Page
Certificate	ii
Acknowledgements	iii
List of Figures	vii
Synopsis	ix
CHAPTER I Introduction	1
CHAPTER II The Mixed Valence Problem in the Hartree Fock Approximation	15
Introduction	15
1. The Anderson Model in the Hartree Fock Approximation	16
2. Analysis of the $C \neq 0$ Anderson Hamiltonian in the Hartree Fock Approximation	19
(a) The HF self consistent equations and stability conditions of the solutions	19
(b) Finding solutions to the HF equations	21
(c) Boundaries of magnetic and non-magnetic regimes	24
(d) The phase transition line	30
(e) Summary of results obtained from HF analysis of Anderson Model with $C \neq 0$	34
3. Two Interacting Impurities	35
(a) The model and the self consistent equations in HFA	35
(b) Two antiparallel moments	39
(c) Two parallel moments	41
(d) Two ions in different valence states	44
(e) Brief discussion of results obtained for a pair of interacting impurities in HFA	47
CHAPTER III The Mixed Valence Lattice	50
1. The Model	50
(a) Single impurity	50
(b) Two impurities	51
2. Possible Phases of the System	55
(a) Ferro- (or antiferro-) magnetic phase	56
(b) The valence fluctuation phase $S_x \neq 0$	60
3. Competition Between Phases	61

CHAPTER IV	Beyond the Hartree Fock Approximation The Path Integral Method for the Anderson Model	63
1.	Introduction	63
2.	The Path Integral Formulation	66
3.	The Choice of Paths and Evaluation of Z	70
	(a) The choice of paths	70
	(b) Evaluation of the integrals ϕ_σ and B_σ	72
	(c) Determination of hopping shape, and of τ_0	76
	(d) The partition function	81
4.	The Mixed Valence (Anderson Model $C \neq 0$) in Path Integral Method	83
CHAPTER V	Beyond the HFA -- The Quasiparticle Method	87
1.	Introduction	87
2.	Formalism	89
	(a) The general quasiparticle formalism	89
	(b) Deriving the self consistent quasi- partical equation	90
	(c) The quasiparticle energies at different temperatures	96
	(i) Analytical forms for quasiparti- cle energy	96
	(ii) Low temperature limit	102
	(iii) Quasiparticle energies at high temperatures	106
3.	The Magnetic Susceptibility	107
	(a) Zero temperature susceptibility	108
	(b) The magnetic susceptibility at high temperatures	114
	(c) Numerical results	116
4.	The Valence Fraction	118
5.	Suggestions on Inclusion of screening terms and of interactions between ions	119
CHAPTER VI	Conclusions	123

Appendix I	Free Energy for the Anderson Model ($C \neq 0$) in HFA and Condition for Minimum Energy Solutions	125
Appendix II	To Show that the Range of Unstable Solutions to II Equations is Bounded by Extreme in ϵ_u	129
Appendix III	Energy of Two Interacting Ions in HFA	131
Appendix IV	Free Energy with Constant Fields in the Path Integral Method for $C \neq 0$ Anderson Model	132
Appendix V	The Integrals Occurring in the Short Range Term in the Path Integral Method and Determination of τ_0	134
Appendix VI	The Integral $I(a) = \int_{-D}^D \frac{f(x) dx}{x+a}$	145
References		149

LIST OF FIGURES

Figure		Page
1(a)	Magnetic susceptibility χ vs temperature for typical MV system ($S_{m-x} V_x B_6$).	4
1(b)	Specific heat C_V vs temperature for a typical MV system.	5
2	Phase diagram for $C=0$ Anderson model.	18
3	Solution to HF self consistent equations.	23
4	F_{HF} (Computer calculations) vs ϵ_d .	27
5	Energies of stable HF solutions.	31
6	d-Occupation in HFA.	32
7	MV regions in parameter space.	33
8	The x and z ordering temperatures within the MV region.	59
9	Time dependent potential (hopping path).	73
10(a)	Hopping path (single hop).	77
10(b)	Hopping path (oscillating hop).	77
11	Graphical solution to equation for minimum energy path ($X=5$).	79
12	Path for $C \neq 0$.	84
13	Irreducible diagram contributing to T_G^* and T_0 .	91
14	Kondo model diagrams.	94
15	Graphical solution to zero temperature quasi-particle equation.	97
16	Diagrams corresponding to truncation of quasi-particle equation.	100
17	Graphical solution to quasiparticle equation for E_0 at different temperatures ($\bar{E}_0 = -4.75$). The curves show $I(a)$ at different temperatures.	105
18	Third order scattering diagram	110
19	Variation of $\tilde{\epsilon}$ with d-energy.	113

Figure

Page

20	The magnetic susceptibility results for $D = 1000\Delta/\pi$, $U =$ (for KW, $D = 2U = 1000\Delta/\pi$).	117
21	Higher order scattering diagrams.	120
22	Shape of the path $\xi(\tau)$.	135
23	Diagram showing the various regions of Fig. 22.	137
24	Contour for integration.	146

SYNOPSIS

Thesis entitled 'Dilute and concentrated Mixed Valence Systems — Some Simple Models' submitted by Keya Sur in partial fulfilment of the requirements of the Ph.D. degree to the Department of Physics, Indian Institute of Technology, Kanpur.

September 1978

Some simple microscopic model Hamiltonians, considered suitable for describing mixed valence systems, are explored theoretically in this thesis.

The introductory chapter of the thesis describes briefly the experimental background and the existing theoretical approaches to the problem. In most solids, ions exist in a state of integral definite valence. However, in a number of metallic systems containing rare earth ions, e.g., Ce, Ce Al₂, Yb Al₃, collapsed Sm S etc., the rare earth ion is in an unusual state of mixed or intermediate valence, n_v , such that $n \leq n_v \leq n + 1$ where n is an integer. The mixed valence systems have many unusual properties, viz., absence of magnetic ordering (even though the ionic state with valence n may be magnetic), anomalous resistivity, large specific heat, complicated (nonmagnetic) phases. The mixed valence phenomenon, specially marked in the early, middle and late lanthanides, occurs also in dilute solutions of these in metallic hosts, and in actinides, as well as some transition metals.

Theoretical attempts at understanding the phenomenon concentrate separately on two different aspects. First there is the question of energetics; i.e., for this interacting electron system, what is the ground state? Why is it one of nonintegral valence? Is the transition (from insulator to metal, and from integral to nonintegral valence) continuous or discontinuous? Since correlation effects are very important, this serious electronic structure problem has been tackled so far largely through phenomenological approaches. Second (and this is the area of our concern), there is the problem of understanding the detailed magnetic, thermal and electrical properties of mixed valence systems. Here, the most common approach uses the microscopic model Hamiltonian introduced by Anderson to describe a magnetic impurity in a metal. The Hamiltonian is

$$H = \sum_{\sigma} \epsilon_d n_{d\sigma} + \sum_{k\sigma} V_{kd} a_{k\sigma}^{\dagger} a_{d\sigma} + \text{h.c.} + \sum_{k\sigma} \epsilon_k n_{k\sigma} + \sum_{\sigma} \frac{U}{2} n_{d\sigma} n_{d-\sigma}$$

where the atomic 'd'-electron (the subscript d refers to electrons in the localized level of the impurity — f-orbital in case of rare-earths or actinides) has energy ϵ_d with respect to the Fermi energy, mixes with amplitude V_k with the conduction electron state of energy ϵ_k , and repels a d-electron of opposite spin with energy U . In a concentrated system, e.g., a lattice, there is a d electron orbital at each lattice site. As ϵ_d (a phenomenological parameter) tends to zero, the states with valence 1 and valence 0 ($\langle n_d \rangle = 1$ and

with probabilities of two

$\langle n \rangle = 0$) become degenerate, and so the possibilities of two different valences and intermediate valence are contained in the model. The model, however, does not include degeneracy of d or f orbitals, crystal field effects, etc. But it is the simplest one exhibiting two valence states. Earlier work on the model has concentrated on the 'good' magnetic impurity, i.e., $\frac{U}{2} \gg \pi |V_{kd}|^2 \rho_{\epsilon_F} \equiv \Delta$ (ρ_{ϵ_F} = conduction electron density of states at Fermi level) and $-\epsilon_d = \frac{U}{2}$ (symmetric Anderson model) or $|\epsilon_d| \gg \Delta$ (Kondo impurity). This and earlier Hartree-Fock work are briefly reviewed in Chapter I.

We start our work on the mixed valence problem with a thorough analysis in the Hartree Fock approximation (HFA). For a single impurity this was done by Anderson, and an important extension to include a d electron conduction-hole attraction (a Falicov Kimball term, $H_{FK} = W \sum_{\sigma} n_{d\sigma} \sum_{kk'} \sum_{\sigma'} a_{k\sigma'}^\dagger a_{k'\sigma}$) has been made by Haldane. Haldane found that when the parameter $C (\sim W^2 \rho_{\epsilon_F})$ is sufficiently large, there is a region in the parameter space ($\frac{\epsilon_d}{\Delta}, \frac{U}{\Delta}$ space) where a nonmagnetic and a doubly degenerate magnetic states are simultaneously stable. In Chapter II we investigate this region in detail, especially around $\epsilon_d \sim 0$, locate the self consistent solutions to the H-F equations by computer calculations, find their energies and the coexistence region. We also obtain approximate analytical forms for the latter and show them to be accurate. We find basically that for $C > \pi \Delta$, there exist in the parameter space around $\epsilon_d = 0$ and $\epsilon_d = -U$, two 'mixed-valence'

regimes of width $\sim C$. Within each such mixed-valence regime there is a line on which the magnetic and nonmagnetic solutions have equal energy, but $\langle n_d \rangle$ and $\langle s_d \rangle$ ($s_d = n_{d+} - n_{d-}$) for the two states are very different; thus this is a line of first order phase transition.

We next consider two such impurities interacting through a hopping term of the type $\lambda (c_{d1\sigma}^\dagger c_{d2\sigma} + \text{h.c.})$, in the HFA, the aim being to obtain the energy of interaction $E_{\text{int}}^{\text{oo}}$ for various single impurity HF configurations ($E_{\text{int}}^{\text{oo}} = E_2 - 2E_1$) for the case $C \neq 0$. Denoting the nonmagnetic state as o and the magnetic state as σ , we calculate the energies E_{int} , $E_{\text{int}}^{\text{oo}}$, $E_{\text{int}}^{\sigma\sigma}$, $E_{\text{int}}^{\sigma-o}$ where the superscripts, oo for example mean that one of the impurities is in the state o and the other in the state σ . In addition to these diagonal terms there is the possibility of transition between individual ion HF product states, i.e., processes of the type $|oo\rangle \rightarrow |o\sigma\rangle$. The amplitude for this is $\sim \lambda$.

The above serves as a preliminary for investigation of the mixed valence lattice (Chapter III). The existence of three states, two magnetic and one nonmagnetic, at each site, is modelled by the eigenstates of an $S=1$ spin, with a single ion anisotropy term ΔS_Z^2 simulating the energy difference between the magnetic ($S_Z^1 = \pm 1$) and nonmagnetic ($S_Z^1 = 0$) states. The interactions obtained above can be written as spin-spin interactions. The important points are that (i) these

interactions arise from states outside the restricted three level manifold, so they should be included in any complete theory working explicitly only with these three states and (ii) the spin - spin interactions are obtained as functions of ϵ_d , C , U and Δ . We discuss the possible phases of this interacting 'spin' system, which has the model Hamiltonian

$$H = L \sum_i S_i^2 + \sum_{ij} J S_z^i S_z^j + \sum_{ij} \lambda S_x^i S_x^j + \sum_{ij} K S_z^i S_z^j + M$$

The orderings $\langle S_z^i \rangle \neq 0$ and $\langle S_z^i \rangle_{\text{sublattice}} \neq 0$ correspond to ferro- and antiferromagnetic phases. We obtain parameter space conditions for this to occur, and mean field estimates of the transition temperature T_C . In addition there is the possibility of $\langle S_x^i \rangle \neq 0$, which is a nonmagnetic coherent valence fluctuation phase. One important result we get is that this new type of phase is more stable than the magnetic phases for a sizeable range of ϵ_d values close to zero. This is in accord with experiment. We compare transition temperatures and briefly discuss the nature of this phase.

The HFA is correct in the gross, but, for a single impurity for instance, misses the Kondo effect, which is due to transitions between the HF states owing to fluctuations beyond the mean field. Due to the Anderson orthogonality catastrophe, such transitions are nearly blocked, the Kondo temperature is small, and the HFA good except for $T \lesssim T_K$. A formalism taking precisely the above fluctuations into account, for the symmetric Anderson model, was discussed by Hamann. We extend (in Chapter IV) this path integral formalism to the nonsymmetrical Anderson model, and show that its

partition function is the same as that of the Kondo model as obtained by Yuval and Anderson. From this analogy we can calculate J_{eff} as a function of ε_d . In contrast to the Schrieffer-Wolff value $J = \frac{\Delta}{\pi} \left(\frac{1}{\varepsilon_d} - \frac{1}{\varepsilon_d + U} \right)$, this does not diverge as $\varepsilon_d \rightarrow 0$, though it does increase to a large value. Thus the asymmetric Anderson model tends to a strong coupling Kondo system with the Kondo temperature $T_K \rightarrow \Delta$ as $\varepsilon_d \rightarrow 0$. We finally discuss the impurity with $C \neq 0$ in this formalism, and show that the partition function is identical with that of a two resonant level model. The latter, unfortunately, is not soluble (in contrast to the one resonant level model the Toulouse limit).

The method of approach of the previous paragraph cannot easily be carried through for more than one impurity, e.g., a lattice of mixed valence ions. The mixed valence problem is characterized by several energies, e.g., the Kondo temperature, the energy difference between two different valence states, the energy of interaction between ions, being nearly the same. This limits the utility of HFA in which $T_K = 0$. The path integral method is tractable only for $E_{\text{int}} = 0$. Thus we need a method which includes all these effects. Preliminary results using such a method are presented in Chapter V. We use Bloch and De Dominicis formulation of expressing the partition function Z of an interacting system as a product

$$Z = Z_0 \cdot Z_{\text{q.p.}}$$

where $Z_{\text{q.p.}}$ is, in appearance, the partition function of a

"quasiparticle" with discrete real energy levels. For the Anderson model with $U = \infty$, we find the energies of these quasiparticles (three in number, one nonmagnetic and two nonmagnetic) within a reasonable approximation, their dependence on temperature and model parameters, and hence thermodynamic quantities, viz., the static magnetic susceptibility for all temperatures and ϵ_d , the valence fraction (defined $\langle n_d \rangle$). The zero temperature susceptibility is found to be $O(\frac{1}{T_K})$, which is consistent with other estimates. The ground state at zero temperature is nonmagnetic with a valence fraction of $1 - \frac{T_K}{\Delta}$ showing that the ground state is a mixture of the two magnetic and the nonmagnetic states of the non-interacting system (the term $V_{kd} c_{k\sigma}^+ c_{d\sigma} + \text{h.c.}$ having been taken as interaction), with a predominant proportion of the former. This corroborates the singlet ground state idea and quantitatively matches the estimate of Yafet and Varma.

It is possible to include the $C \neq 0$ and finite U cases within the formalism although we have not gone into the details of these. For the two impurity problem also it is possible to find out the energies of interaction between quasiparticle product states, and tackle the lattice problem via a pseudospin model. This pseudospin model is, however, very different from that obtained from the HFA, as the magnetic and nonmagnetic states themselves are different. The problem is treating two impurities in this formalism arises in proving the fundamental

relation $E_2 = 2E_1$ (for $E_{int} = 0$, or two noninteracting impurities).

Lastly, we must mention that the outcome of the above treatments are not yet in a state to be compared with experimental data. The theory or the models, as already mentioned, are too simplistic and therefore comparison with experiments would be premature. But we expect these models and their treatments to provide a basis for further improvements and make the theory more realistic.

CHAPTER I

INTRODUCTION

Some rare earth compounds such as chalcogenides, intermetallic compounds, Cerium metal, and more recently, some actinides have been the subject of a wide range of experimental investigations for some time. The interest in rare earth (RE) chalcogenides such as SmS, SmSe, TmSe, Tm Te etc., arises from the fact that although under normal pressure they are semiconducting and usually in a 2^+ (atomic configuration $4f^n$) valence state, on application of hydrostatic pressure, they undergo an abrupt isostructural change with a large change in the lattice constant, to a conducting state with an unusual valence in between 2^+ and 3^+ (configurations $4f^{n-1} 5d^x 6s^{1-x}$) state. In this phase (which is also called a "collapsed" phase) lattice constant corresponds to the weighted average of those corresponding to the 2^+ and 3^+ states. It is possible to find the ratios of fractions of 2^+ and 3^+ states quite accurately because in lanthanide series, due to lanthanide contraction, lattice constants vary very systematically with the valence or number of electrons in the atom. This metallic phase (collapsed) shows anomalous magnetic properties — saturation of the moment at low temperature and absence of magnetic ordering; resistivity minimum; specific heat anomaly, and so on. The intermetallic compounds Ce Al₂, Ce Al₃, Yb Al₃ etc., and the actinide metals such as Np, Pu and some

compounds of U, Pu such as USn_3 , UAl_2 , $NpRh_3$ and $PuAl_3$ show behaviour similar to this collapsed metallic or mixed valence (MV) phase. The mixed valence phenomenon is also seen in numerous metallic hosts containing RE impurities.

The interest in intermediate valence or fluctuating valence compounds has been significant and is growing as is evident from the large number of recent publications and conferences on the subject. Since extensive and upto date review articles¹ exist on both experimental and theoretical aspects of the subject we do not consider it necessary to attempt a detailed review here. We will, however, discuss the salient experimental features wherever necessary to explain or justify our choice of models.

Theoretical attempts at understanding the mixed valence phenomenon concentrate on two different aspects. First there is the question of energetics i.e., for this interacting electronic system, what is the ground state? Why is it of nonintegral valence? Is the phase transition continuous or discontinuous? In this electronic structure problem, correlation effects are very important as, clearly, the extremely localized f-orbitals are involved. This problem has so far been tackled largely through phenomenological approaches and we have not gone into these, although at times we have based our models on these approaches. The second aspect of the problem forms the area of our concern. It is that of understanding the detailed magnetic, thermal and electrical properties of the mixed valence system.

The magnetic susceptibility, specific heat and resistivity of MV compounds are similar to those of a Kondo system. This, and the lack of magnetic ordering, indicate that intersite interactions are extremely weak and the study of a single MV ion will take us a long way towards understanding the whole system.

The physical properties which we seek to explain are intermediate valence (fluctuation or mixing), static magnetic susceptibility and magnetic ordering. There has been some speculation in the literature about the time nature of mixed valence in these compounds — whether valence in a sample is spatially homogeneous and fluctuating in time or whether different valence ions are spatially distributed like an alloy. The dynamic probes for this are Mossbauer effect, neutron diffraction and XPS. The first of these methods gives only an average valence but the much faster probe, XPS, clearly shows the two valence states. Thus it is established beyond doubt that these are actually fluctuating valence systems with characteristic time typically of the order of 10^{-14} seconds. The typical magnetic susceptibility versus temperature curves have been shown in fig. 1(a). They are characterized by a mild peak below which the susceptibility is slowly varying and at zero temperature has a finite value (non-magnetic behaviour). At much higher temperature the susceptibility shows Curie-Weiss like behaviour characteristic of a magnetic moment. Thus, while the high temperature susceptibility does show the ion to carry magnetic moment, all search for ferromagne-

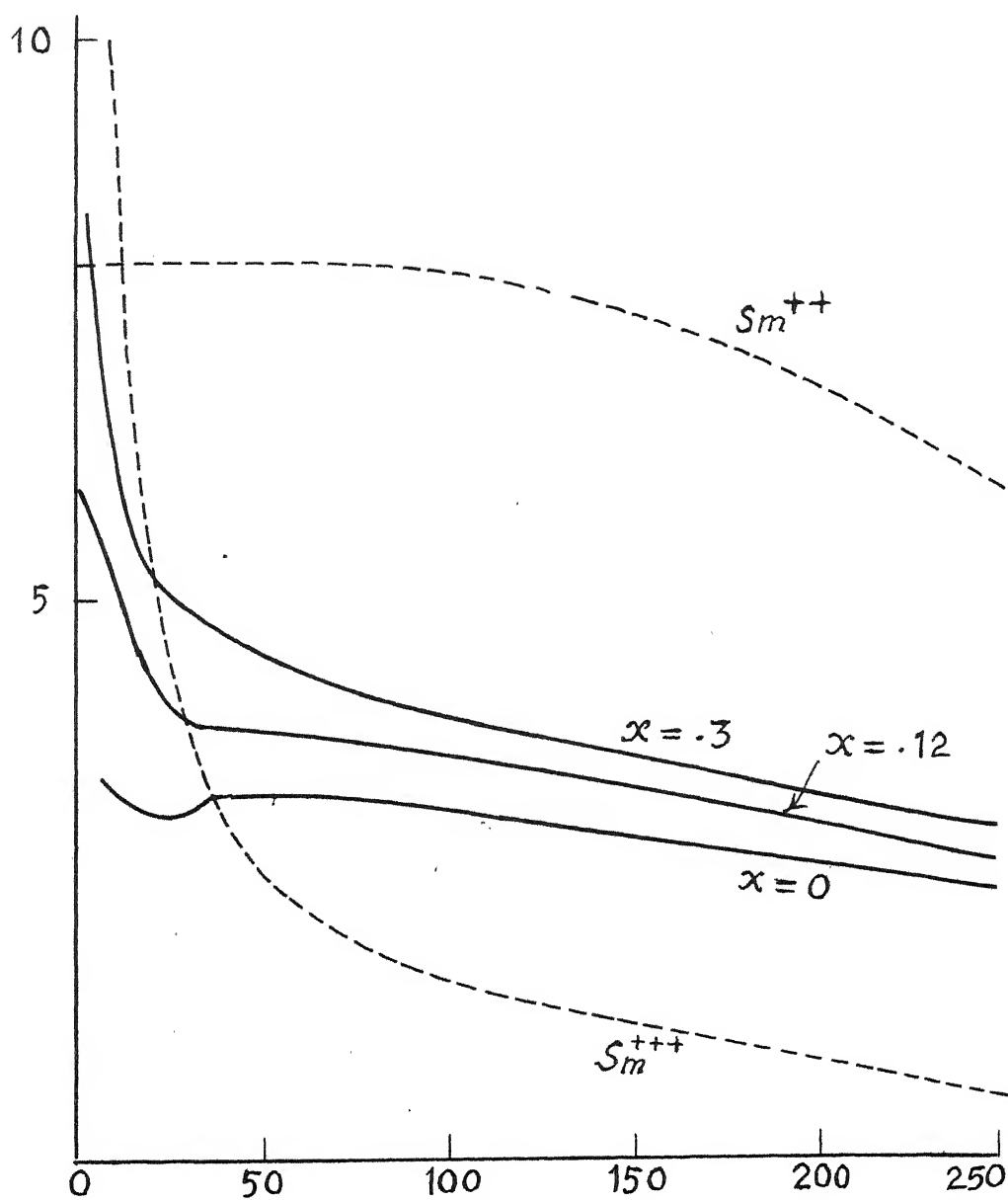


FIG. 1- The magnetic susceptibility χ per Sm ion in $Sm_{1-x}V_xB_6$. Values for free Sm^{++} and Sm^{+++} are shown. (From ref. 38)

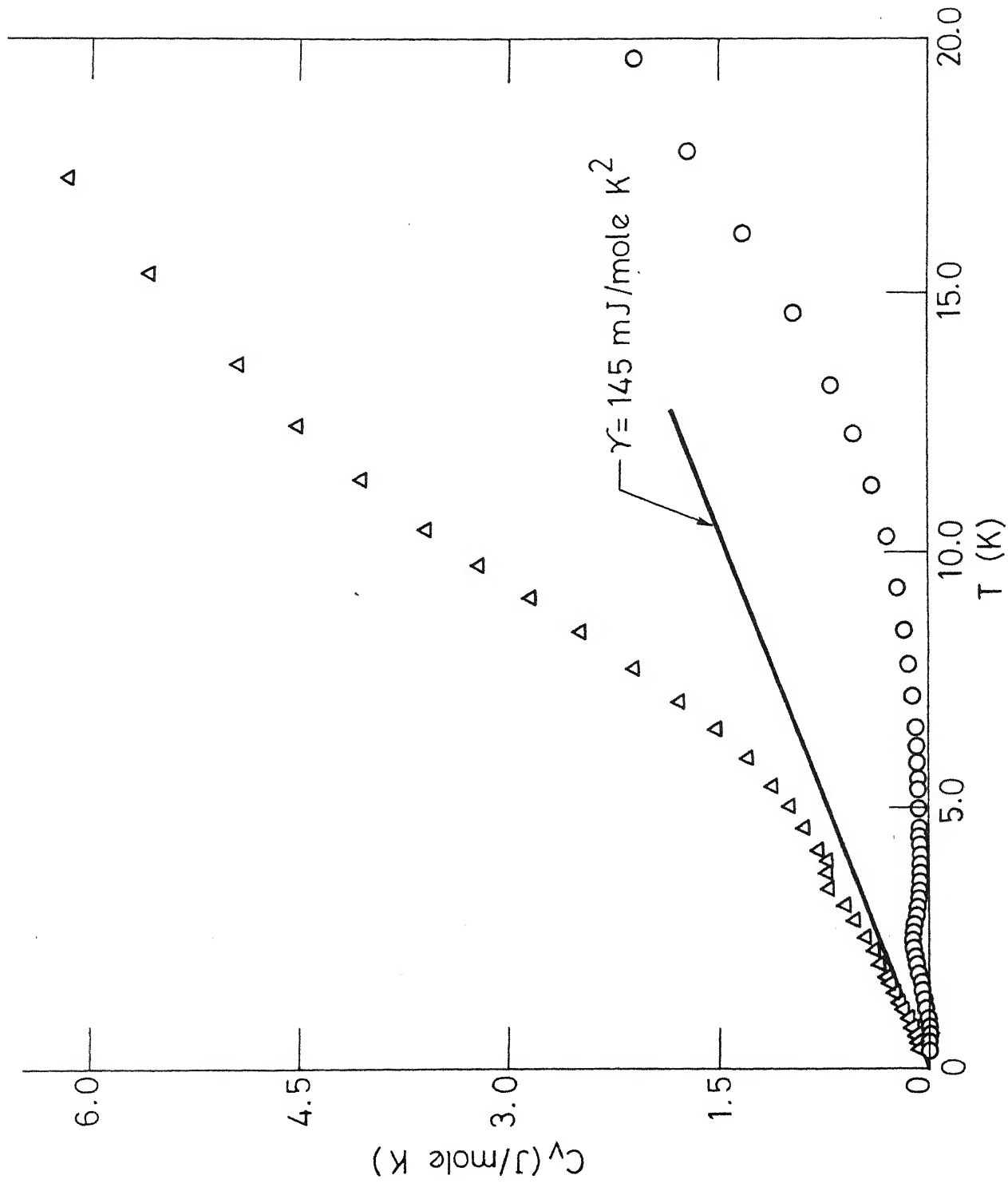


Fig.1(b) C_v Vs. T for typical M.V. system ($S_m B_6$) (from Maple⁴⁰).

tic ordering has been futile; only one compound TmTe shows antiferromagnetic ordering at low temperature; and Ce Al₂ is thought to do so, though not conclusively shown yet. A typical specific heat curve is shown in fig. 1(b). Zero temperature behaviour of these properties suggest heavy Fermi liquid.

Any theoretical model for such systems must start with a narrow f-band (4-f for RE 5-f for actinides) or f-state in case of a single ion, and a wide conduction band. Then the strong correlation between highly localized f-state must be taken into account. One such model is the Anderson model for localized impurity in metals² and we start with the simplest non-degenerate or single orbital Anderson model, the Hamiltonian for which is,

$$H = \sum_{k\sigma} \epsilon_{k\sigma} c_{k\sigma}^+ c_{k\sigma} + \sum_{\sigma} \epsilon_{d\sigma} c_{d\sigma}^+ c_{d\sigma} + \sum_{k\sigma} V_{k\sigma} (c_{k\sigma}^+ c_{d\sigma} + c_{d\sigma}^+ c_{k\sigma}) + \frac{U}{2} \sum_{\sigma} n_{d\sigma} n_{d\sigma} \quad (1)$$

The first two terms describe the conduction band and the ionic local level (subscripted 'd' for historical reasons but actually describes f-states) and the last one correlation between local electrons. The third term describes a hybridisation between local and conduction states and arises from the fact that dissolved in a solid, the local level is no longer orthogonal to the band levels even if originally of a different symmetry. The single orbital case is not too unrealistic because in systems under investigation, due to large Coulomb correlation

(U), only two ionic levels are close enough to each other and to the Fermi level to matter. It however gives wrong magnetic moment values. But we believe that the essential statistics and qualitative features will not be damaged due to this choice. In RE systems under consideration, the coulomb repulsion $U \sim 5$ to 10 eV, the mixing term V is responsible for the width of the local state ($\Delta = \pi \rho_{\text{eF}} |V|^2$) and typically we have $\Delta \sim .1$ eV. The distance ϵ_d of the local level from the Fermi level decides the extent of valence mixing — closer it is to the Fermi level, more energetically favourable for it to empty into the conduction band. Therefore for valence fluctuation phenomena, the case of interest is when ϵ_d is close to the Fermi level or $|\epsilon_d| \lesssim \Delta$. The Anderson model is a strong candidate for MV systems also because the properties of these systems are close to a Kondo impurity and so are those of the Anderson model as shown by S. W. transformation.³ The S.W. transformation, however, does not apply to $|\epsilon_d| \lesssim \Delta$ the region of interest here. The correspondence to Kondo model, therefore, does not become clear right at the outset. It becomes clear, in this work, only in the Path Integral treatment (chapter III) of the Anderson model.

But, as is well known, the treatment of the Kondo model in time representation (the Path Integral method (PIM) reduces the Anderson model to this) takes only spin fluctuations into account and valence fluctuations do not explicitly enter the picture. This is because in the Hartree-Fock approximation (HFA), which is the starting point of PIM, the two solutions of the Anderson

model are of the same valence. To accomodate fluctuations between different valence states in the HFA we incorporate into the Anderson model a term

$$g \left(\sum_{k', \sigma} c_{k\sigma}^+ c_{k'\sigma} \right) \sum_{\sigma} n_{d\sigma} \quad \dots (2)$$

This represents a Coulomb repulsion of the conduction electrons by the localized electron. This is the term in the Falicov-Kimball model⁴ responsible for the phase transition to a different valence state. The bracketed part in (2) can be represented in terms of Tomonaga bosons. (2) then represents coupling of the local electrons with a boson field. Thus coupling with bosons such as phonons can also be treated in the same way.

In Chapter I we have taken up this modified Anderson model in the Hartree-Fock approximation at zero temperature. For a single impurity this was done by Anderson² who found that there exist two regimes in the parameter space $(\frac{\Delta}{U}, \frac{\epsilon_d}{U})$; one for which $\langle n_{d\uparrow} \rangle = \langle n_{d\downarrow} \rangle$ signifying a nonmagnetic regime, and another for which $\langle n_{d\uparrow} \rangle \neq \langle n_{d\downarrow} \rangle$, signifying a magnetic regime. The implications of this phase diagram and transition are discussed briefly in section 1 of chapter II. In the next section we add Falicov-Kimball like screening term to the model as done by Haldane⁵, and proceed with its Hartree-Fock(HF) analysis. We concentrate on the large U , large C case for varying ϵ_d . We write down the HF equations, and their stability conditions. Haldane found that when the parameter C is sufficiently large,

there are two regions in the parameter space $(\frac{\epsilon_d}{\Delta}, \frac{U}{\Delta})$ around $\epsilon_d = 0$ and $\epsilon_d = -U$, where a stable nonmagnetic solution coexists with a stable magnetic one. We investigate these coexistence regions, especially around $\epsilon_d = 0$, in detail by locating the solutions to HF equations by computer calculations. We show that the coexistence region is of width $\sim C$. From the calculated energies and d-occupation numbers ($\langle n_d \rangle = \langle n_{d\uparrow} \rangle + \langle n_{d\downarrow} \rangle$) of the solutions we show that within this MV regime (coexistence region) there is a line in the $(\frac{\epsilon_d}{\Delta}, \frac{U}{\Delta})$ space on which the magnetic and nonmagnetic solutions have equal energy, but different $\langle n_d \rangle$. Thus this is a line of first order phase transition. This phase transition is, of course, spurious, although it is believed that the energies are of correct order of magnitude. This spurious phase transition disappears and gives rise to a gradual change from magnetic to nonmagnetic behaviours when one takes into account effects beyond the mean (or HF) field. This has been done in Chapter IV. In section 2 of chapter II we find appropriate analytical expressions for the energies and boundaries (in the parameter space) of magnetic and nonmagnetic solutions for large $C (\gg \pi\Delta)$ and show them to agree quite well with the computer calculations.

In the next section (sec. 3) of this chapter, we consider two impurities each described by a modified Anderson model, and interacting through a hopping term of the type $C_{d1}^{\dagger} C_{d2} + \text{h.c.}$, as done by Alexander and Anderson.⁶ We find within the HFA at zero temperature the energies of interaction E_{int} where $E_{\text{int}} =$

$E_2 - 2E_1$, for various configurations of the two impurity system. Here E_2 is the energy of the interacting ions, E_1 is the HF energy of a single noninteracting ion, and by "configuration", e.g., denoted by superscripts 0σ in $E^{0\sigma}$, we mean that one of the ions is in the nonmagnetic state and the other in the magnetic state σ . Thus we find the interaction energies E_{int}^{00} , $E_{int}^{0\sigma}$, $E_{int}^{\sigma\sigma}$ and $E_{int}^{\sigma-\sigma}$. In addition to these diagonal terms, there is the possibility of moment transfer or exchange as a result of interaction. We show that the processes of the type $|0\sigma\rangle \rightarrow |\sigma 0\rangle$ have an amplitude $\sim \lambda$. The results of this section are used in the next chapter to construct a Hamiltonian for a lattice of such interacting ions.

Thus, in Chapter III, we consider a lattice of mixed valence impurities, the preliminary energetics of which are provided by the HF treatment of the previous chapter. In chapter III we show that each impurity (with $C \neq 0$) in the MV regime can exist in either of the two degenerate magnetic or the nonmagnetic HF state, the magnetic and the nonmagnetic states being of different energies (generally). This situation is simulated by representing each ion by an $S = 1$ spin and adding a single ion anisotropy term, AS_Z^2 , where A is the difference between the energies of the two HF states. Now the interactions obtained in Chapter II can be written as spin-spin interactions. These interactions, say between an ion at site i and another at j , are of the type $J_{ij} S_Z^i S_Z^j$, $B_{ij} S_Z^{i2} S_Z^{j2}$, $\lambda_{ij} S_X^i S_X^j$, ..., where all the parameters can be obtained from the results of the last section of Chapter II. Thus we have the Hamiltonian of the

MV lattice as

$$H = \sum_{ij} J_{ij} S_z^i S_z^j + \sum_{ij} B_{ij} S_z^{i2} S_z^{j2} + A \sum_i S_z^{i2} + \lambda \sum_{ij} S_x^i S_x^j + M \quad (3)$$

Next, in section 2 of Chapter III, we consider the various possible orderings of the above Hamiltonian within the mean field approximation (MFA). We find parameter space conditions and transition temperatures T_c for the various orderings, ferromagnetic ($\langle S_z \rangle = 0$), antiferromagnetic ($\langle S_z \rangle \neq 0$) and a third kind of ordering characterized by $\langle S_z \rangle \neq 0$, $\langle S_x \rangle \neq 0$. This last is the coherent valence fluctuation (VF) phase. On comparison of transition temperatures we find that this nonmagnetic VF phase dominates over most of the temperature range upto very low temperatures. At very low temperatures, we expect Kondo fluctuations to take over which makes the ions nonmagnetic anyway. Thus it seems to bear out the experimental results of absence of magnetic ordering in MV systems.

As has been already pointed out, the HFA is correct in the gross, but, for a single impurity for instance, misses the Kondo effect which has been shown to exist for an Anderson model. The HF wave functions which are eigenfunctions of different effective one electron Hamiltonians, are not orthogonal to each other though nearly so as shown by Anderson⁷ orthogonality catastrophe. The small overlap between these states causes fluctuations, which are beyond the mean field approach, and gives rise to Kondo effect and a vanishing moment at very low temperatures. To take these effects beyond the HFA into account,

we follow Hamann's path integral method⁸ which he used for the symmetric Anderson model. We extend his method to the case of asymmetric Anderson model (with $C = 0$) in Chapter IV. The method consists of choosing hopping paths between the two HF solutions which correspond to minima in the free energy functional, and calculating their contribution to the partition function. We show that the partition function Z has the same form as that obtained by Yuval and Anderson⁹ for the Kondo model. From this analogy we find the parameters J, τ of the equivalent Kondo model. By this method we are able to reach upto $\varepsilon_d = 0$ which the Schrieffer-Wolff transformation fails to do as it breaks down as $|\varepsilon_d| \lesssim \Delta$. We show that the effective exchange coupling J_{eff} does increase to a large value but remains finite as $|\varepsilon_d| \rightarrow 0$, taking the system to strong coupling Kondo limit. In section 4 of Chapter IV we turn to the $C \neq 0$ case and show that the Z for this, when scaled following Anderson and Yuval's method, reduces to that for a two resonant level model in contrast to the one resonant level model obtained by scaling of the $C = 0$ Anderson model. Unfortunately, the two resonant level model is not soluble and therefore this method cannot give physical quantities for the $C \neq 0$ case.

This path integral method of Chapter IV cannot be easily carried through to describe a many impurity situation either. The treatment of a lattice of MV impurities in Chapter III is meaningful only when Kondo fluctuations are on a much smaller scale ($T_K \sim 0$) compared to ion-ion interactions. Around $\varepsilon_d = 0$,

these various energies, the Kondo temperature, energy difference between different valence states, energy of interaction between ions, are all of the same magnitude. This limits the utility of the HF approach of chapter III. These difficulties prompt us to investigate another method which holds the promise of accomodating nonzero C as well as many impurities, for all parameter ranges. Chapter V presents preliminary results using such a method, the quasiparticle method.

In section 2 of Chapter V we very briefly describe the formulation of Bloch and De Dominicis, of expressing Z of a large interacting system as that of a 'quasiparticle' with discrete real energy levels. The self consistent equations determining the quasiparticle energies for a $U = \infty$ Anderson model ($C = 0$) are approximated upto certain terms in section 2 and the implications of these approximations discussed. Among the three quasiparticles, two magnetic and one nonmagnetic, we show the nonmagnetic one to be the ground state at zero and low temperatures, while at higher temperatures the magnetic states lie lower. Once the energies of these quasiparticles and hence Z has been found, one can calculate thermodynamic quantities as derivatives of Z . In sections 3 and 4 we find the static magnetic susceptibility, and valence fraction ($\langle n_d \rangle$). Numerical values have been obtained by computer calculations. The results on susceptibility are compared with the renormalization group calculations of Krishnamurti, Wilson and Wilkins¹⁰, and it is found that around $|\epsilon_d| \lesssim \Delta$,

our magnetic susceptibility curve has the same general shape as their calculated ones, although our results are higher by a factor of ~ 4 (not uniform over the whole range of temperature). This may be due to the approximations involved, or the difference between a $U = D/2$ (KWW) and $U = \infty$ (this work) model. For the $\epsilon_d < 0$, $|\epsilon_d| \gg \Delta$ case we show that χ_k matches standard results at zero and high temperatures. So we conclude that the approximations involved are good.

In the last section, 5, of this chapter, we briefly discuss further possibilities in the method. The $C \neq 0$ case does not seem intractable. The interaction between two impurities is also possible to deal with. The difficulty in this arises because of the formal difficulty in showing $E_2 = 2E_1$ for a pair of non-interacting ions. But we believe that the method is capable of dealing with these problems and hence that of a lattice of MV impurities.

In the concluding chapter we summarize the results obtained in, and wisdom gained from chapters II through V. Finally, we suggest that although in the present state, the results can only be compared qualitatively with experimental data, more realistic features like multiple orbitals, crystal fields etc., can be incorporated into the model in treatment of chapter V; then the results on physical quantities will be more ripe for comparison with experimental data.

CHAPTER II

THE MIXED VALENCE PROBLEM IN THE HARTREE-FOCK APPROXIMATION

In this chapter we apply the simplest, the Hartree Fock approximation (HFA), to the Anderson model and its modified version advocated by Haldane⁵ ($C \neq 0$ case), and then to a pair of such ions.

The HFA results for the Anderson model are well known and in section 1 we briefly describe it.

In section 2, we take up the modified Anderson model ($C \neq 0$). With Haldane's work as background, we discuss in detail the mixed valence regime in the parameter space. We find the boundaries of this regime, the energies of the two solutions, and their valences by computer calculations. Then we find these quantities for large C ($C > \Delta$) in approximate analytical form and show them to be close to numerical results.

In section 3 of this chapter, we consider, in the HFA, two such impurities interacting via a hopping term of the type $\lambda c_{d1}^+ c_{d2} + \text{h.c.}$ Vermell¹ has partially addressed himself to this work. We analyse the problem following Alexander and Anderson's⁶ HF approach and find the various energies of interaction.

Section 1 : THE ANDERSON MODEL IN THE HARTREE FOCK APPROXIMATION

The nondegenerate Anderson model has been treated in the HFA by Anderson himself. The Hamiltonian

$$H = \sum_{k\sigma} \epsilon_{k\sigma} c_{k\sigma}^+ c_{k\sigma} + \sum_{\sigma} \epsilon_{d\sigma} c_{d\sigma}^+ c_{d\sigma} + \frac{U}{2} \sum_{\sigma} n_{d\sigma} n_{d-\sigma} + \sum_{k\sigma} V_{kd} (c_{k\sigma}^+ c_{d\sigma} + c_{d\sigma}^+ c_{k\sigma})$$

represents conduction electrons in a wide band, with energies ϵ_k , mixing with the localized impurity level of energy ϵ_d (energies measured from the Fermi level) via a mixing term of strength V_{kd} while local electrons of opposite spin repel each other with coulomb energy U . In the HFA, each local electron of spin σ is supposed to be governed by the one-electron Hamiltonian

$$\sum_k \epsilon_k c_{k\sigma}^+ c_{k\sigma} + (\epsilon_d + \frac{U}{2} \langle n_{d-\sigma} \rangle) n_{d\sigma} + \sum_k (V c_{k\sigma}^+ c_{d\sigma} + \text{h.c.})$$

(V is an average mixing strength, $(V_{kd})_{av}$).

This resonant level Hamiltonian has well known solutions and gives, at zero temperature,

$$\langle n_{d\sigma} \rangle = \int_{-\Delta}^0 \rho_{d\sigma}(\epsilon) d\epsilon$$

$$\text{where } \rho_{d\sigma}(\epsilon) = \frac{1}{\pi} \frac{\Delta}{(\epsilon - \epsilon_{d\sigma} - \frac{U}{2} \langle n_{d-\sigma} \rangle)^2 + \Delta^2}$$

$$\text{with } \Delta = \pi \rho_{\epsilon_F} |V|^2$$

Collecting expressions for local electrons of both spins one obtains the self consistent equations,

$$\langle n_{d\uparrow} \rangle = \frac{1}{\pi} \cot^{-1} \frac{\epsilon_d + U \langle n_{d\uparrow} \rangle}{\Delta}$$

$$\langle n_{d\downarrow} \rangle = \frac{1}{\pi} \cot^{-1} \frac{\epsilon_d + U \langle n_{d\downarrow} \rangle}{\Delta}$$

This set of equations has two types of solutions, magnetic, with $\langle n_{d\uparrow} \rangle \neq \langle n_{d\downarrow} \rangle$ and nonmagnetic when $\langle n_{d\uparrow} \rangle = \langle n_{d\downarrow} \rangle$. The magnetic solutions exist only when $U \geq \pi\Delta$. When this condition is satisfied, the magnetic solution exists only within a range of ε_d specified by $-U \lesssim \varepsilon_d \lesssim 0$. Within this range, the nonmagnetic solution is unstable (stability of solutions will be discussed in the next section), and outside only the nonmagnetic one exists. Thus we have the phase diagram shown in fig. 2.

This phase diagram shows a sharp transition between magnetic and nonmagnetic character at particular points in the phase space. This, however, should not be taken literally. Keeping in view the character of HFA, which precludes slow oscillations between, say, the two degenerate magnetic solutions. Such oscillations are the heart of the Kondo effect and are nearly blocked by Anderson's orthogonality catastrophe⁷ according to which the matrix element between two determinantal wave functions constructed from different scattering states (as in the HFA for Anderson model for local electron of each spin, for a magnetic solution) is vanishingly small when the phase shifts at the Fermi surface of the two scattering states are greatly different. Thus in the HFA we miss the Kondo effect. However, it gives us correct energetics deep within the magnetic or nonmagnetic states (far away from the phase transition line), in that the ordinary theory of nonmagnetic impurities is applicable in the nonmagnetic regime and in the magnetic regime, Kondo

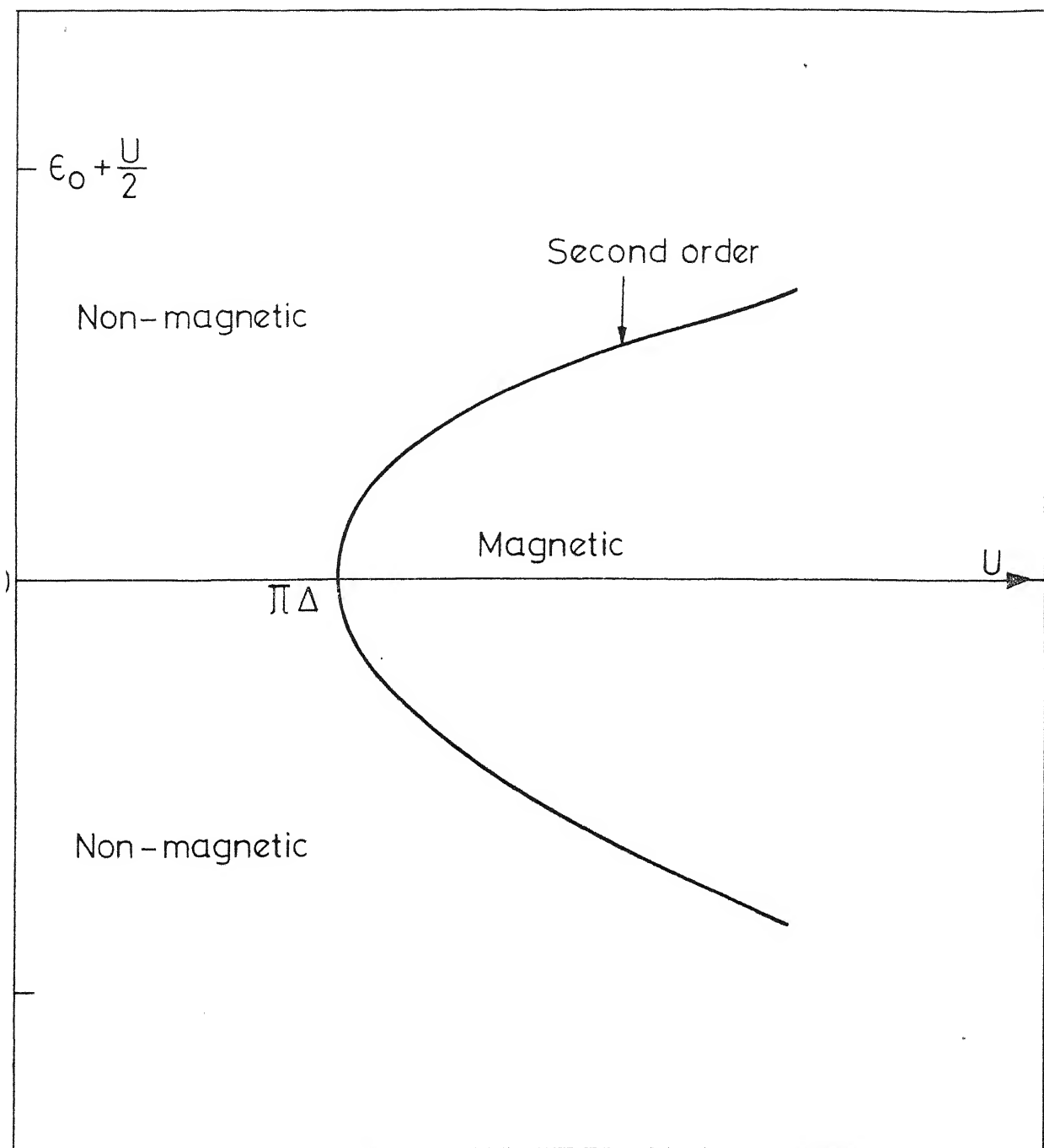


Fig. 2 Phase diagram for $C=0$ Anderson model.
(from Verma³⁹)

effect is regained if upon the HF solutions we impose the above mentioned oscillations. Hence the importance of an HF analysis. These points have been discussed in detail by Blending.¹²

Section 2 : ANALYSIS OF THE $C \neq 0$ ANDERSON HAMILTONIAN IN THE HARTREE-FOCK APPROXIMATION

The Anderson model has been recently generalized by Haldane⁵ to include local electron conduction electron Coulmb repulsion by including in the Anderson Hamiltonian a term $g \left(\sum_{\sigma} n_{d\sigma} \right) \left(\sum_{k,k',\sigma'} c_{k\sigma}^+ c_{k'\sigma'} \right)$. It has been shown that by taking terms upto second order in g (the approximation within which Haldane and Riseborough¹³ have worked), an effective Hamiltonian can be written as follows :

$$H = \sum_{\sigma} \epsilon_{d\sigma} c_{d\sigma}^+ c_{d\sigma} + \sum_{\sigma} c_{k\sigma}^+ c_{k\sigma} + U n_{d\uparrow} n_{d\downarrow} - \frac{C}{2} (n_{d\uparrow} + n_{d\downarrow})^2 + V \sum_{k\sigma} (c_{k\sigma}^+ c_{d\sigma} + c_{d\sigma}^+ c_{k\sigma}) \quad \dots (1)$$

$$\text{where } C = 4\pi^2 \rho_{\epsilon_F} g^2$$

The above type of interaction also appears in the case of interaction of the local electrons with a Boson field.¹³

We now analyse the Hamiltonian (1) in the HFA.

Section 2(a) : THE HF SELF CONSISTENT EQUATIONS AND STABILITY CONDITIONS OF THE SOLUTIONS.

The effective field seen by a single d electron of

spin σ is,

$$x_{\sigma} = \varepsilon_{d\sigma} + (U - C) \langle n_{d-\sigma} \rangle - C \langle n_{d\sigma} \rangle$$

Thus for the two spins we write

$$x_{+} = \varepsilon_d + (U - C) \langle n_{-} \rangle - C \langle n_{+} \rangle \quad \dots (2)$$

$$x_{-} = \varepsilon_d + (U - C) \langle n_{+} \rangle - C \langle n_{-} \rangle \quad \dots (3)$$

The average occupations $\langle n_{\pm} \rangle$ are derived from the effective d-electron Green's function as

$$\begin{aligned} \langle n_{\pm} \rangle &= \frac{\Delta}{\pi} \int_{-\Delta}^0 \frac{d\omega}{(\omega - x_{\pm})^2 + \Delta^2} \\ &= \frac{\Delta}{\pi} \left(\frac{\pi}{2} - \tan^{-1} \frac{x_{\pm}}{\Delta} \right) \quad \dots (4) \end{aligned}$$

Equations (2) and (3) with $\langle n_{\pm} \rangle$ given by (4) constitute the HF equations for the two spins, to be solved self consistently. For $C = 0$, they reduce to those found for the Anderson model (section 1).

In this case also two types of solutions exist - the non-magnetic ones, for which $x_{+} = x_{-}$ and the magnetic ones for which $x_{+} \neq x_{-}$. The conditions and regions of parameter space in which either type of solution exists, or both kinds coexist, will be investigated in detail in section 2(b). Before that we look into the conditions for stability of these solutions.

The self consistent equations (2) and (3) do not indicate the stability of their solutions. For this we must first write the free energy in HFA :-

$$\begin{aligned} F_{\text{HF}} &= \frac{\Delta}{\pi} \int_{-\Delta}^0 \frac{\omega d\omega}{(\omega - x_{+})^2 + \Delta^2} + \frac{\Delta}{\pi} \int_{-\Delta}^0 \frac{\omega d\omega}{(\omega - x_{-})^2 + \Delta^2} - U \langle n_{+} \rangle \langle n_{-} \rangle \\ &\quad + \frac{C}{2} (\langle n_{+} \rangle + \langle n_{-} \rangle)^2 \quad \dots (5) \end{aligned}$$

The first two terms represent energies of the two resonant d-electrons and the last two those that are left after part of the correlation terms have been absorbed in the effective d-electron Hamiltonians. The derivation of F_{HF} and the matrix of its derivatives is described in appendix 1. It is clear from (5) that F_{HF} is a function of the variables x_+ and x_- . The extrema represent the HF solutions. The stability conditions, viz., the conditions that these are minima, are derived in the appendix and are,

$$2 + C \{ n'(x_+) + n'(x_-) \} > 0 \quad \dots (6)$$

$$1 + C \{ n'(x_+) + n'(x_-) \} - \{ (U-C)^2 - C^2 \} n'(x_+) n'(x_-) > 0 \quad \dots (7)$$

$$\text{where } n'(x_{\pm}) = \frac{1}{\pi} \left(\frac{\pi}{2} - \tan^{-1} \frac{x_{\pm}}{\Delta} \right) \quad \dots (8)$$

It can be easily shown, by putting the LHS of (6) equal to zero into (7) that now (7) is not satisfied, i.e., (6) does not imply (7). On the other hand, (7) implies (6). Therefore, (7) is a more severe condition and hereafter we shall consider only (7) for examining the stability of the solutions (assuming all the time, $U > 2C$).

Section 2(b) : FINDING SOLUTIONS TO THE HF EQUATIONS

The HF equations are, from equations (2), (3), (4) and (8),

$$x_+ = \epsilon_d + (U - C) n(x_-) - C n(x_+) \quad \dots (2')$$

$$x_- = \epsilon_d + (U - C) n(x_+) - C n(x_-) \quad \dots (3')$$

Subtract (2') from (3'). Then

$$x_- - x_+ = U \{ n(x_+) - n(x_-) \}$$

$$\text{or } x_- + U n(x_-) = x_+ + U n(x_+) = K \quad \text{say} \quad \dots (9)$$

We recall from (8) that $n(x_{\pm})$ are functions of the form

$$n(x_{\pm}) = \frac{1}{\pi} \left(\frac{\pi}{2} - \tan^{-1} \frac{x_{\pm}}{\Delta} \right).$$

So, graphically, solutions to equation (9), for either x_+ or x_- , lie on the intersection of $n(z)$ and the straight line $-\frac{z}{U} = \frac{K}{U}$, shown in fig. 3. K is the intercept on z axis and varies from solution to solution according to ϵ_d .

The solutions are magnetic or nonmagnetic according as x_+ and x_- are different or same. In the straight line $-\frac{z}{U} = \frac{K}{U}$, when K is too small (e.g., on the left, line N_1) it cuts the $n(z)$ curve at only one point, and therefore only one, a nonmagnetic, solution exists. As K becomes larger (the line moves to the right) the line reaches a position when it is tangent to $n(z)$ (dotted line 1). This is when the magnetic solution becomes just about possible. We call it the extreme magnetic or extreme nonmagnetic solution. As the straight line moves further to the right, three magnetic solutions become possible (e.g., the line N_3), for which $(x_+, x_-) = (x_1, x_2)$, (x_2, x_3) or (x_1, x_3) ; and also the three nonmagnetic solutions (x_1, x_1) , (x_2, x_2) and (x_3, x_3) . On moving K further to the right, we again reach an extreme magnetic solution (dotted line 2), after which, again, only nonmagnetic solutions exist (e.g., line N_2).

For nonmagnetic solutions of the kind given by line N_1 , i.e., when the d level is deep beneath the Fermi level, both spins occupy the level and the d -electron occupation number

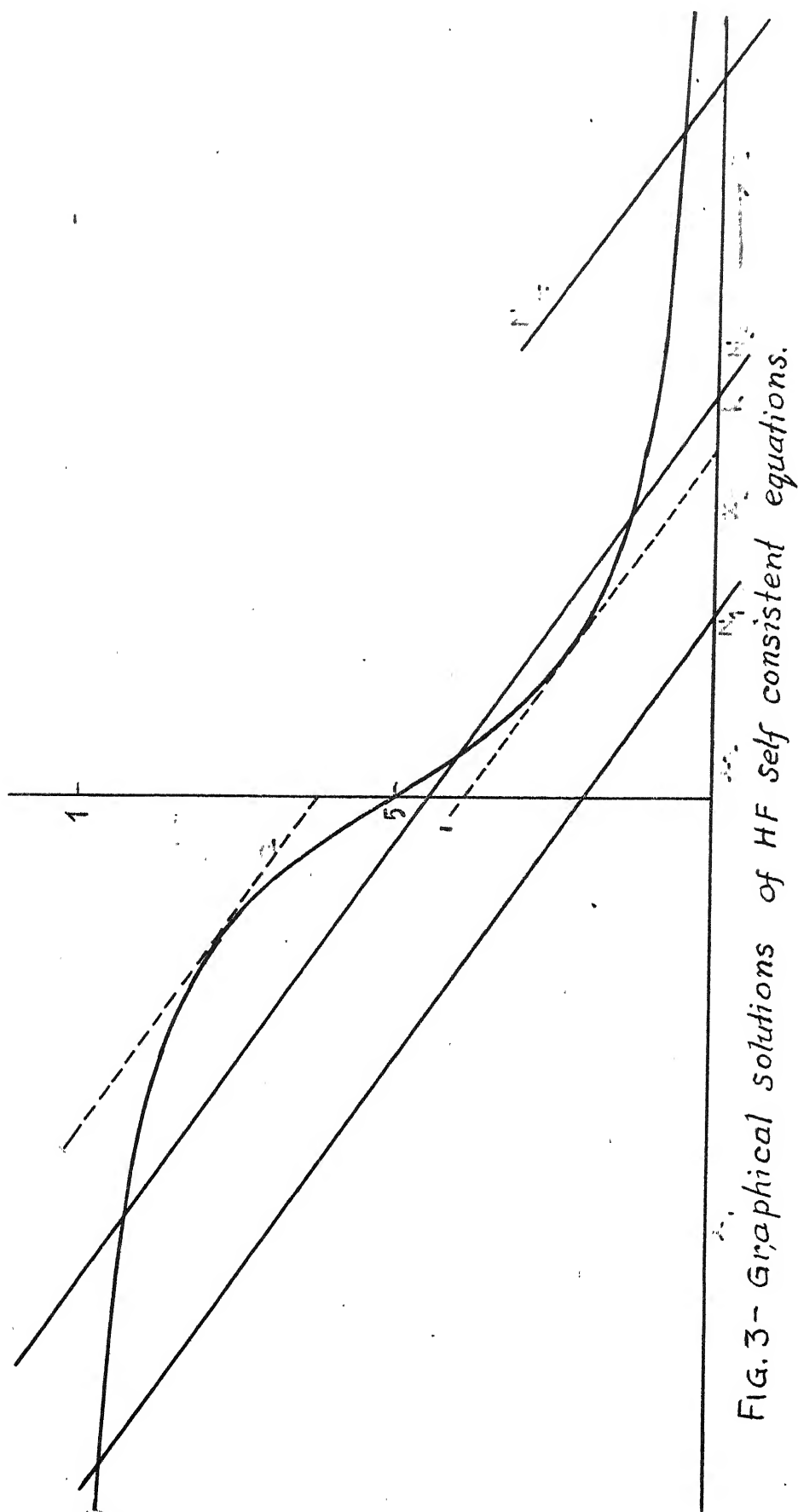


FIG. 3- Graphical solutions of HF self consistent equations.

is ≈ 2 . For good magnetic solutions (x_+ and x_- well separated) the d-occupation is ≈ 1 . The approximate solutions x_{\pm} for the three regions (provided they do not come too close to the limiting ones) are the following :

In nonmagnetic regime 1, i.e., $\varepsilon_d + U - 2C \lesssim \Delta$

$$x_+ = x_- \approx \varepsilon_d + U - 2C$$

In nonmagnetic regime 2, i.e., $\varepsilon_d \geq 0$, $x_+ = x_- \approx \varepsilon_d$

In good magnetic regime, $x_{\pm} \approx \varepsilon_d - C$, $x_{\mp} \approx \varepsilon_d - C + U$

The range of ε_d for which above regimes exist, are discussed in the next sub-section.

Section 2c : BOUNDARIES OF MAGNETIC AND NONMAGNETIC REGIMES

In this sub-section, we use the stability criterion (7) to sift, out of the various possible solutions described in the previous subsection, those which are stable. This enables us to discuss stable magnetic and nonmagnetic solutions, and their possible coexistence for certain range of values of ε_d , U , C etc.

Boundaries of Nonmagnetic Solutions :

For nonmagnetic solutions, $x_+ = x_- \equiv x$ (say). The condition (7) becomes, for stable nonmagnetic solutions to exist,

$$1 + 2C n'(x) - U(U - 2C) \{n'(x)\}^2 > 0$$

$$\text{or, } \{(U - 2C) + n'(x) U(U - 2C)\} \{U - n'(x) U(U - 2C)\} > 0$$

... (10)

We have taken $U > 2C$ and $n'(x) < 0$. So the second factor in (10) is > 0 . So we must also have the other factor > 0 , or

$$1 + U n'(x) > 0 \quad \text{or} \quad |n'(x)| < \frac{1}{U},$$

for stable solutions. Clearly, this holds for all nonmagnetic solutions to the left of extreme solution 1 (see fig. 3) or to the right of extreme solution 2, i.e., for $\varepsilon_d < (>)$ that corresponding to extreme solution 1 (2). These solutions are

$$n'(x) = -\frac{1}{U} = -\frac{\Delta}{\pi} \frac{1}{x^2 + \Delta^2}$$

or

$$x = \pm \sqrt{U/\pi - \Delta^2}$$

$$\pm \sqrt{\Delta U/\pi} \quad \text{for } U \gg \pi \Delta$$

Thus for nonmagnetic solutions to be stable,

$$x > \sqrt{\frac{\Delta U}{\pi}} \quad \text{or } x < -\sqrt{\frac{\Delta U}{\pi}}. \quad \text{With } \sqrt{\frac{\Delta U}{\pi}} > x > -\sqrt{\frac{\Delta U}{\pi}},$$

nonmagnetic solutions exist, but are unstable.

The value of ε_d corresponding to the lower boundary

$$x = -\sqrt{\frac{\Delta U}{\pi}} \text{ is given using e.g., (2')} \text{ or (3')} \text{ as}$$

$$\begin{aligned} \varepsilon_d &= x' - (U - 2C) n(x) \\ &= -\left(\frac{\Delta U}{\pi}\right) - \frac{U-2C}{\pi} \left(\frac{\pi}{2} + \tan^{-1} \sqrt{\frac{\Delta U}{\pi}}\right) \\ &\quad - U + 2C - 2C \sqrt{\frac{\Delta}{\pi U}} + O\left(\Delta \sqrt{\frac{\pi \Delta}{U}}\right) + O\left(\frac{C\Delta}{U} \sqrt{\frac{\pi \Delta}{U}}\right) \end{aligned}$$

Similarly, the upper nonmagnetic boundary, where $x = +\sqrt{\frac{\Delta U}{\pi}}$, is obtained as

$$\varepsilon_d = 2C \sqrt{\frac{\Delta}{\pi U}} + O\left(\Delta \sqrt{\frac{\pi}{U}}\right) + O\left(\frac{C\Delta}{U} \sqrt{\frac{\pi \Delta}{U}}\right) \dots (12)$$

Comparing (11) and (12) we find that nonmagnetic solutions are

stable beyond the region bounded by,

$$(\varepsilon_d + \frac{U}{2} - C) \gtrless \pm \left(\frac{U}{2} - C + 2C \sqrt{\frac{\Delta}{\pi U}} \right) \quad \dots (13)$$

Boundaries of Magnetic Solutions :

It is difficult to locate analytically boundaries of magnetic solutions. However we present here some arguments enabling us to do this approximately. We support these results by computer calculations. The computer results and conclusions drawn from this analysis are discussed later in this section.

Fig. 4 shows a plot of energy F_{HF} (arbitrary base) of the HF solutions vs. ε_d , as obtained from computer calculations. According to this, there is a region of ε_d in which two magnetic solutions exist. We now show that the dotted portion of the line representing magnetic solutions corresponds to unstable ones. For this it is sufficient to show that the condition for stability is the same as that for an extremum to occur in the curve, i.e., the condition $\frac{\partial \varepsilon_d}{\partial V} = 0 \implies$ minimum in F , or equation (7). This has been done in appendix II where we first show that $\frac{\partial \varepsilon_d}{\partial x_+} = 0 \implies \frac{\partial \varepsilon_d}{\partial V} = 0$ and that this condition is the same as (7) with an equality sign; the branch denoted by the solid line satisfies the inequality and therefore corresponds to stable solutions.

Thus we show that there exist ranges of ε_d for given U and C within which not two but one magnetic, and one nonmagnetic solutions are stable. We call these the mixed valence (MV) regimes, since, as has been already mentioned, the valence or d-occupation numbers for the two kinds of solution are very different. The

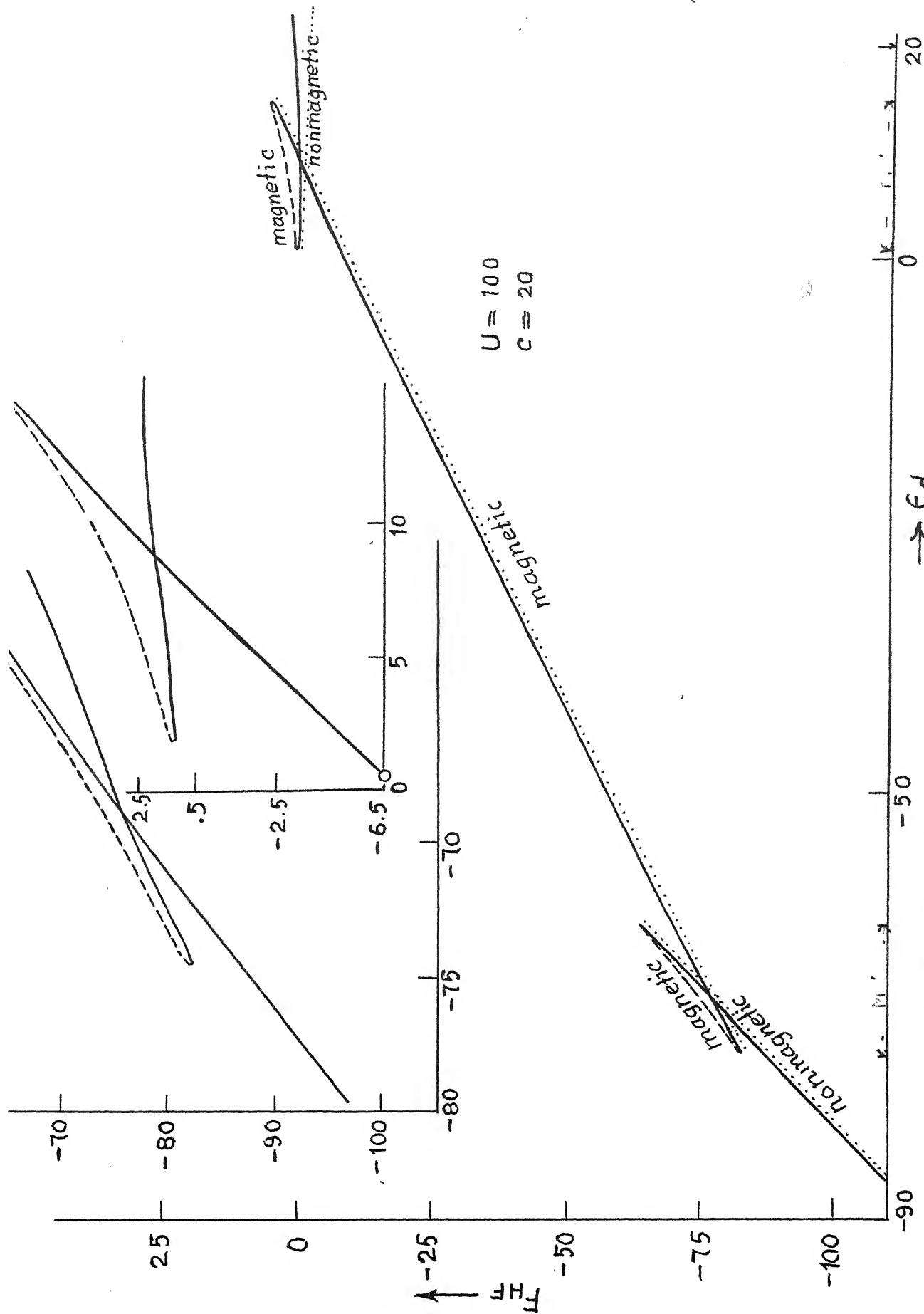


FIG. 4- F_{HF} (computer calculations) Vs. ϵ_d

Insertions show detail of mixed valence (MV) regimes.

extrema of nonmagnetic solutions have already been found. To find the limits of magnetic solutions, we must solve the equation obtained from (7)

$$1 + C \{ n'(x_+) + n'(x_-) \} - \{ (U - C)^2 - C^2 \} n'(x_+) n'(x_-) = 0 \quad \dots (14)$$

We are able to solve (14) analytically only approximately and for large C . To solve it, substitute for $n'(x_{\pm})$ in (14) and we obtain

$$1 - \frac{C \Delta / \pi}{x_+^2 + \Delta^2} - \frac{C \Delta / \pi}{x_-^2 + \Delta^2} - \frac{U(U-C) \Delta^2 / \pi^2}{(x_+^2 + \Delta^2)(x_-^2 + \Delta^2)} = 0 \quad \dots (15)$$

Suppose (x_+, x_-) is a 'good' magnetic solution, i.e., $n(x_+) \simeq 1$, $n(x_-) \simeq 0$. Then we can neglect the last term in (15) since $x_- \gg \Delta$ and $|x_+| \sim O(U)$. In any magnetic solution forming the boundary, one of the levels has to be within $\pm \sqrt{\Delta U / \pi - \Delta^2}$ (the limiting solution). Suppose x_+ is this level. Then the other level, x_- , in a good magnetic solution must be such that $|x_-| \gg x_+$. Then (15) reduces to

$$1 - \frac{C \Delta / \pi}{x_+^2 + \Delta^2} = 0 \quad \dots (16)$$

This has the solution.

$$x_+ = \pm \sqrt{\frac{C \Delta}{\pi} - \Delta^2} \simeq \pm \sqrt{\frac{C \Delta}{\pi}} \quad \text{for } C \gg \Delta \pi \quad \dots (17)$$

To find out x_- for above x_+ , we use the relation (9),

$$x_+ - x_- = -U \{ n(x_+) - n(x_-) \}.$$

For $x_+ = +\sqrt{\frac{\Delta C}{\pi}}$ this gives,

$$\sqrt{(\Delta C / \pi)} - x_- = -U \left(\sqrt{(\Delta / \pi C)} - 1 + \Delta / \pi x_- \right), \quad \dots (18)$$

after expanding the \tan^{-1} function involved in $n(x)$, to lowest order. The solution to (18) is,

$$x_- \simeq \sqrt{\frac{\Delta C}{\pi}} - U + U \sqrt{\frac{\Delta}{\pi C}} \quad \dots (19)$$

For x_+ given by (17) and (19), $n(x_+)$ and $n(x_-)$ are,

$$n(x_+) \simeq \sqrt{\frac{\Delta}{\pi C}} \quad ; \quad n(x_-) \simeq 1 - \Delta/[U - (U+C)\sqrt{(\Delta/\pi C)}]$$

and using the relation (3') we find ε_d :

$$\begin{aligned} \varepsilon_d &= x_- - (U - C) n(x_+) + C n(x_-) \\ &\simeq \sqrt{\frac{\Delta C}{\pi}} - U + U \sqrt{\frac{\Delta}{\pi C}} - (U - C) \sqrt{\frac{\Delta}{\pi C}} - O\left(\frac{\Delta C}{U}\right) \\ &\simeq -U + C + 2\sqrt{\frac{\Delta C}{\pi}} \quad \dots (20) \end{aligned}$$

Thus (20) gives the lower magnetic boundary. The upper magnetic boundary can be found likewise, taking $x_+ = -\sqrt{\frac{\Delta C}{\pi}}$ from (17). The equation for the line in phase space bounding the magnetic region then becomes,

$$\varepsilon_d - C + \frac{U}{2} \simeq \pm \left(\frac{U}{2} - 2\sqrt{\frac{\Delta C}{\pi}} \right) \text{ for } U, C \gg \pi\Delta \quad \dots (21)$$

Comparing this with the expression obtained for boundaries of nonmagnetic regimes, eqn. (13), we find that the width (in ε_d) of either MV regime is

$$W_{MV} \simeq C - 2\sqrt{\frac{\Delta C}{\pi}} - 2C\sqrt{\frac{\Delta}{\pi U}} \quad \dots (22)$$

Equations (21) and (13) determine the boundaries of magnetic

and nonmagnetic stable solutions, within the approximations mentioned.

Section 2d : THE PHASE TRANSITION LINE

As is clear from fig. 5, the HF energy curves cross each other within the MV regime. In the parameter space this represents a line across which the HF solution with lowest energy changes character, i.e., on one side it is the magnetic one and on the other it is the nonmagnetic one that has the lowest energy. Thus this is a line of phase transition. Around this line, the valence fluctuations are expected to be the most prominent. Fig. 6, which shows a plot of valence or $\langle n_d \rangle$ against ε_d , shows that at this line in parameter space, or the value of ε_d where the two solutions have equal energy, $\langle n_d \rangle$ for magnetic and nonmagnetic solutions are very different from each other. So this indicates a first order phase transition, unlike in the case of $C = 0$ Anderson model in which the solutions show continuous change in energy and $\langle n_d \rangle$ as the character changes and there is no MV regime.

To find the line of phase transition we make linear approximations to the HF free energies of magnetic and nonmagnetic solutions, given in appendix I.

$$F_{HF} = U n(x_+) n(x_-) - C \{n(x_+) + n(x_-)\}^2 + \varepsilon_d \{n(x_+) + n(x_-)\} + \\ + \frac{\pi \Delta}{2} \ln \left\{ \frac{x_+^2 + \Delta^2}{\Delta^2} \cdot \frac{x_-^2 + \Delta^2}{\Delta^2} \right\} + \text{const.}$$

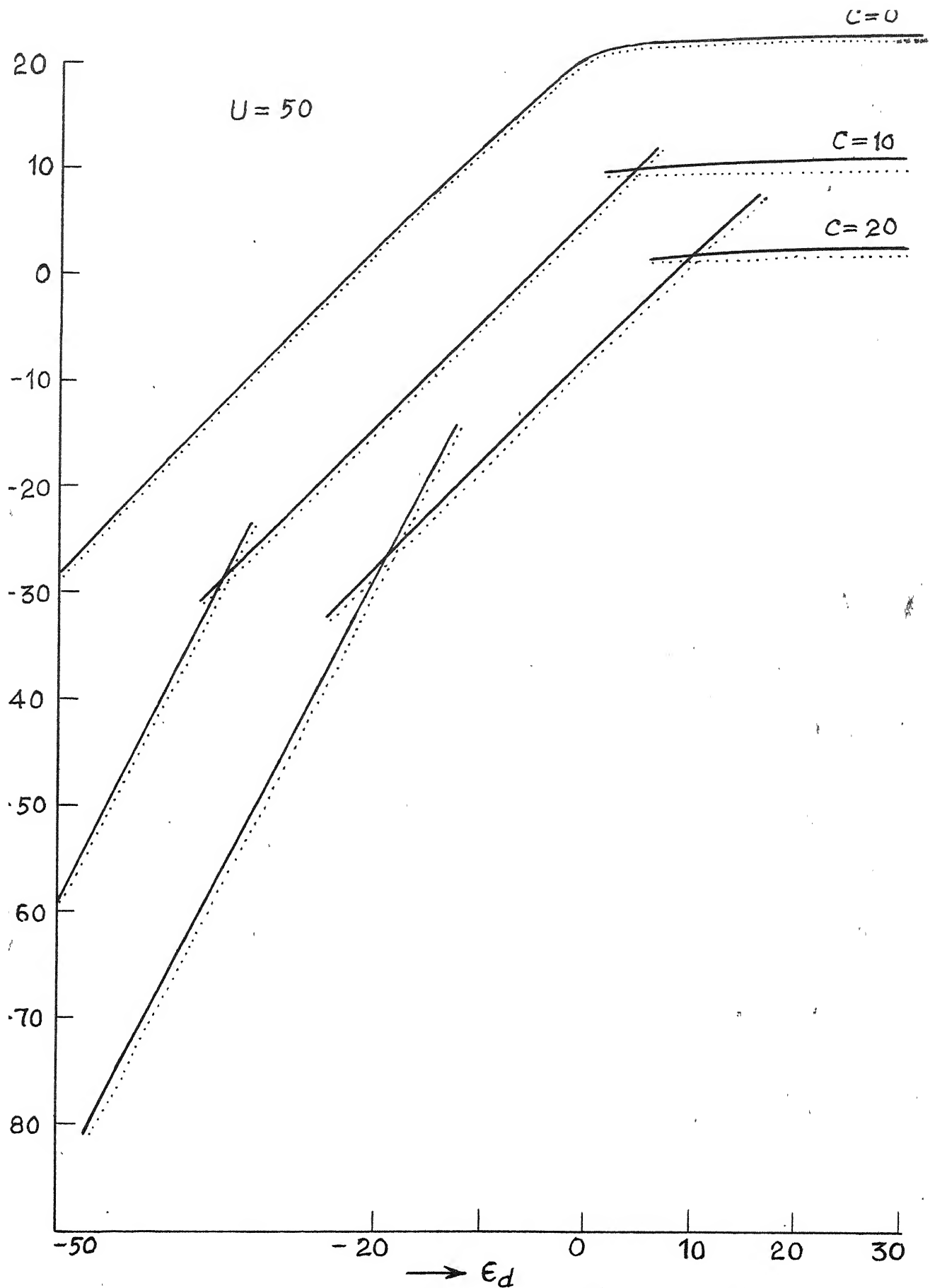


FIG. 5 Energies of stable HF solutions (arbitrary amount has been added to F_{HF} for each C)

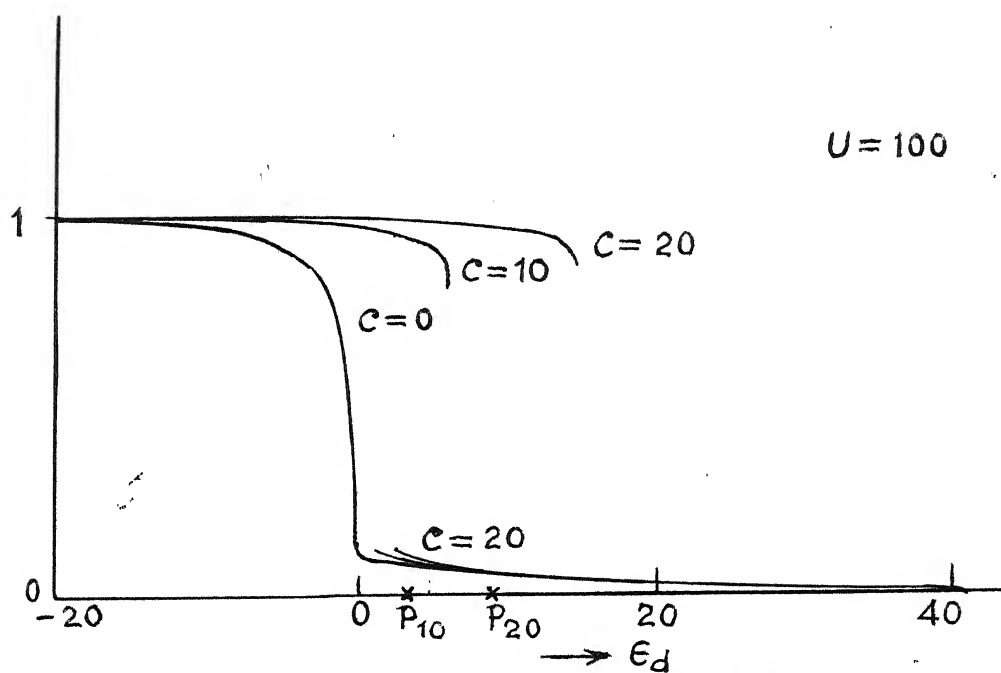
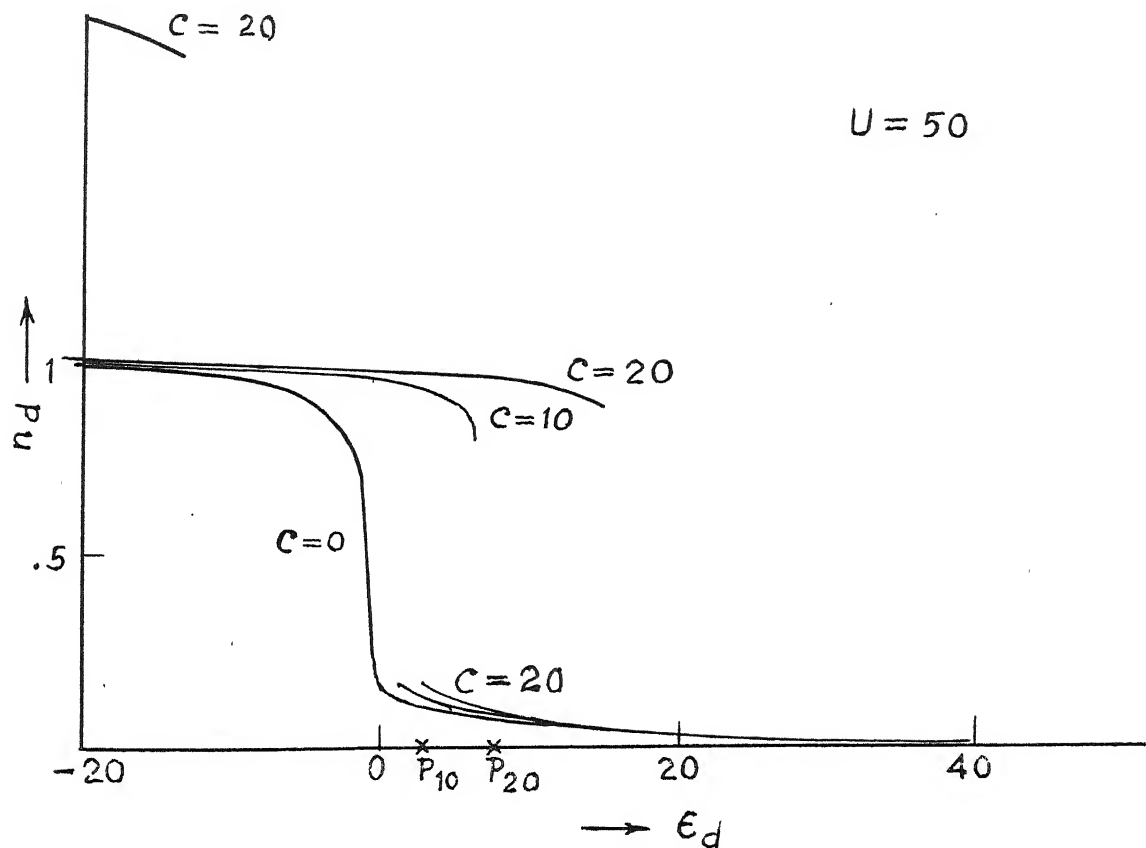


FIG. 6. d -occupation in HFA
Crosses denote the points where phase transitions occur.

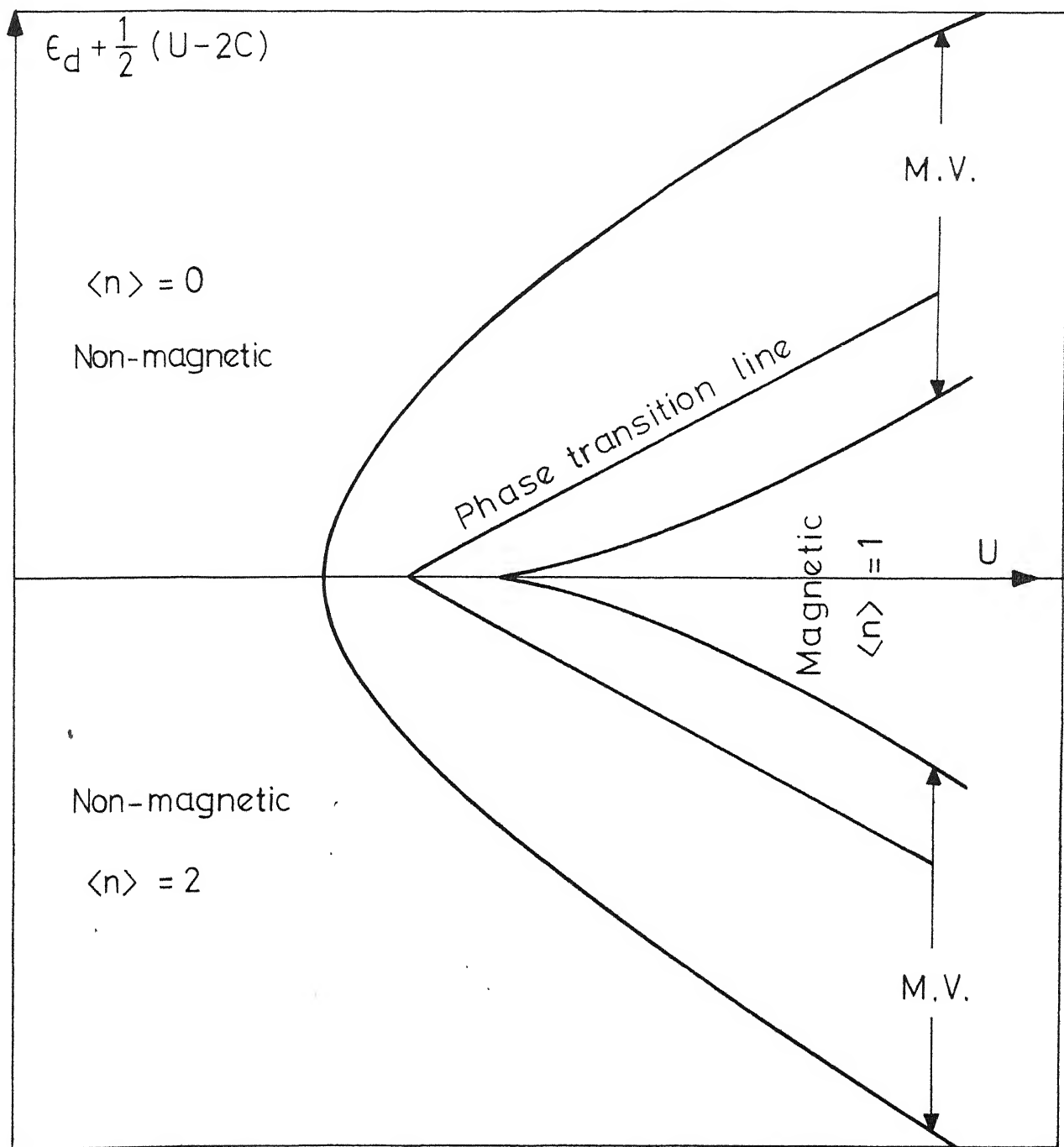


Fig. 7 M.V. Regions in parameter space.

In the lower nonmagnetic regime, $n(x_+) = n(x_-) \simeq 1$.

$$\therefore F_{HF} \simeq U - 4C + 2\varepsilon_d \quad \dots (23)$$

neglecting the logarithmic terms.

In the upper nonmagnetic regime, $n(x_+) = n(x_-) \simeq 0$.

$$\therefore F_{HF} \simeq 0 \quad \dots (24)$$

In the magnetic regime, $n(x_+) \simeq 1$, $n(x_-) \simeq 0$

$$\therefore F_{HF} \simeq \varepsilon_d - C \quad \dots (25)$$

The upper (lower) phase transition line is obtained by equating (25) with (24) ((23))

So the equations for these two phase transition lines are found to be

$$\varepsilon_d - C + \frac{U}{2} = \pm \left(\frac{U}{2} - \frac{C}{2} \right) \quad \dots (26)$$

Section 2e : SUMMARY OF RESULTS OBTAINED FROM HF ANALYSIS OF ANDERSON MODEL WITH $C \neq 0$

Figures 5 through 7 show results of numerical calculation compared with our analytical estimates. We find our estimates to be correct to within $O(\Delta)$. For the display of graphs, the parameters are so chosen because, as mentioned in Chapter I, U is expected to be of the order of $\sim 100 \Delta$. The parameter C is expected to be much smaller, an order of magnitude smaller than U . ε_d is a free parameter of the theory.

The salient features found are :

- (i) Magnetic solutions exist only when $U > \pi\Delta$
- (ii) MV regime exists only when $C > \pi\Delta$
- (iii) There are two MV regimes, around $0 \lesssim \epsilon_d \lesssim C - 2\sqrt{\frac{\Delta C}{\pi}}$
and $-U + C + 2\sqrt{\frac{\Delta C}{\pi}} \lesssim \epsilon_d \lesssim -U + 2C$ with width of
 $\sim C - 2\sqrt{\frac{\Delta C}{\pi}}$
- (iv) Energy differences between magnetic and nonmagnetic solutions in the MV regime are $\sim \Delta$
- (v) The phase transition within the MV regime is a first order phase transition.

Section 3 : TWO INTERACTING IMPURITIES, $C \neq 0$

Section 3a : THE MODEL AND THE SELF-CONSISTENT EQUATIONS IN HFA

In this section we consider the interaction between two impurities, each of which is described by the generalized ($C \neq 0$) Anderson Hamiltonian. The only extra term introduced is $\lambda^0 c_{d1\sigma}^+ c_{d2\sigma} + \text{h.c.}$, representing the transfer of d-electrons between sites 1 and 2 due to wave function overlap. Another source of coupling between the impurities is via the conduction electrons with which the d-states mix. The Hamiltonian can thus be written as

$$H = \sum_{k\sigma} \epsilon_k c_{k\sigma}^+ c_{k\sigma} + \sum_{i,\sigma} (\epsilon_d c_{di\sigma}^+ c_{di\sigma} + \frac{U}{2} n_{di\sigma} n_{di-\sigma}) + V \sum_{\sigma,i,k} (c_{di\sigma}^+ c_{k\sigma} e^{ik \cdot r_i} + \text{h.c.}) + (\lambda^0 c_{d1\sigma}^+ c_{d2\sigma} + \text{h.c.}) \dots (27)$$

where $i = 1, 2$.

We investigate this Hamiltonian in the HFA, i.e., we reduce it to an effective one body Hamiltonian,

$$H_{HF} = \sum_{k,\sigma} \epsilon_k c_{k\sigma}^+ c_{k\sigma} + \sum_{i,\sigma} (\epsilon_d c_{di\sigma}^+ c_{di\sigma} + U \langle n_{di-\sigma} \rangle n_{di\sigma}) \\ + V \sum_{\sigma,i,k} (c_{di\sigma}^+ c_{k\sigma} e^{ik \cdot r_i} + h.c.) + (\lambda^0 c_{d1\sigma}^+ c_{d2\sigma} + h.c.) - U \sum_i \langle n_{di\sigma} \rangle \langle n_{di-\sigma} \rangle \quad \dots (28)$$

Thus the Hamiltonian reduces to that of two resonant levels at sites 1 and 2 interacting with each other via the mixing term proportional to λ^0 . The quantities $\langle n_{di\sigma} \rangle$ in (28) are to be determined self consistently. The self consistent equations for these are obtained as,

$$n_{\sigma} = (N_+ + N_-)/2 \quad \dots (29)$$

$$d_{\sigma} = -(1/2V^{-\sigma})(N_+ - N_-) \{ (U-C)d^{\sigma} - Cd^{-\sigma} \} \quad \dots (30)$$

$$\text{where } N_{\pm} = [\pi/2 - \tan^{-1} \{ (\epsilon_d + (U-C)n^{-\sigma} - Cn^{\sigma} \pm V^{-\sigma})/\Delta \}]/\pi$$

$$\sigma = \pm; n^{\sigma} = (\langle n_{d1\sigma} \rangle + \langle n_{d2\sigma} \rangle)/2; d^{\sigma} = (\langle n_{d1\sigma} \rangle - \langle n_{d2\sigma} \rangle)/2$$

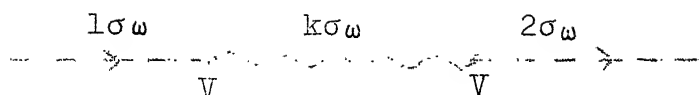
$$V^{\sigma} = V[\{ (U-C)d^{-\sigma} - Cd^{\sigma} \}^2 + \lambda^2] \quad \text{and } |\lambda^2| = |\lambda^0 + \lambda_{12}^c|^2 \quad \dots (31)$$

$$\dots (31)$$

λ_{12}^c is a transfer term arising out of the localized conduction electron mixing and is given by

$$\lambda_{12}^c = -V^2 \sum_k \frac{e^{ik \cdot (r_1 - r_2)}}{\epsilon_k} \quad \dots (32)$$

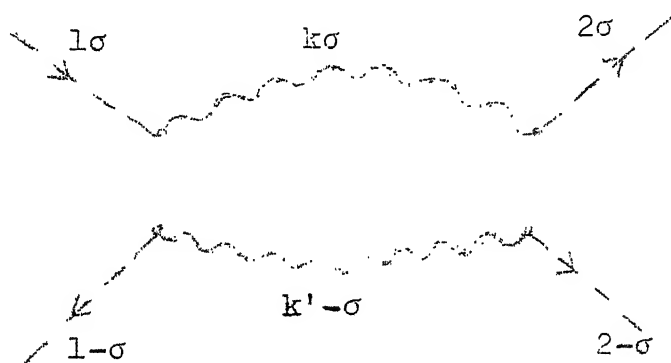
Diagrammatically, it originates from propagators of the type



where dotted lines denote d-electron propagators and curly ones, those for conduction electrons. From the above diagram it is clear that we should actually have

$$\lambda_{12}^c(\omega) = V^2 \sum_k \frac{e^{ik \cdot (r_1 - r_2)}}{\omega - \epsilon_k} \quad \dots (33)$$

In the next order, i.e., $O(\lambda_{12}^c)^2$, the form (33) produces RKKY exchange interaction via scatterings of the type



However, for the sake of simplicity, we omit ω -dependence of λ_{12}^c , use the form (32) and lump both kinds of hopping, direct and through conduction electrons, into λ and hereafter use only λ . The four equations (29) and (30) (two for each σ) have been obtained in a straightforward manner following Alexander and Anderson⁶ and are the same as those found by Varma¹¹. So we do not give the derivation here.

The general solution of these equations is quite difficult, and we consider only the case of weak coupling between the impurities, i.e., retain only the leading order terms in λ . We further assume that the solution to HF equations for the system is very close to one of the direct product HF states of the noninteracting impurities. The energy shift of these states due to interaction is calculated to leading order in λ (actually to order λ^2). For a single impurity, the HF states can be labelled $+$, $-$ or 0 , i.e., the two degenerate magnetic states and the nonmagnetic state. All three are locally stable in a certain range of ε_d (the mixed valence regime). For two noninteracting impurities therefore, the HF states are direct product states denoted by $|\sigma\sigma\rangle$, $|00\rangle$, $|\sigma-\sigma\rangle$, $|0\sigma\rangle$ and $|\sigma 0\rangle$ where the first letter within the ket denotes the spin state of impurity 1 and the second that of impurity 2. Each of the above product states, with the exception of the second, is doubly degenerate. The first represents magnetic HF states at both sites with spins aligned parallel; the second corresponds to nonmagnetic HF states at both sites, etc. In the absence of interaction between impurities, the states with parallel and antiparallel alignment are also degenerate. We now calculate the energy shift of these states due to interaction, to order λ^2 . This is in the spirit of the usual perturbation theory, i.e., the effects due to the change in HF states caused by λ , and the direct effect of λ are properly included. We take up the various configurations one by one.

Section 3b : TWO ANTIPARALLEL MOMENTS

In the antiparallel configuration, by symmetry, $n_1^\sigma = n_2^{-\sigma}$.

So we define quantities n and d ,

$$n^\sigma = \frac{n_1^\sigma + n_1^{-\sigma}}{2} = n = \frac{n_2^\sigma + n_2^{-\sigma}}{2} \quad \dots (34)$$

$$d = \frac{n_1^\sigma - n_1^{-\sigma}}{2} = d = \frac{-n_2^\sigma + n_2^{-\sigma}}{2} = -d^{-\sigma} \quad \dots (35)$$

Equations (29) and (30) then reduce to

$$n = \frac{1}{2} \left(\frac{\pi}{2} - \frac{1}{2} \tan^{-1} \frac{\epsilon_d + (U-2C)n+V}{\Delta} - \frac{1}{2} \tan^{-1} \frac{\epsilon_d + (U-2C)n-V}{\Delta} \right) \quad \dots (36)$$

$$V = \frac{U}{2\pi} \left(\tan^{-1} \frac{\epsilon_d + (U-2C)n+V}{\Delta} - \tan^{-1} \frac{\epsilon_d + (U-2C)n-V}{\Delta} \right) \quad \dots (37)$$

Equation (31) gives, when (35) is substituted,

$$V = \sqrt{(U^2 d^2 + \lambda^2)} \quad \dots (38)$$

Define ϵ_\pm as,

$$\epsilon_\pm = \epsilon_d + (U - 2C)n \pm V \quad \dots (39)$$

Then, from (36) and (37) we get

$$\epsilon_\pm = \epsilon_d + \frac{U-C}{\pi} \left(\frac{\pi}{2} - \tan^{-1} \frac{\epsilon_\mp}{\Delta} \right) - \frac{C}{\pi} \left(\frac{\pi}{2} - \tan^{-1} \frac{\epsilon_\pm}{\Delta} \right) \quad \dots (40)$$

Equations (40) are the same as HF self consistent equations for a single impurity, equations (2') and (3') of section 2(b). We must therefore have $\epsilon_\pm = x_\pm$, where (x_+, x_-) is the magnetic

solution to (2') and (3'); the nonmagnetic solution ($\varepsilon_+ = \varepsilon_-$) is not permissible since then we would have $d = 0$ or $n_1^\sigma = n_1^{-\sigma} = n_2^\sigma$ which is contrary to the supposition of antiparallel moments. Now we compare the energy of the two interacting ions written in terms of x_\pm , with that of two noninteracting ions written in terms of x_\pm . The energy of two noninteracting ions, from equation (A1.10) of appendix I is,

$$F^{ni} = -2 \int_{-\infty}^{x_+} dZ \cdot Z \cdot n'(Z) - 2 \int_{-\infty}^{x_-} dZ \cdot Z \cdot n'(Z) + x_+ n(x_+) + x_- n(x_-) - 2U n(x_+) n(x_-) + C \{n(x_+) + n(x_-)\}^2 \quad \dots (41)$$

The energy of two interacting ions in the HFA is given in Appendix III and becomes, after substitutions from equations (34), (35) and (40) for antiparallel spins,

$$F^{a.p} = \frac{2\Delta}{\pi} \left[\int_{-D}^0 \frac{\varepsilon d\varepsilon}{(\varepsilon - \varepsilon_+)^2 + \Delta^2} + \int \frac{\varepsilon d\varepsilon}{(\varepsilon - \varepsilon_-)^2 + \Delta^2} \right] - 2U(n^2 - d^2) + 4Cn^2 \quad \dots (42)$$

The first term in (42), that within square brackets, can be reduced to the same form as the sum of first four terms in (41); and since $x_\pm = \varepsilon_\pm$, these cancel when F^{ni} is subtracted from $F^{a.p}$. So we have the energy of interaction of two antiparallel impurities :-

$$E_{int} = F^{a.p} - F^{ni} = -2U(n^2 - d^2) + 4Cn + 2Un(x_+) n(x_-) - C \{n(x_+) + n(x_-)\}^2 \quad \dots (43)$$

In equation (43) the last two terms can be expressed in terms of x_\pm through the self consistent equations (2') and (3'), and

the first two terms in ε_{\pm} through equations (38) and (39).

Then most of the terms cancel and we get

$$E_{\text{int}}^{\sigma-\sigma} = - \frac{2\lambda^2}{U} \quad \dots(44)$$

The physical origin of this term is well known and corresponds to a coupling via an intermediate state where both \uparrow and \downarrow spins are at site 1 or at 2; the intermediate state thus has an extra energy U , and hence the energy denominator U in (44). This result is exact within the HFA and differs from Alexander and Anderson's result by terms $O(\frac{\lambda^2 \Delta}{\varepsilon_d})$ + higher order in Δ .

Section 3c : TWO PARALLEL MOMENTS

When the two ions are in parallel configuration, one has,

$$n_1^{\sigma} = n_2^{\sigma} = n^{\sigma} \quad , \quad d^{\sigma} = d^{-\sigma} = 0 \quad , \quad V^{\sigma} = V^{-\sigma} = \lambda \quad \dots (45)$$

The self consistent equations (29) and (30) then become

$$n^{\sigma} = 1/2 - (1/2\pi) \tan^{-1} [\{\varepsilon_d + (U-C)n^{-\sigma} - Cn^{\sigma} + \lambda\}/\Delta] \\ - (1/2\pi) \tan^{-1} [\{\varepsilon_d + (U-C)n^{-\sigma} - Cn^{\sigma} - \lambda\}/\Delta] \quad \dots (46)$$

where $\sigma = \pm$

If we put in (46)

$$\varepsilon_{\pm} = \varepsilon_d + (U - C) n^{\mp} - C n^{\pm} \quad \dots (47)$$

then equations (46) give us, in lowest order in λ ,

$$\varepsilon_{\pm} = \varepsilon_d + \frac{U-C}{\pi} \left\{ \frac{\pi}{2} - \tan^{-1} \frac{\varepsilon_{\pm}}{\Delta} + 2\lambda^2 \frac{\Delta \varepsilon_{\pm}}{(\varepsilon_{\pm}^2 + \Delta^2)^2} \right\}$$

$$- \frac{C}{\pi} \left\{ \frac{\pi}{2} - \tan^{-1} \frac{\varepsilon_+}{\Delta} + 2\lambda^2 \frac{\Delta \varepsilon_+}{(\varepsilon_+^2 + \Delta^2)^2} \right\} \dots (48)$$

The HF energy given by e.g. (AIII.2) of appendix III can be written in terms of ε_{\pm} as,

$$F^{\text{parll}} = -2 \{ (\varepsilon_+ - \varepsilon_d)(\varepsilon_- - \varepsilon_d) \} / (U - 2C) - C(\varepsilon_+ - \varepsilon_-)^2 / \{ U(U - 2C) \} \\ - \frac{\lambda^2 \Delta}{\pi} \sum_{\sigma} (\varepsilon_{\sigma}^2 + \Delta^2)^{-1} + \frac{2\Delta}{\pi} \sum_{\sigma} \int_{-D}^0 \frac{\varepsilon d\varepsilon}{(\varepsilon - \varepsilon_{\sigma})^2 + \Delta^2}, \quad \sigma = \pm \dots (49)$$

Comparing this with $F^{\text{n.i}}$ we find the interaction energy for two parallel moments as,

$$E_{\text{int}}^{\sigma\sigma} \equiv F^{\text{parll}} - F^{\text{n.i}} = -2[\delta\varepsilon_+(\varepsilon_- - \varepsilon_d) + \delta\varepsilon_-(\varepsilon_+ - \varepsilon_d)] / (U - 2C) \\ - \frac{2C(\varepsilon_+ - \varepsilon_-)}{U(U - 2C)} (\delta\varepsilon_+ - \delta\varepsilon_-) - \frac{\lambda^2 \Delta}{\pi} \sum_{\sigma} (\varepsilon_{\sigma}^2 + \Delta^2)^{-1} \\ - \frac{2\Delta}{\pi} \sum_{\sigma} \delta\varepsilon_{\sigma} \int \varepsilon d\varepsilon \frac{d}{d\varepsilon} \{ (\varepsilon - \varepsilon_{\sigma})^2 + \Delta^2 \}^{-1}, \\ \sigma = \pm \dots (50)$$

where we have put $\delta\varepsilon_{\pm} = \varepsilon_{\pm} - x_{\pm}$, x_{\pm} being magnetic solutions for a noninteracting impurity in HFA. From (48) we can see that $\varepsilon_{\pm} - x_{\pm} \sim O(\lambda^2)$. Therefore, in order to evaluate (50) to lowest order in λ , we replace ε_{\pm} in (50) by x_{\pm} , and obtain,

$$E_{\text{int}} = -2 \sum_{\sigma} \delta\varepsilon_{\sigma} (x_{\sigma} - \varepsilon_d) / (U - 2C) - \frac{2C(x_+ - x_-)(\delta\varepsilon_+ - \delta\varepsilon_-)}{U(U - 2C)}$$

$$-\frac{\lambda^2 \Delta}{\pi} \sum_{\sigma} (x_{\sigma}^2 + \Delta^2)^{-1} = \frac{2}{\pi} \sum_{\sigma} \delta \epsilon_{\sigma} \int \epsilon d\epsilon \frac{d}{d\epsilon} \{(\epsilon - x_{\sigma})^2 + \Delta^2\}^{-1},$$

$$\sigma = \pm \dots (51)$$

The sum of last two terms in (51) is equal to,

$$2 \delta \epsilon_{+} \cdot n(x_{+}) + 2 \delta \epsilon_{-} \cdot n(x_{-})$$

Writing this in terms of x_{\pm} using noninteracting ion HF self consistency conditions, and substituting in (51) we find that the only surviving terms give

$$E_{int}^{\sigma\sigma} = -\lambda^2 \frac{\Delta}{\pi} \left(\frac{1}{x_{+}^2 + \Delta^2} + \frac{1}{x_{-}^2 + \Delta^2} \right) \equiv -\lambda^2 (\rho_{+} + \rho_{-}) \dots (52)$$

where ρ_{\pm} are density of d-states at Fermi level when the levels are x_{\pm} .

The expression (52) has the same form as that found by Alexander and Andersen and shows that the exchange between two parallel spins proceeds necessarily through the d-conduction mixing.

When both ions are in the nonmagnetic HF state the shift is found exactly in the same way to be

$$E_{int} = -2 \lambda^2 \rho_0 \dots (53)$$

ρ_0 being the density of states at Fermi level for the single ion nonmagnetic HF state.

We now proceed to find the interaction energy when the two ions are in different valence states.

Section 3d : TWO IONS IN DIFFERENT VALENCE STATES

The general expression for HF energy of two interacting ions, found in appendix III is,

$$\begin{aligned}
 E^{(2)} = & -U(n_1^\uparrow n_1^\uparrow + n_2^\uparrow n_2^\uparrow) + \frac{C}{2} (n_1^\uparrow + n_1^\downarrow) + (n_2^\uparrow + n_2^\downarrow)^2 + \\
 & + \frac{\Delta}{\pi} \sum_{\sigma, \alpha} \int \frac{\varepsilon \, d\varepsilon}{(\varepsilon - \varepsilon_d - (U-C)n^\sigma + Cn^{-\sigma} - \alpha V^\sigma)^2 + \Delta^2} \\
 & \alpha = 1, 2
 \end{aligned} \quad \dots (54)$$

Let us first examine V^σ . By definition,

$$V = \sqrt{[(U-C)d^\sigma - Cd^{-\sigma}]^2 + \lambda^2} \quad \dots (55)$$

By definition of d^σ ,

$$(U-C)d^\sigma - Cd^{-\sigma} = (U-C)(n_1^\sigma - n_2^\sigma) - C(n_1^{-\sigma} - n_2^{-\sigma}) \quad \dots (56)$$

Suppose ion 1 is in the nonmagnetic lower valence state and 2 is in one of the magnetic states. Then (56) gives, if HF levels remained unshifted from their noninteracting values,

$$(U-C)d^\sigma - Cd^{-\sigma} = (U-C)\{n(x_0) - n(x_+)\} - C\{n(x_0) - n(x_-)\}$$

where x_0 is the nonmagnetic HF level and x_\pm are the magnetic levels in the VF regime for a single noninteracting ion. With the help of self consistent equations for a single ion, the above quantity can be written as

$$(U-2C)n(x_0) - \{(U-C)n(x_+) - Cn(x_-)\} = x_0 - x_- \quad \dots (57)$$

In the HF analysis of one impurity we showed that when

$C \gg \pi \Delta$, the stable magnetic solutions are in 'good' magnetic regime, i.e., in the VF regime around $\varepsilon_d=0$; $x_{\pm} \approx \varepsilon_d - C$ and $x_{\pm} \approx \varepsilon_d - C + U$. Also, in the VF regime, $x_0 \approx \varepsilon_d$. So the non-magnetic level x_0 does not come closer than C to either of the magnetic levels. So, for sufficiently large C and sufficiently small λ , we can expand (55) in powers of λ ,

$$V^{\sigma} = (U-C) d^{\sigma} - C d^{-\sigma} + \frac{\lambda^2}{2\{(U-C)d^{\sigma} - C d^{-\sigma}\}} + O(\lambda^4) \quad \dots (58)$$

Substituting (58) into (54) we get

$$F^{(2)} = -U(n_1^{\uparrow} n_1^{\downarrow} + n_2^{\uparrow} n_2^{\downarrow}) + C[(n_1^{\uparrow} + n_1^{\downarrow})^2 + (n_2^{\uparrow} + n_2^{\downarrow})^2]/2 \\ + \sum_{\sigma, i} \frac{\Delta}{\pi} \int_{-D}^0 \frac{\varepsilon d\varepsilon}{[\varepsilon - \varepsilon_d - (U-C)n_i^{\sigma} - Cn_i^{-\sigma} + (i - \frac{3}{2})\lambda^2/\{(U-C)d^{\sigma} - C d^{-\sigma}\}]^2 + \Delta^2} \\ i = 1, 2 \quad \dots (59)$$

The energy expression for two noninteracting impurities is the same as (59), except for the absence of the terms proportional to λ in the denominators of integrands within the square brackets, and that the n_i 's have their noninteracting HF values. So, we can straightaway write the interaction energy as,

$$E_{\text{int}} = F^{(2)} - F^{n.i} = -U \sum_{i, \sigma} (\delta n_i^{\sigma} \cdot n_i^{\sigma}) + C \sum_i \left(\sum_{\sigma} \delta n_i^{\sigma} \right) \left(\sum_{\sigma'} n_i^{\sigma'} \right) \\ + \sum_{\sigma, i} \left[\{ -(U-C) \delta n_i^{\sigma} + C \delta n_i^{-\sigma} - \frac{(i-3/2)\lambda^2}{(U-C)d^{\sigma} - C d^{-\sigma}} \} \cdot \right. \\ \left. \cdot \int_{-D}^0 \varepsilon d\varepsilon \frac{d}{d\varepsilon} \{ (\varepsilon - \varepsilon_i^{-\sigma})^2 + \Delta^2 \}^{-1} \right] \\ i = 1, 2 \quad \dots (60)$$

To find the lowest order correction to F , we substitute in (60) the noninteracting impurity values for ε_i^σ and n_i^σ and obtain,

$$E_{\text{int}} = \frac{\lambda^2 d^\dagger}{(U-C)d^\dagger - C d^\dagger} + \frac{\lambda^2 d^\dagger}{(U-C)d^\dagger - C d^\dagger} + O(\delta n \cdot \delta n) + O(\lambda^2 \cdot \delta d) \quad \dots (61)$$

The last two terms in (61) can be shown to be weaker than λ^2 .

If we take $n_1^\sigma = n_1^{-\sigma} = n_2(x_0)$ and $n^+ = n(x_+)$, $n_2^+ = n(x_-)$,

then

$$d^\dagger = \frac{n(x_0) - n(x_+)}{2} \quad \text{and} \quad d^\dagger = \frac{n(x_0) - n(x_-)}{2}$$

Using these and the single ion self consistency conditions, we get

$$E_{\text{int}}^{0\sigma} \sim \lambda^2 \left[n(x_0) \left(\frac{1}{x_0 - x_-} + \frac{1}{x_0 - x_+} \right) - \frac{n(x_-)}{x_0 - x_-} - \frac{n(x_+)}{x_0 - x_+} \right] \quad \dots (62)$$

In the MV regime around $\varepsilon_d = 0$, as we have already shown, $x_+ \sim \varepsilon_d - C + U$ and $n(x_+) \sim \Delta / (\varepsilon_d - C + U)$. Therefore we omit terms involving x_+ in (62) and have

$$E_{\text{int}}^{0\sigma} \sim \lambda^2 \frac{n(x_+) - n(x_-)}{x_0 - x_-} \quad \dots (63)$$

If $x_0 > x_-$, $n(x_0) < n(x_-)$.

Thus the interaction energy (63) is always negative, and is roughly $\sim -\frac{\lambda^2}{C}$.

Section 3e : A BRIEF DISCUSSION OF RESULTS OBTAINED FOR A PAIR OF INTERACTING IMPURITIES IN HFA

The results obtained in the above subsections are

$$E_{int}^{\sigma\sigma} = -\lambda^2 (\rho_+ + \rho_-)$$

$$E_{int}^{00} = -2\lambda^2 \rho_0$$

$$E_{int}^{\sigma-\sigma} = -2\lambda^2/U$$

$$E_{int}^{0\sigma} \approx \lambda^2 \frac{n(x_0) - n(x_0)}{x_0 - x_0} \approx -\frac{\lambda^2}{C}$$

upto lowest order in λ .

The first two of these, the interaction energy for parallel configurations, are dependent on itinerancy (the parameter Δ) and becomes stronger as the relevant HF level moves closer to the Fermi surface or ρ increases. As pointed out by Alexander and Anderson, this is a Zener type of exchange. $E_{int}^{\sigma-\sigma}$ does not depend on Δ . However, in perturbation theory one expects to have further terms as in $E_{int}^{\sigma\sigma}$ since all the mechanisms for parallel spins are applicable here. However, as we have mentioned in section 3b, our result is exact within the HFA and differs from Alexander and Anderson's in nonleading terms. For $U = \infty$, the interaction energy for antiparallel configurations vanishes and the parallel configuration is favoured throughout the range of ε_d . But for finite U , antiparallel configuration is favoured when

$$\frac{\lambda^2}{U} > \lambda^2 (\rho_+ + \rho_-)$$

or, roughly, when

$$\frac{\Delta/\pi}{(\varepsilon_d - C)^2 + \Delta^2} < 1/U$$

in the parameter range of our interest,

$$\text{or when } |\varepsilon - C| \lesssim \sqrt{\frac{\Delta U}{\pi}}$$

In the mixed valence regime of our interest, $-C \lesssim \varepsilon_d - C \lesssim -2\sqrt{\frac{\Delta C}{\pi}}$, as found in section 2. So, if $C < \sqrt{\frac{\Delta U}{\pi}}$, the antiparallel configuration is favoured throughout the MV regime. If $C > \sqrt{\frac{\Delta U}{\pi}}$, the antiparallel configuration is favoured when $C - \sqrt{(\Delta U/\pi)} \lesssim \varepsilon_d \lesssim -2\sqrt{\frac{\Delta C}{\pi}}$ (upper portion of MV regime), and parallel configuration when $\varepsilon_d < C - \sqrt{(\Delta U/\pi)}$

When $\varepsilon_d \lesssim C/2$, $\rho_0 \approx \rho_{\pm}$. Then the state $|00\rangle$ has energy lower than either parallel or antiparallel state.

The energy shifts obtained above for specified individual impurity HF configuration can be viewed as diagonal terms of an interaction Hamiltonian, e.g., $E_{\text{int}}^{\sigma\sigma} = \langle \sigma\sigma | H_{\text{int}} | \sigma\sigma \rangle$.

There is an important off diagonal term left out in the above discussion. This is the coupling between the noninteracting HF states $|0\sigma\rangle$ and $|\sigma 0\rangle$. In the perturbation theory, the λ dependent term in the Hamiltonian removes the degeneracy between these two states and introduces an energy difference of 2λ between the symmetric and antisymmetric combination states. However, in the HFA this effect is not present and we must put $\langle 0\sigma | H_{\text{int}} | \sigma 0 \rangle \sim \lambda$ as the most important

off-diagonal term, causing transitions between the two HF states. In the next chapter we make use of such effective interaction Hamiltonian matrix elements to discuss a lattice of such ions.

CHAPTER III

THE MIXED VALENCE LATTICE

We have seen in Chapter II that for a $C \neq 0$ Anderson model impurity, there are three locally stable states for a certain range of ϵ_d values (mixed valence regions; actually there are two mixed valence regions, one around $\epsilon_d \approx -U$ and another around $\epsilon_d \approx 0$. We are interested in the latter). Two of these, corresponding to magnetic solutions ($\langle n_{d\sigma} \rangle \approx 1$, $\langle n_{d-\sigma} \rangle \approx 0$) are degenerate, while the third low valence nonmagnetic state ($\langle n_{d\sigma} \rangle = \langle n_{d-\sigma} \rangle \approx 0$) has an energy which may be lower or higher than that of the former two depending on ϵ_d . Further, the energy shifts due to interaction between two such 'mixed valence' impurities have been calculated. These results are most simply expressed in a pseudospin ($S = 1$) model. In this form, generalization to a mixed valence lattice is immediate, and one can discuss the thermodynamic properties of a mixed valence lattice, especially the question of possible phases of the system. This is done below.

Section 1 : THE MODEL

Section 1a : SINGLE IMPURITY

Consider first a single impurity at site i . The three locally stable HF states are denoted $|+\rangle$, $|+\rangle$, $|0\rangle$ and have energies E_σ , E_σ and E_0 respectively. E_σ and E_0

can be calculated in terms of the model parameters ϵ_d , Δ , U , C (see Chapter II, sec. 2). This manifold is represented by the states of an $S = 1$ system, with a single ion anisotropy term, i.e.,

$$H = (E_G - E_0) S_z^2 + E_0 \quad \dots (1)$$

The states $S_z^1 = \pm 1$ are degenerate and represent the magnetic HF states. $S_z^1 = 0$ represents the nonmagnetic state.

A Hamiltonian of the form (1) with additional off diagonal terms of the type λS_z^1 has been used by de Chatel¹⁴ as a model for a mixed valence impurity. Such a term leads to the magnetic susceptibility being always finite at $T = 0$. However, it is well known that the effect of terms beyond the HFA is to cause transitions between the HF eigenstates with long time transients (Anderson and Yuval⁹, Hamann⁸, this thesis, Chapter IV). As a consequence there is Kondo quenching of the moment at low temperatures. Their effect cannot be simulated by a simple off diagonal term such as the above.

Section 1b : TWO IMPURITIES

Consider the following model Hamiltonian for two interacting $S = 1$ systems at sites i and j ,

$$H = J_{ij} S_z^i S_z^j + B_{ij} S_z^{i2} S_z^{j2} + A(S_z^{i2} + S_z^{j2}) + M \quad \dots (2)$$

This Hamiltonian is diagonal in the S_z^i , S_z^j space, and the eigenstates are in one to one correspondence with the two impurity HF eigenstates discussed in II.3. Further, we see

that the interaction energy shifts obtained there are reproduced exactly by (2), if

$$J_{ij} = \frac{1}{2} (E_{int}^{\sigma\sigma} - E_{int}^{\sigma-\sigma}) \quad \dots (3a)$$

$$B_{ij} = \frac{1}{2} (E_{int}^{\sigma\sigma} + E_{int}^{\sigma-\sigma}) - 2E_{int}^{\sigma 0} - E_{int}^{00} \quad \dots (3b)$$

$$A = E_{\sigma} - E_0 + E_{int}^{\sigma 0} - E_{int}^{00} \quad \dots (3c)$$

$$M = 2E_0 + E_{int}^{00} \quad \dots (3d)$$

The interaction λ , being the direct overlap between f orbitals on different sites plus hopping via conduction electrons, is very small. We therefore consider only nearest neighbour interactions.

As we have pointed out in Chapter II, Sec. 3, the interaction λ has off diagonal matrix elements in the HF basis, between states $|0\sigma\rangle$ and $|\sigma 0\rangle$. This is easily included in the pseudospin model through the term

$$H_{ij}^X = \lambda S_i^X S_j^X \quad \dots (4)$$

Since the axis of spin quantization is arbitrary and the system is actually rotationally invariant (though not in HFA), there ought to be a transverse spin coupling in addition to the longitudinal or Ising coupling between the spins. This coupling flips the HF state at site i from $|+\rangle$ to $|-\rangle$ (say) and simultaneously the HF state at site j from $|+\rangle$ to $|+\rangle$. Its magnitude is easily obtained from the condition of

rotational invariance. Combining all these terms, the results obtained in the HFA for two interacting MV impurities can be described by the model Hamiltonian,

$$H = J_{ij} S_z^i S_z^j + B_{ij} S_z^{i2} S_z^{j2} + A(S_z^{i2} + S_z^{j2}) + \lambda S_x^i S_x^j + M \dots (5)$$

where the coupling parameters are expressible in terms of the basic Anderson model parameters ε_d , Δ , U , C , λ .

An objection can be made that by introducing (4) we completely include the effect of λ , and hence other terms are superfluous. This is not so. The antiferromagnetic coupling arises from intermediate states of the type $n_{i\uparrow} = n_{j\uparrow} = 1$, not included in the three level manifold being used here. The ferromagnetic and other couplings (viz., $\delta E_{\sigma\sigma}$, $\delta E_{0\sigma}$, δE_{00}) are results of itinerancy or mixing with conduction electron states. That also is a feature not included in the three-level scheme.

The Hamiltonian (5) does not have two important features and because of this it is a poor model for explicit discussion of valence transitions in the concentrated (lattice) system. These missing features are the following :

(i) In mixed valence systems the transition to a low valence state takes place with promotion of the extra electron to the conduction band. For a mixed valence impurity this leads to nothing new. However, in a concentrated system, the fermi energy becomes dependent on the valence fraction. In our

model, where the fermi energy is always kept zero, such an electron count effect¹⁵ can be phenomenologically taken into account by making ϵ_d a function of $\langle S_z^{i2} \rangle$ or the valence fraction. It is generally believed to have the effect of pinning the d level to the fermi level.¹⁶ The functional form is to be computed from knowledge of density of conduction band states etc.

(ii) As pointed out by Chui and Anderson¹⁷ ions of different radii in an elastic medium (the solid) cause long range strain effects due to size mismatch. Presumably, this can be partially taken into account by an additional long range coupling term $B_{ij}^{l.r.} S_z^{i2} S_z^{j2}$.

Because of these shortcomings, we do not use the above Hamiltonian to explicitly discuss valence transitions as are observed in S_m chalcogenides, Ce , $Ca_x Th_{1-x}$ etc. However, the model is quite suitable for a discussion of the phases possible in a mixed valence lattice. We note, though, that an important phenomenon, namely the Kondo effect, is missing in this HFA modelling of the system. We discuss the consequences of this omission later, and in Chapter V suggest a scheme which includes the Kondo effect as well.

A Hamiltonian of the form

$$H = \delta S_1^{x2} + \omega S_1^x + J S_1 \cdot S_j$$

has been used by Ghatak¹⁸ to discuss the valence transition.

This has a single ion transverse spin term ωS_1^x whose microscopic origin is unclear. It does not have the longitudinal and

transverse near neighbour spin - spin couplings which we have found in Chapter II. Further, the two features mentioned above are also missing. It cannot therefore be a good model for discussion of valence transition or for various possible phases.

Section 2 : POSSIBLE PHASES OF THE SYSTEM

Consider the Hamiltonian,

$$H = A \sum_i S_z^{i2} + M + \sum_{i,j} J_{ij} S_z^i S_z^j + \sum_{i,j} B_{ij} S_z^{i2} S_z^{j2} + \lambda \sum_{ij} S_x^i S_x^j \dots (6)$$

This represents an $S = 1$ lattice system with

- (i) single ion anisotropy
- (ii) anisotropic exchange
- (iii) a kind of quadrupolar interaction.

Such $S = 1$ models (generally with more symmetric couplings) have been extensively discussed in the literature^{19,20}.

The possible phases depending on system parameters, are

- (i) Ferromagnetic, viz., $\langle S_z^i \rangle \neq 0$
- (ii) Antiferromagnetic, viz., $\langle S_z^{\text{sublattice}} \rangle \neq 0$
- (iii) and (iv) Similar phases, with alignments in the xy plane, e.g., $\langle S_x^i \rangle \neq 0$
- (v) Singlet, i.e., a phase with $\langle S_\alpha^i \rangle = 0$,
 $\langle S_\alpha^{\text{sublattice}} \rangle = 0$, $\alpha = x, y, z$.

and $\langle S_z^1 \rangle$ (we have assumed here that J_{ij} is negative, i.e., the coupling is ferromagnetic). The Curie temperature is obtained by requiring that self consistent solutions with $\langle S_z^1 \rangle \neq 0$ exist. In this way one obtains the self consistent equations as,

$$\langle S_z \rangle = \frac{-2e^{-\beta(A+B)\langle S_z^2 \rangle} \cosh(\beta J \langle S_z \rangle)}{1 + 2e^{-\beta(A+B)\langle S_z^2 \rangle} \cosh(\beta J \langle S_z \rangle)} \sinh(\beta J \langle S_z \rangle) \quad \dots (8)$$

$$S_z^2 = \frac{2e^{-\beta(A+B)\langle S_z^2 \rangle} \cosh(\beta J \langle S_z \rangle)}{1 + 2e^{-\beta(A+B)\langle S_z^2 \rangle} \cosh(\beta J \langle S_z \rangle)} \quad \dots (9)$$

where $B = \sum_{j(n.n.)} B_{ij}$ and $J = \sum_{j(n.n.)} J_{ij}$, and we have omitted the site index.

A simple special case arises when $B_{ij} = 0$. In that case, one finds that the self consistency condition for $\langle S_z \rangle$, equation (8) gives the condition for $\langle S_z \rangle \neq 0$ to be just possible as,

$$\frac{-2\beta J e^{-\beta A}}{1 + 2e^{-\beta A}} = 1 \quad \dots (10)$$

This equation determines T_C , which can also be seen from the usual susceptibility expression in MFA -

$$\chi^{-1}(T) = \chi_0^{-1}(T) + J \quad \dots (11)$$

where $\chi_0^{-1}(T)$ is the susceptibility of a single noninteracting ion and is in this case

$$\chi_0 = \frac{2\beta e^{-\beta A}}{1 + 2e^{-\beta A}} \quad \dots (12)$$

So the condition for the susceptibility to blow up is the same as eq. (10) above. From this equation, it is clear that for $A < 0$

$$k_B T_c \simeq |J| \quad \dots (13)$$

the well known Curie-Weiss result. For $A > 0$, the transition temperature decreases exponentially, satisfying the relation,

$$\frac{k_B T_c}{2} \simeq |J| e^{-A/(k_B T_c)} \quad \dots (14)$$

It is well known, however, that for $A > A_c$, the transition is first order, the point $A_c, T_c(A_c)$ being the well known tricritical point. Further, for $A > .463 |J|$ the ground state is nonmagnetic (a singlet or $\langle S_z \rangle = 0$ state), since in that case no real solution exists to the equation (10) which determines T_c .

In our calculations, the results of which are shown in fig. 8, we find that generally $A \sim \Delta$ and $|J| \sim 10^{-3} \Delta$. (for the chosen parameters U, C and λ) unless we are very close to the HF phase transition line where $A \sim 0$. Thus, the results which are crude solutions to equations (13) and (14) and basically show that as ϵ_d increases within the MV regime, starting from its lower reach, T_c slowly increases to a maximum around the HF phase transition, and then falls off exponentially over a range $\sim 10^{-3} \Delta$. The assumption of $B = 0$ is not unrealistic since we find $B \sim 10^{-3} \Delta \ll \Delta$ over most of the range. In any case, it can only shift the peak in T_c and will not change its character in any significant way.

$$U = \frac{1000}{\pi}$$

$$C = 10$$

$$\lambda = 0.25$$

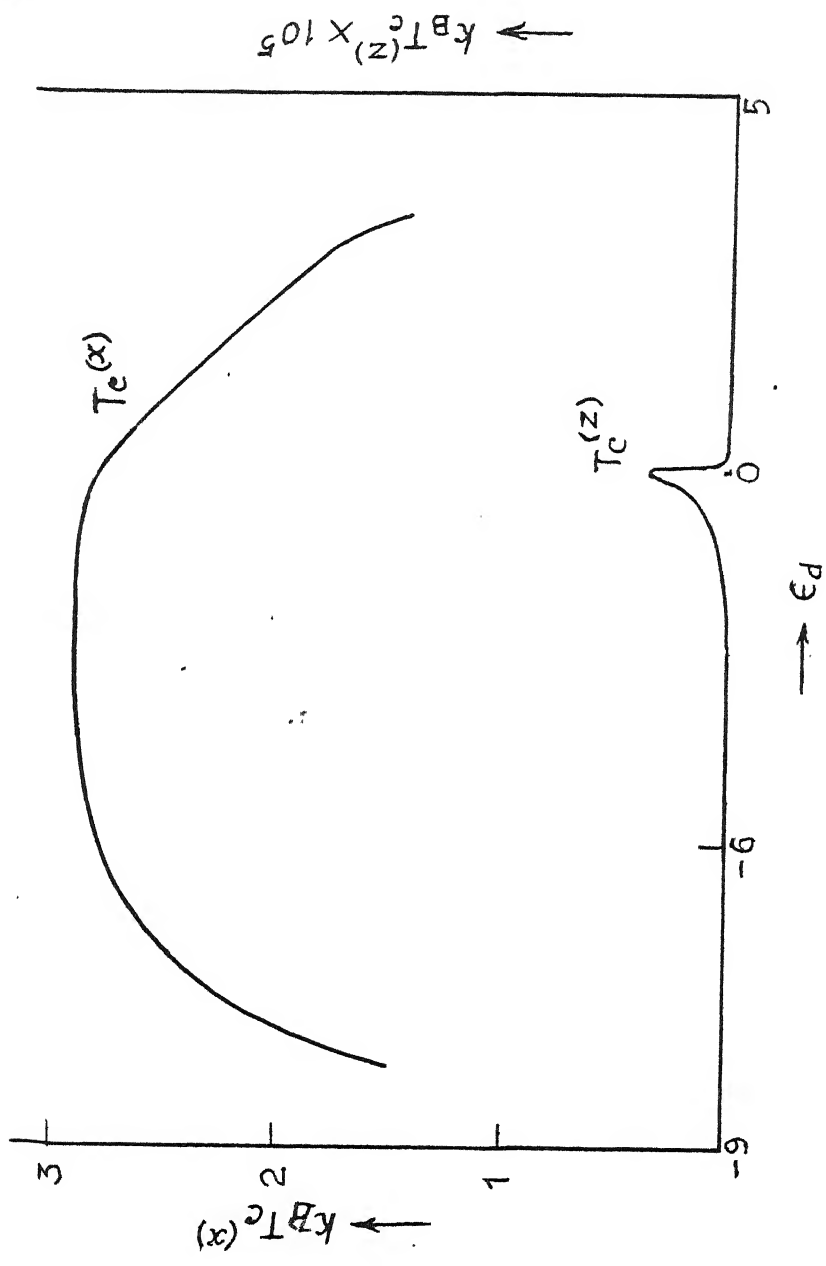


FIG. 8 - The x and z ordering temperatures within the MV regime.

Section 2b : THE VALENCE FLUCTUATION PHASE, $\langle S_x \rangle \neq 0$

To investigate the $\langle S_x \rangle$ ordering in MFT, we consider the mean field Hamiltonian,

$$H = \sum_i A' S_z^2 + \lambda_x \sum_i S_x^2 \quad \dots (15)$$

where, $A' = A + B \langle S_z^2 \rangle$

and $\lambda_x = \sum_j \lambda_{ij} \langle S_x \rangle$.

Thus, we are looking for a kind of ordering where $\langle S_z \rangle = 0$, $\langle S_x \rangle \neq 0$. Within the mean field theory we have the usual expression for susceptibility,

$$\chi_x^{-1} = \chi_x^{o-1} + \lambda_x \quad \dots (16)$$

where χ_x^o is the single(noninteracting) ion x susceptibility and is found to be

$$\chi_x^o = \frac{4}{A'} \frac{1 - e^{-\beta A'}}{1 + 2e^{-\beta A'}} \quad \dots (17)$$

$$\therefore \chi_x^{o-1} = \frac{A'}{8} [1 + 3 \coth \frac{\beta A'}{2}] \quad \dots (18)$$

So the solution to the equation $\chi_x^{-1} = 0$ is

$$k_B T_c = \frac{A'}{2 \tan^{-1} \left(\frac{3}{8\lambda_x/A' - 1} \right)} \quad \dots (19)$$

From the above expression it is clear that when $2\lambda_x < A' (A' > 0)$ the transition temperature is nonexistent or negative, so that the system does not order in this particular mode.

Fig. 8 shows the results of calculation of T_c from (19). It is nearly constant over the MV regime and is $\sim \frac{4}{3} \lambda$ as expected from (19).

Section 3 : COMPETITION BETWEEN PHASES

We now discuss which of the possible phases the system will actually have at a given temperature and for a given set of system parameters. The problem can be approached from the high temperature side (comparison of T_c 's) and from the low temperature side (ground state).

The comparison of T_c 's for system parameters in the MV range are shown in fig. 8. For simplicity, we consider $C < \sqrt{U\Delta}$ so that only Ferromagnetic ordering is possible. We find that over almost the whole range, the $\langle S_x \rangle$ ordering dominates. The possibility of $\langle S_z \rangle$ ordering arises only at very low temperatures. We show below that such temperatures are too close to the Kondo temperature to be meaningful, since, as we have already mentioned, the theory does not hold at these temperatures and below.

In fig. 8, we show the variation of critical temperatures for $\langle S_x \rangle$ and $\langle S_z \rangle$ orderings. The parameters chosen are $U = 200 \Delta$, $C = 8 \Delta$, $\lambda = .25 \Delta$. Computer calculations show that the MV regime extends from $\epsilon_d \sim .7$ to $\epsilon_d \sim 6$. When $\epsilon_d \sim 6$, the magnetic HF solution is $(x, y) \sim (-1.5 \Delta, 160 \Delta)$ which corresponds to a Kondo temperature, $T_K \sim .15 \Delta$. At the

other end of the MV regime, the spin fluctuation lifetime is expected to be $\sim \Delta^{-1}$. These temperatures are below the x -ordering temperatures (T_c^x) but well above the z -ordering temperatures. Thus, if at all any ordering occurs, it will be the valence fluctuation type of phase. If λ is too small, say by another order of magnitude than that considered here, this phase is also unlikely to occur.

CHAPTER IV

BEYOND THE HARTREE FOCK APPROXIMATION THE PATH INTEGRAL METHOD FOR THE ANDERSON MODEL

Section 1 : INTRODUCTION

The HFA discussed in the previous two chapters suffers from a serious shortcoming. For a single impurity described by the Anderson model (with $U \gg \pi\Delta$), it predicts a magnetic ground state (for $\epsilon_d < 0$), whereas experimental evidence available in abundance shows that the state changes over smoothly into a nonmagnetic ground state well below the Kondo temperature T_K . Thus the conclusions derived in the previous chapter are unreliable if, e.g., the transition temperatures T_C or T_C^x are of order T_K . In this and the succeeding chapter we attempt to include the Kondo phenomenon in our theoretical description of dilute systems described by the Anderson model. We largely concentrate on the case $C = 0$.

Schrieffer and Wolff²² (SW) showed in perturbation theory that the magnetic properties of the Anderson model with $\epsilon_d < 0$ and $|\epsilon_d| \gg \Delta$, are the same as those of the Kondo model,

$$H = \sum_{k\sigma} \epsilon_k c_{k\sigma}^+ c_{k\sigma} - J \vec{S} \cdot \vec{S} + \sum_{kk'\sigma} V_{kk'} c_{k\sigma}^+ c_{k'\sigma} \quad \dots (1)$$

$$\text{with } J \simeq 2|V_{kd}|^2 \left(\frac{1}{\epsilon_d} - \frac{1}{\epsilon_d + U} \right) \quad \dots (2)$$

$$V_{kk'} \approx V - \frac{|V_{kd}|^2}{2} \left(\frac{1}{\epsilon_d} + \frac{1}{\epsilon_d + U} \right) \quad \dots (3)$$

Here, \vec{S} is the spin of the local moment and \vec{s} is the conduction electron spin density at the local moment site.

It is well known that a Kondo impurity described by eq.(1) has a nonmagnetic ground state. Approximately, $x = \mu_{\text{eff}} / (T + T_K)$ where $T = D_{\text{eff}} \sqrt{J_\rho} e^{-1/J_\rho}$ for $J_\rho \ll 1$, D_{eff} being an effective bandwidth. The correspondence between Anderson and Kondo models is strengthened by the results of Krishnamurthy, Wilkins and Wilson¹⁰ (KWW). Doing a renormalization group calculation which amounts to a numerical nonperturbative calculation of energy levels of the system, they showed that the symmetric Anderson model ($\epsilon_d = -\frac{U}{2}$; and in (1) and (3), $V = 0$) is identical with the Kondo model in its thermal magnetic properties, with J given by the SW value, with $D_{\text{eff}} = U/12$.

For systems of interest to us, viz., $U \gg \pi \Delta$, $\epsilon_d \rightarrow 0$, the SW transformation is of limited value, since $J_{\text{eff}} \rightarrow \infty$ as $\epsilon_d \rightarrow 0$; this explosive situation arising because of the breakdown of the perturbative basis of SW transformation as $\epsilon_d \rightarrow 0$. The question then is whether the connection between Anderson model and Kondo model (for magnetic properties of the former system) breaks down or is modified in a definite way. KWW have studied this question in their numerical renormalization group approach and have found deviations from Kondo like behaviour for $|\epsilon_d| \lesssim \Delta$. We study the same problem here in

an analytical, albeit more crudely approximate, framework.

The method we use is a generalization of that due to Hamann⁸ for the symmetric Anderson model. This method has as its special feature, the starting point of Hartree-Fock states rather than the ground states of an unperturbed model which are then perturbatively expanded either in terms of $\Delta |\epsilon_d|$ or U/Δ . Such perturbation expansions would be useless for the range of parameters of interest to us. Hamann's method then proceeds to describe the system in terms of 'paths' or fluctuations between the HF states arising out of processes beyond the HFA. In his treatment he has chosen only special types of paths - linear hops between the HF states - which correspond to sudden (though not discrete) changes in the effective d electron HF potential. Nozieres and De-Dominicis²³ have shown that such changes excite low energy electron-hole pairs in the conduction electron system which are responsible for Kondo divergences. With this approximation, Hamann has shown that the partition function for the symmetric Anderson model is the same as that of the Kondo model as obtained by Anderson and Yuval⁹. This approach shows that because of the near orthogonality of the two HF states, the "communication" between them via excited electron hole states is small and T_K is, consequently low. Hamann obtained the Kondo model parameters for a given set of values of U and Δ (he has taken $\epsilon_d = -U/2$). The parameters are,

$$J_\rho = 4\Delta/U \quad \dots (4)$$

$$D_{\text{eff}} = U/12 \quad \dots (5)$$

agreeing completely with the later results of KWW. We extend here this approach to the somewhat more complicated asymmetric case.

Section 2 : THE PATH INTEGRAL FORMULATION

In this section we closely follow Hamann and obtain a formal expression for the partition function, the evaluation of which is done in the next section.

The Anderson model is broken up as

$$H = H_0 + H_1$$

$$\text{where } H_0 = \sum_{k\sigma} \epsilon_{k\sigma} n_{k\sigma} + \sum_{\sigma} \epsilon_{d\sigma} n_{d\sigma} + U n_{d\uparrow} n_{d\downarrow} \quad \dots (6)$$

$$\text{and } H_1 = V \sum_{k\sigma} (c_{k\sigma}^+ c_{d\sigma} + c_{d\sigma}^+ c_{k\sigma}) \quad \dots (7)$$

The partition function can be written as,

$$Z = Z_0 \langle T_{\tau} \int \exp(-H_1(\tau)) d\tau \rangle \quad \dots (8)$$

where the quantity after Z_0 is an abbreviated notation for the usual perturbation expansion, T_{τ} denoting time ordering, and

$$H_1(\tau) = e^{H_0\tau} H_1 e^{-H_0\tau} \quad \dots (9)$$

when right hand side of (8) is expanded, we have sums of time ordered products of the form $\dots H_1(\tau_{i+1})H_1(\tau_i)H_1(\tau_{i-1}) \dots$ integrated over the τ 's. The operators H_1 change the d electron occupation numbers $n_{d\sigma}$, but H_0 conserves them; therefore, within the trace (8), exponential factors arising

from (9) contribute numerical factors of the form $e^{-U n_{d+} n_{d+} \tau}$ from H_0 , with $n_{d\sigma}$ now denoting the eigenvalue of the corresponding operator. The product $n_{d+} n_{d+}$ can be written as

$$n_{d+} n_{d+} = \frac{1}{4} [(n_{d+} + n_{d+})^2 - (n_{d+} - n_{d+})^2] \quad \dots (10)$$

then the above exponential factors involving $n_{d+} n_{d+}$ can be written out using Gauss integral formula,

$$e^{a^2} = \int_{-\infty}^{\infty} dx e^{-\pi x^2 - 2\sqrt{\pi} a x}$$

After carrying out these steps, we get the expression for Z as,

$$Z = Z_0 \int \delta X \int \delta Y Z_{+}(X, Y) Z_{+}(X, Y) e^{-\int_0^{\beta} (\frac{X^2}{U} + \frac{Y^2}{U}) d\tau} \quad \dots (11)$$

In (11), Z_{+} and Z_{+} are partition functions for $+$ and $+$ spin d electrons with d energies, $\varepsilon_d \pm X + iY$, with the $+(-)$ sign for $+$ ($+$) electron, mixing with conduction electrons via the mixing given by H_1 (equation (7)). The U term has been removed by the above mentioned steps and results in the general time dependent fields X and Y . Thus X and Y are general functions of τ .

To evaluate Z (expression (11)) for a general path, we look first into $Z_{\sigma}(X, Y)$, which is given by

$$Z_{\sigma}(X, Y) = e^{C_{\sigma}} \quad \dots (12)$$

where C_{σ} is the well known closed loop sum. This can easily be shown to be equal to (e.g., see Hamann)

$$C_{\sigma} = - \int_0^1 d\lambda \int_0^{\beta} d\tau v_{\sigma}(\tau) G_{d\sigma}^{(\lambda)}(\tau, \tau^+) \quad \dots (13)$$

where $\lambda v_\sigma = \lambda(iY(\tau) + \sigma X(\tau))$ is the external potential acting on a d electron of spin σ ; $G_{d\sigma}^{(\lambda)}$ is the Green's function for the d-electron in this potential.

Formally, the Green's function for an arbitrary time dependent potential can be found from Dyson's equation,

$$G = G^0 + G^0 V G \quad \dots (14)$$

where G^0 is the Green's function in the absence of any time dependent potential, i.e., when the d electron is in the level E_d (say) and mixes with the conduction band as usual in the one body HF theory. $G_{d\sigma}^0(\tau)$ is the Fourier transform of $G_{d\sigma}^0(\varepsilon) = (\varepsilon - E_{d\sigma} - i\Delta)^{-1}$, and is found to be, in the long time approximation,

$$G_{d\sigma}^0(\tau) \approx -\frac{\Delta}{E_{d\sigma}^2 + \Delta^2} \left[\frac{P}{\pi\tau} + \frac{E_d}{\Delta} \delta(\tau) \right] \quad \dots (15)$$

The Dyson equation (14) with $G_{d\sigma}^0$ given by (15) and with $E_d = 0$ has been solved by Hamann, using Muskhelivili's²⁴ method for singular integral equations. We also put $E_d = 0$ so that the instantaneous potentials for a d electron of spin σ is,

$$V_\sigma = \varepsilon_d + iY(\tau) + \sigma X(\tau) \quad \dots (16)$$

Hamann's result for $G_d(\tau)$ is (we have dropped the spin indices which are to be substituted back when necessary),

$$G_d(\tau, \tau') = G_d^0(\tau, \tau', \xi(\tau)) + \frac{1}{4\pi i \Delta \xi(\tau)} \left[\frac{1}{A^+(\tau)} - \frac{1}{A^-(\tau)} \right] \Delta \\ \times \left[\frac{A^+(\tau) + A^-(\tau) - A^+(\tau') - A^-(\tau')}{\tau - \tau'} \right] \quad \dots (17)$$

where $\xi(\tau)$ is a dimensionless quantity defined as

$$\xi_{\sigma}(\tau) = V_{\sigma}(\tau)/\Delta \quad \dots (18)$$

$$\text{and } A^{\pm}(\tau) = \exp (\pm i\eta(\tau)A(\tau)) \quad \dots (19)$$

$$\text{where } A(\tau) = \exp \left[\frac{P}{\pi} \int_0^{\beta} \frac{d\tau'}{\tau' - \tau} \eta(\tau') \right] \quad \dots (20)$$

$$\text{with } \eta(\tau) = -\tan^{-1} \xi(\tau) \quad \dots (21)$$

After having found $G_{d\sigma}(\tau, \tau')$, the next step towards evaluating Z_{σ} is to find the linked cluster sum C^{σ} given by (13). Hamann has shown that this can be broken up into an adiabatic and a transient part corresponding to adiabatic and transient parts of $G_{d\sigma}$ -- the first and second terms of r.h.s. of (17). respectively. The adiabatic part of C_{σ} , which we denote by A_{σ}

$$A_{\sigma} = -\frac{\Delta}{\pi} \int_0^{\beta} d\tau \xi_{\sigma}(\tau) \left[\frac{\pi}{2} - \tan^{-1} \xi_{\sigma}(\tau) + \frac{1}{2\xi_{\sigma}(\tau)} \ln(1 + \xi_{\sigma}^2(\tau)) \right] \dots (22)$$

The transient part of C_{σ} is denoted by B_{σ} and is obtained by substituting into (13),

$$G_d^{tr}(\tau, \tau^+) = \frac{1}{\pi \Delta \xi(\tau)} \left[\sin^2 \eta(\tau) \frac{d\eta(\tau)}{d\tau} - \sin \eta(\tau) \cos \eta(\tau) \frac{d}{d\tau} \ln A(\tau) \right] \quad \dots (23)$$

The first term of this contributes to C_{σ} an integral -

$$-\frac{1}{\pi} \int \frac{d\lambda}{\lambda} \int_0^{\beta} d\tau \sin^2 \eta(\tau) \frac{d\eta(\tau)}{d\tau}$$

This integral vanishes if $\eta(\beta) = \eta(0)$ which must be the case for periodicity of G_β . So only the second term of (23) gives a nonvanishing contribution to B_σ . We find that

$$B = -\frac{P}{\pi^2} \int \frac{d\tau d\tau'}{\tau - \tau'} \int \frac{d\lambda}{\lambda} \frac{\sin 2\eta(\tau)}{2} \frac{d\eta(\tau')}{d\tau'} \dots (24)$$

The condition $\eta(\beta) = \eta(0) = 0$ has been used in (24). Substituting $\eta(\tau) = \tan^{-1} \lambda \xi(\tau)$ in (24) the coupling constant integral (over λ) becomes,

$$\begin{aligned} & \int_0^1 d\lambda \frac{\lambda \xi(\tau)}{\{1 + \lambda^2 \xi^2(\tau)\} \{1 + \lambda^2 \xi^2(\tau')\}} \frac{d\xi(\tau')}{d\tau'} \\ &= \frac{\xi(\tau)}{2\{\xi^2(\tau) - \xi^2(\tau')\}} \ln \frac{1 + \xi^2(\tau)}{1 + \xi^2(\tau')} \cdot \frac{d\xi(\tau')}{d\tau'} \dots (25) \end{aligned}$$

and putting this in (24) we get

$$B = -\frac{P}{2\pi^2} \int_0^\beta \frac{d\tau d\tau'}{\tau - \tau'} \cdot \frac{d\xi(\tau')}{d\tau'} \cdot \frac{\xi(\tau)}{\xi_\sigma^2(\tau) - \xi_\sigma^2(\tau')} \ln \frac{1 + \xi_\sigma^2(\tau)}{1 + \xi_\sigma^2(\tau')} \dots (26)$$

So, finally, for Z we get,

$$Z = Z_0 \int \delta X \int \delta Y \exp \left\{ \sum_\sigma (\mathcal{L}_\sigma + B_\sigma) - \Delta^2 \int_0^\beta d\tau \sum_\sigma \xi_\sigma^2/U \right\} \dots (27)$$

where \mathcal{L}_σ and B_σ are given by the expressions (22) and (26) with appropriate spin indices put in.

Section 3 : THE CHOICE OF PATHS AND EVALUATION OF Z

Section 3a : THE CHOICE OF PATHS

Before evaluating Z for general time dependent X and Y

We look into it for time independent X and Y , i.e., the d electrons of opposite spins moving in fields constant in time; which is equivalent to HFA. It is, however, not clear rightaway which values of X and Y give us exactly the HF solutions. In the spirit of the path integral method, we first write down the free energy of the system and find the values of X and Y for which this has minima, with the intention of then taking into account fluctuations around or among these minima.

In appendix IV, the free energy for constant fields is written and extremized w.r.t. X and Y . The extremum conditions are found to be the same as self consistent HF equations (2 , 3) of Chapter II. Further we show that the conditions for the extrema to be minima are the same as stability conditions for HF solutions (equation (6) and (7) of chapter II). The solutions of these HF equations together with the above conditions, were shown in chapter II to give magnetic solution for $-U < \varepsilon_d < 0$ ($U \gg \pi\Delta$), and nonmagnetic ones for rest of the range of ε_d . Let us denote by X_0 and Y_0 the fields which minimize the free energy.

Clearly, small fluctuations around the HF minima do not significantly affect the ground state which continues to be magnetic. However, transitions between \uparrow and \downarrow spin HF solutions, i.e., between the broken symmetry solutions, can lead to a nonmagnetic or symmetry restored ground state. Therefore, like Hamann, we make the choice of hopping paths -

the d electron initially being in one of the HF states and a sequence of time dependent potential flipping it to the other HF state, then back again, and so on. Such a time dependent potential is shown in fig. 9. Most of the times the potential has the value at either of the HF solutions and the time taken to cross over from one to the other, the hopping time denoted τ_0 is short compared to time spent at these. Such paths correspond to long time spin fluctuations. For the time being we keep the shape of the potential within each hop arbitrary. This, and the hopping time, which we assume to be the same for each hop, will be determined in a later section.

Section 3b : EVALUATION OF THE INTEGRALS A_σ AND B_σ .

We first evaluate the term B_σ given by eq. (26) -

$$B_\sigma = - \frac{P}{2\pi^2} \int_0^\beta \int_0^\beta \frac{d\tau d\tau'}{\tau - \tau'} \frac{d\xi_\sigma(\tau')}{d\tau'} \cdot \frac{\xi_\sigma(\tau)}{\xi_\sigma^2(\tau) - \xi_\sigma^2(\tau')} \ln \frac{1 + \xi_\sigma^2(\tau)}{1 + \xi_\sigma^2(\tau')}$$

In the above we first integrate over τ by parts and put the condition $\xi_\sigma(\beta) = \xi_\sigma(0) = 0$. Then ,

$$B_\sigma = \frac{1}{2\pi^2} \int_0^\beta \int_0^{\beta'} d\tau d\tau' \frac{d\xi_\sigma(\tau')}{d\tau'} \ln |\tau - \tau'| \left\{ \frac{d}{d\tau} \left[\frac{\xi_\sigma(\tau)}{\xi_\sigma^2(\tau) - \xi_\sigma^2(\tau')} \right] \right. \\ \left. \ln \frac{1 + \xi_\sigma^2(\tau)}{1 + \xi_\sigma^2(\tau')} \right\} \dots (28)$$

For a hopping path ξ_σ is constant except during the hops. So unless τ is inside a hop, $d\xi_\sigma(\tau)/d\tau' = 0$. Therefore, non-vanishing contributions to (28) come only when τ and τ' both

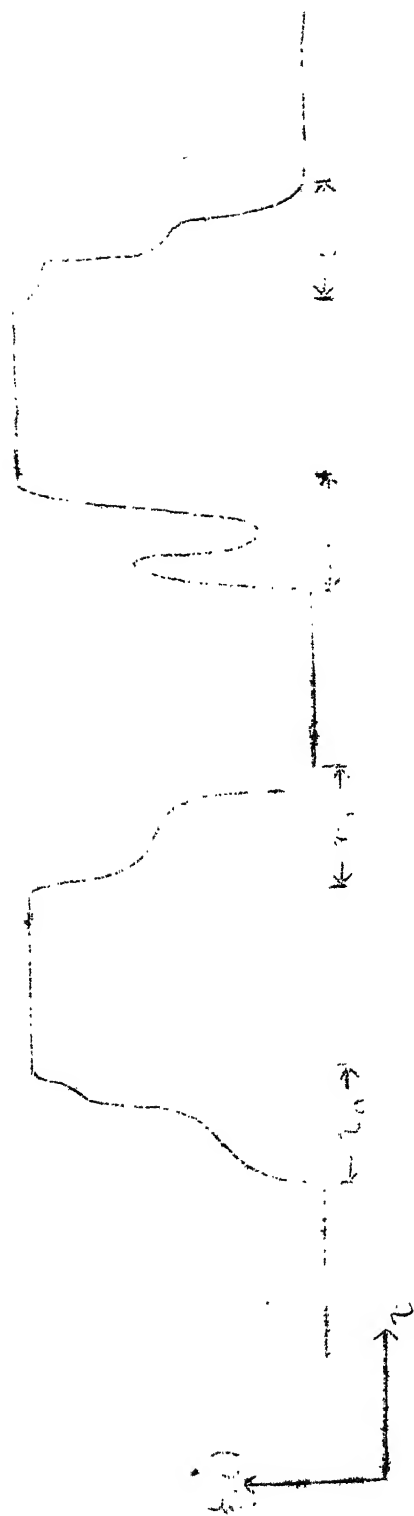


Fig 1. Time dependant potential (hopping path)

are inside hops. If we denote by L_{ij}^σ the contributions when i is within the i^{th} hop and τ' within the j^{th} ($i \neq j$), and by S_i the contribution when τ and τ' are both within the i^{th} hop, then B_σ can be written as,

$$B_\sigma = \sum_{ij} L_{ij}^\sigma + \sum_i S_i \quad \dots (29)$$

With

$$L_{ij}^\sigma = \frac{1}{2\pi^2} \int_{t_i}^{t_i+\tau_0} d\tau' \int_{t_j}^{t_j+\tau_0} d\tau \frac{d\xi_\sigma(\tau)}{d\tau'} \ln |\tau - \tau'| \frac{d}{d\tau} \left\{ \frac{\xi_\sigma(\tau)}{\xi_\sigma^2(\tau) - \xi_\sigma^2(\tau')} \right. \\ \left. \ln \frac{1 + \xi_\sigma^2(\tau)}{1 + \xi_\sigma^2(\tau')} \right\} \quad \dots (30)$$

and

$$S_i = \frac{1}{2\pi^2} \int_{t_i}^{t_i+\tau_0} d\tau \int_{t_i}^{t_i+\tau_0} d\tau' \frac{d\xi_\sigma(\tau')}{d\tau'} \ln |\tau - \tau'| \frac{d}{d\tau} \left\{ \frac{\xi_\sigma(\tau)}{\xi_\sigma^2(\tau) - \xi_\sigma^2(\tau')} \right. \\ \left. \ln \frac{1 + \xi_\sigma^2(\tau)}{1 + \xi_\sigma^2(\tau')} \right\} \quad \dots (31)$$

These two terms are known as the long and short range terms respectively. In evaluating L_{ij}^σ to lowest order, we do not need to know the hopping shape or time. In the lowest order we simply write (30) as,

$$L_{ij}^\sigma = \frac{1}{2\pi^2} \ln |t_i - t_j| \int_{t_i}^{t_i+\tau_0} d\tau' \int_{t_j}^{t_j+\tau_0} d\tau \frac{d\xi_\sigma(\tau')}{d\tau'} \cdot \frac{d}{d\tau} \left\{ \frac{\xi_\sigma(\tau)}{\xi_\sigma^2(\tau) - \xi_\sigma^2(\tau')} \right. \\ \left. \ln \frac{1 + \xi_\sigma^2(\tau)}{1 + \xi_\sigma^2(\tau')} \right\} + 0 \left(\frac{\tau_0}{|t_i - t_j|} \right) \quad \dots (32)$$

In (32), the τ integral can immediately be done and we obtain,

$$L_{ij}^\sigma = (-)^j \frac{1}{2\pi^2} \ln |t_i - t_j| \int_{t_i}^{t_i+\tau_0} d\tau' \frac{d\xi_\sigma(\tau')}{d\tau'} \left[\frac{\xi}{\xi^2 - \xi_\sigma^2(\tau')} \right. \\ \left. \ln \frac{1 + \xi^2}{1 + \xi_\sigma^2(\tau')} \right] \quad \dots (33)$$

where the limits ξ_1 and ξ_2 are the HF values and pertain to ξ within the bracket. The overall factor $(-)^j$ takes care of the fact that the initial state is ξ_2 and alternate hops will be $\xi_2 \rightarrow \xi_1$ and $\xi_1 \rightarrow \xi_2$. Next we denote $\xi_\sigma(\tau')$ by ξ' and change the integration variable to ξ' and write (33) as

$$L_{ij}^\sigma = (-)^{i+j} \frac{1}{2\pi^2} \ln |t_i - t_j| \int_{\xi_1}^{\xi_2} d\xi' \left[\frac{\xi}{\xi^2 - \xi'^2} \ln \frac{1 + \xi^2}{1 + \xi'^2} \right]_{\xi=\xi_1}^{\xi_2} \dots (34)$$

Using the coupling constant integration given in equation (25), the above can be written as,

$$\begin{aligned} L_{ij}^\sigma &= \frac{(-)^{i+j}}{2\pi^2} \ln |t_i - t_j| \int_0^1 d\lambda \int_{\xi_1}^{\xi_2} d\xi' \frac{\lambda}{1 + \lambda^2 \xi'^2} \left(\frac{\xi_2}{1 + \lambda^2 \xi_2^2} - \frac{\xi_1}{1 + \lambda^2 \xi_1^2} \right) \\ &= \frac{(-)^{i+j}}{\pi^2} \ln |t_i - t_j| \int_0^1 d\lambda \{ \tan^{-1} \lambda \xi_2 - \tan^{-1} \lambda \xi_1 \} \left\{ \frac{\xi_2}{1 + \lambda^2 \xi_2^2} - \frac{\xi_1}{1 + \lambda^2 \xi_1^2} \right\} \\ &= \frac{(-)^{i+j}}{2\pi^2} \ln |t_i - t_j| \{ \tan^{-1} \xi_2 - \tan^{-1} \xi_1 \}^2 \dots (35) \end{aligned}$$

The method used by Hamann in going from eq. (34) to (35) for the symmetric case cannot be extended to the asymmetric case, whereas the above trick makes this possible.

Now we take up the short range term, eq. (31)

$$S_i^\sigma = \frac{1}{2\pi^2} \int_{t_i}^{t_i + \tau_0} \frac{d\tau}{\tau} \int_{t_j}^{t_i + \tau_0} \frac{d\tau'}{\tau'} \frac{d\xi_\sigma(\tau')}{d\tau'} \ln |\tau - \tau'| \left\{ \frac{\xi_\sigma(\tau)}{\xi_\sigma^2(\tau) - \xi_\sigma^2(\tau')} \right. \\ \left. \ln \frac{1 + \xi_\sigma^2(\tau)}{1 + \xi_\sigma^2(\tau')} \right\}$$

Integrating by parts over τ we get

$$S_i^\sigma = \frac{(-)^i}{2\pi^2} \int_{t_i}^{t_i+\tau_0} d\tau' \frac{d\xi_\sigma(\tau')}{d\tau'} \left\{ \ln |t_i+\tau_0-\tau'| \cdot \frac{\xi_2}{\xi_2^2 - \xi_\sigma^2(\tau')} \ln \frac{1+\xi_2^2}{1+\xi_\sigma^2(\tau')} \right. \\ \left. - \ln |t_i-\tau'| \cdot \frac{\xi_1}{\xi_1^2 - \xi_\sigma^2(\tau')} \ln \frac{1+\xi_1^2}{1+\xi_\sigma^2(\tau')} \right\} - \frac{1}{2\pi^2} \int_{t_i}^{t_i+\tau_0} d\tau \int_{t_i}^{t_i+\tau_0} d\tau' \frac{d\xi_\sigma(\tau')}{d\tau'} \cdot \\ \cdot \frac{P}{\tau-\tau'} \left[\frac{\xi_\sigma(\tau)}{\xi_\sigma^2(\tau) - \xi_\sigma^2(\tau')} \ln \frac{1+\xi_\sigma^2(\tau)}{1+\xi_\sigma^2(\tau')} \right]$$

To evaluate (36) we need to know $\xi_\sigma(\tau)$ explicitly. So next we determine the hopping shape, or the shape of the potential within each hop.

Section 3c : DETERMINATION OF HOPPING SHAPE, AND OF τ_0

Two types of hop are shown in figure 10(a) and (b). We choose a single hop (a) rather than an oscillating one (b), the reason being as follows:

The short range contribution from a single straight hop, as shown by Hamann is a factor $O(J \tau_0)$. An oscillating path of the type shown in fig. 10(b) will contribute a factor $O((J \tau_0)^5)$. The long range contribution does not depend on τ_0 or the shape of hops and will therefore be the same for both type of paths. Therefore contribution to Z from the second type of path (b), is smaller than that from the type (a) by factor $O((J \tau_0)^4)$, since $J \tau_0$ is generally < 1 ; and therefore can be neglected. So we do not consider paths with many short time oscillations.

Hamann has chosen a steady straight path by keeping the

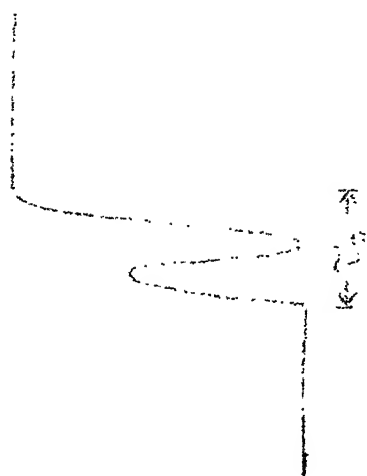


Fig 10(b)

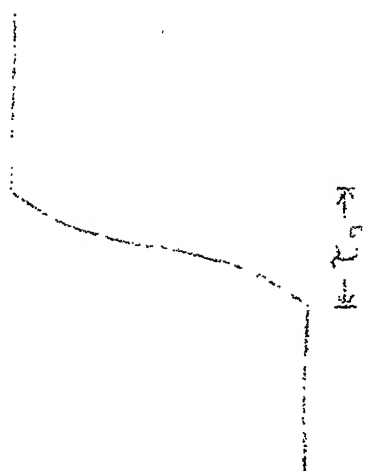


Fig 10(a)

valence field, Y , constant. For an asymmetric Anderson model, however, the path should be so chosen that as X moves from one HF value to the other, Y changes in such a way that the free energy is a minimum w.r.t. it (the Y field). In other words, we must minimize the free energy for the static path w.r.t. Y for a given X . This energy is written as (see appendix IV),

$$V = \frac{X^2}{U} + \frac{Y^2}{U} + \frac{\Delta}{\pi} \sum_{\sigma} \int \frac{\epsilon d\epsilon}{(\epsilon - \epsilon_d - iY + \sigma X)^2 + \Delta^2}, \quad \sigma = \pm \dots (37)$$

Differentiating (37) we get

$$\frac{\partial V}{\partial Y} = \frac{2Y}{U} + \frac{i}{\pi} \left[\pi - \tan^{-1} \frac{\epsilon_d + iY + X}{\Delta} - \tan^{-1} \frac{\epsilon_d + iY - X}{\Delta} \right] \dots (38)$$

When the r.h.s. of (38) is equated to zero, the solution of the equation for Y will give an extremum. To check whether this extremum is a minimum we differentiate (38) again and obtain

$$\frac{\partial^2 V}{\partial Y^2} = \frac{2}{U} + \frac{\Delta/\pi}{(\epsilon_d + iY + X)^2 + \Delta^2} + \frac{\Delta/\pi}{(\epsilon_d + iY - X)^2 + \Delta^2}$$

This quantity is > 0 for all real Y . Therefore, all paths found by the equation $\frac{\partial V}{\partial Y} = 0$ are minima in Y . To find the paths we must solve

$$\frac{2iY}{U} = \frac{1}{\pi} \left(\pi - \tan^{-1} \frac{\epsilon_d + iY + X}{\Delta} - \tan^{-1} \frac{\epsilon_d + iY - X}{\Delta} \right) \dots (39)$$

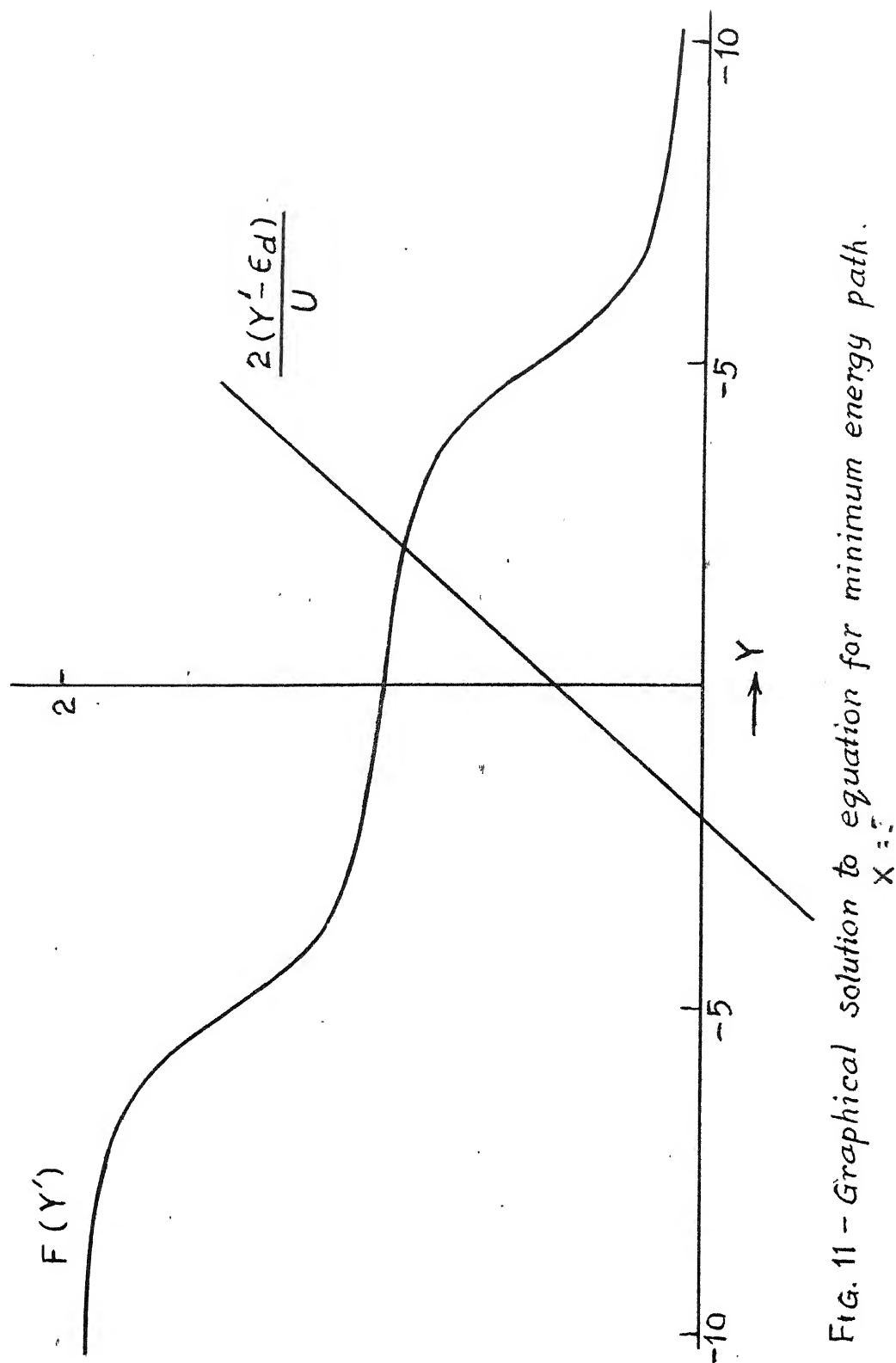


FIG. 11 - Graphical solution to equation for minimum energy path.

A graphical solution to (39) is shown in fig. 11. The approximate solution is,

$$Y' \simeq \varepsilon_d + \frac{U}{2}, \quad |X| > \varepsilon_d + \frac{U}{2} \quad \dots (40)$$

$$Y' \simeq |X|, \quad |X| < \varepsilon_d + \frac{U}{2} \quad \dots (41)$$

We take X to be varying linearly with time, within a hop, i.e.,

$$X(\tau) = X_2 + \frac{-X_2 + X_1}{\tau_0} (\tau - t_1) \quad \dots (42)$$

within the i^{th} hop, if it is from X_2 to X_1 ; otherwise in (42) X_1 and X_2 should be interchanged.

Thus, equations (40), (41) and (42) determine the hopping shape.

When this hopping shape is substituted into the short range term given by eq. (36), many integrals result, which have been shown in appendix V. It has also been shown there that the only τ_0 dependent term is $\frac{1}{2} \left\{ \frac{\tan^{-1} \xi_2 - \tan^{-1} \xi_1}{\pi} \right\}^2 \ln |\tau_0|$.

To determine τ_0 in terms of the model parameters, we collect all the τ_0 -dependent terms in the exponent of Z for a given path. These contributions are, (i) from the short range term mentioned above, and (ii) from the integration of adiabatic (\mathcal{A}_0) plus Gaussian factor terms. Then this τ_0 -dependent contribution is minimized w.r.t. τ_0 . This is also done in appendix V and we get

$$\tau_0 \sim \frac{4}{|\epsilon_d|(1 - \frac{4}{5} \frac{|\epsilon_d|^2}{U^2})} \dots (43)$$

the result being valid for $|\epsilon_d| \gg \Delta$. The result (43) has the KWW or Hamann value for $\epsilon_d = -\frac{U}{2}$

The remaining short range terms contribute to the amplitude associated with each flip which can be identified with $J_{\perp} \tau_0$. For the symmetric case and for $U \gg \pi \Delta$, Hamann has estimated the leading term in this integral, and has shown $J_{\perp} \tau_0 \sim \frac{\Delta}{U} \sim J_2 \tau_0$. However, the coefficient is uncertain, this being a deficiency of this method which is poor for short time properties. We find our integrals to be much more complicated, but for the $U \rightarrow \infty$, large negative ϵ_d case,

$$J_{\perp} \tau_0 \sim \frac{\Delta}{|\epsilon_d|}$$

Unfortunately no precise statement can be made of the approximate size of J_{\perp} or τ_0 for small ϵ_d except to say that the integrals are all finite, so these quantities stay finite as $\epsilon_d \rightarrow 0$.

Section 3d : THE PARTITION FUNCTION

The partition function is the sum of contributions from all possible paths, each path containing $2n$ hops (n is an integer). The contribution from a path with hops at $t_1, t_2, \dots, t_1, \dots$, is obtained by collecting contributions from the long range, short range and adiabatic terms :

$$Z = Z_0 \sum_n Z_n$$

where $Z_n = (J \tau_0)^{2n} \int dt_1 \dots dt_{2n} \exp \left\{ \sum_{ij} (-)^{i-j} (2-\varepsilon) \ln \left| \frac{t_i - t_j}{\tau_0} \right| \right\}$

$$2 - \varepsilon = 2 \left(\frac{\tan^{-1} \varepsilon_2 - \tan^{-1} \varepsilon_1}{\pi} \right)^2$$

This form of the partition function is identical with that of the Kondo model obtained by Yuval and Anderson⁹. The Kondo model parameters, τ_0 , ε , etc., can be obtained as functions of Anderson model parameters, ε_d , Δ , U .

It is clear that as $\varepsilon_d \rightarrow 0$ we go into a very strong coupling Kondo model. However, effective J_z remains finite for $\varepsilon_d \rightarrow 0$. This is an important qualitative conclusion. We also assume that isotropy continues so that $J_\perp \simeq J_z$. However, when $J_\perp \tau_0$ is large, flips are frequent, and the above picture based on well separated hops breaks down. So the Anderson-Kondo analogy is, unfortunately, not very accurate as $\varepsilon_d \rightarrow 0$.

Using the above Anderson-Kondo connection, and known results for Kondo model, we can calculate T_K , $\chi(T)$ etc. There is, however, an additional feature, important near $|\varepsilon_d| \simeq \Delta$. This is the fact of temperature dependent occupation of the bare state ε_d since

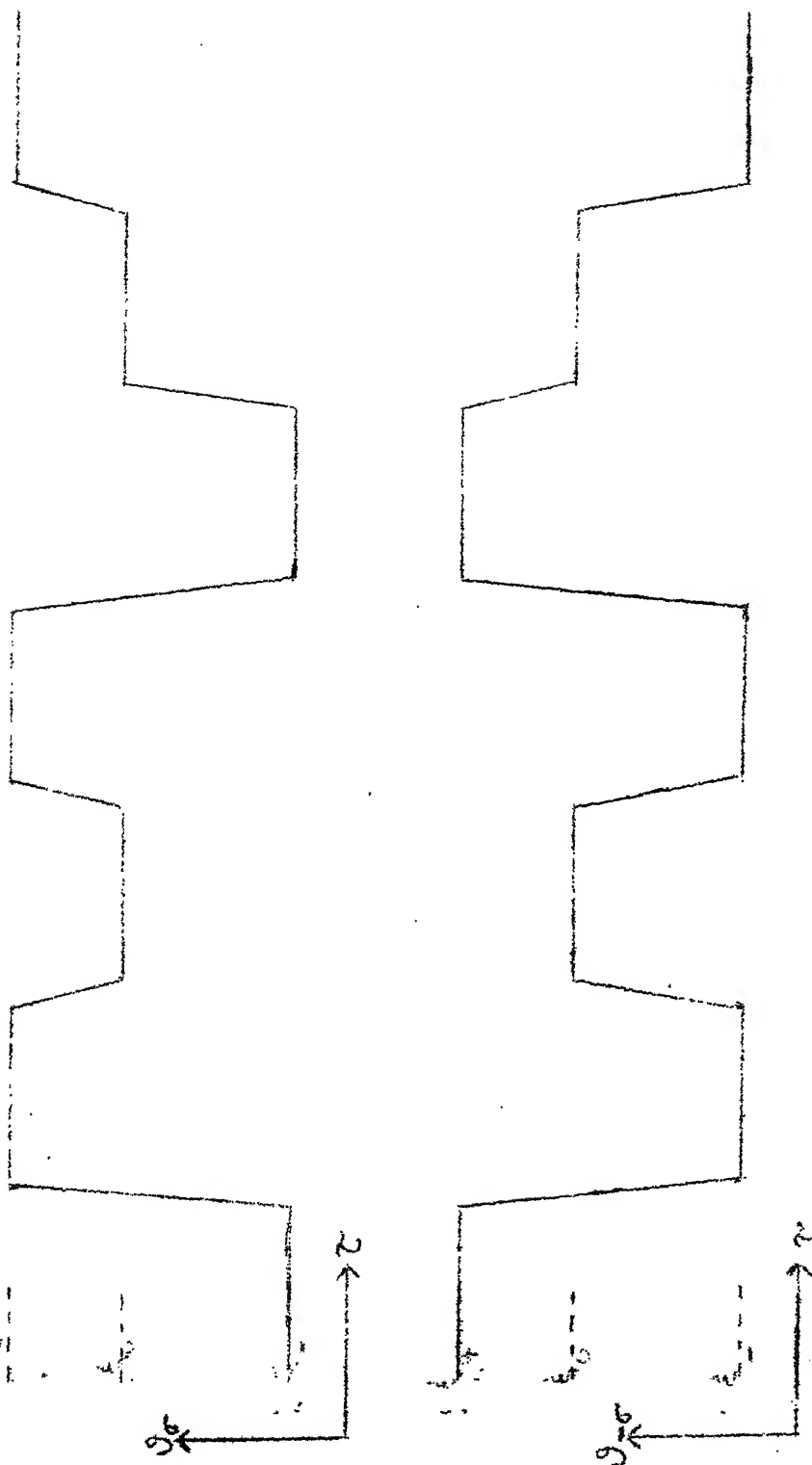
$$Z = Z_0 \cdot Z_{\text{Kondo}}$$

where Z_0 is the product of conduction electron partition function and a local level at ε_d with correlation U . At temperatures $\sim \varepsilon_d$, the level will begin to change occupancy,

and for $T \gg |\epsilon_d|$ it and the nonmagnetic level will be equally occupied, so that now, $\mu_{\text{eff}} \sim \frac{2}{3} \mu_{\text{lowT}}$. If $|\epsilon_d| \sim \Delta \sim T_K$, then this thermal emptying can lead to serious changes in $\chi(T)$ behaviour over the temperature scale $T_K \sim \Delta$ with respect to the pure Kondo dependence. In particular, it is easily seen that for ϵ_d +ve and of order Δ , $\chi(T)$ varies non-monotonically with temperature. This has been found also by KWW. They find a peak in χ setting in at about $\epsilon_d \sim -\frac{\pi\Delta}{2}$.. We have not done detailed calculations in this regime since we do not expect our connection to be numerically accurate there.

Section 4 : THE MIXED VALENCE (ANDERSON MODEL $C \neq 0$) IN PATH INTEGRAL METHOD.

For this case, the formalism runs parallel to the $C = 0$ case - we take the Gaussian integrals in the same way, take terms only upto 2nd order in g , and arrive at an expression for free energy in static fields the minima of which give us the HF solutions for $C \neq 0$ Anderson model. The formal expressions for A_σ and B_σ , the adiabatic and transient terms, are also the same. The main difference is that the path now fluctuates among three values of ξ rather than two. Let us denote the three potentials, corresponding to the three HF solutions, by ξ_+ , ξ_- and ξ_0 . Then a typical path can be shown by figure 12. Note the relation between potentials acting on opposite spin local electrons.

Fig 12

The long range part of the transient term contributes (expression (32)).

$$L_{ij}^{\sigma} = \frac{1}{2\pi^2} \ln |t_i - t_j| \int_{t_j}^{t_j + \tau_0} d\tau \int_{t_i}^{t_i + \tau_0} d\tau' \frac{d\xi_{\sigma}(\tau')}{d\tau'} \left\{ \frac{\xi_{\sigma}(\tau)}{\xi_{\sigma}(\tau) - \xi_{\sigma}^2(\tau')} \ln \frac{1 + \xi_{\sigma}^2(\tau)}{1 + \xi_{\sigma}^2(\tau')} \right\}$$

Following the same tricks as in (34) and (35) and adding the contributions from both spins we find the coefficient of

$(1/\pi^2) \ln |t_i - t_j|$ to be,

$$(\tan^{-1} \xi_a - \tan^{-1} \xi_b)(\tan^{-1} \xi_c - \tan^{-1} \xi_d) + (\tan^{-1} \xi_a - \tan^{-1} \xi_{b'}) \times \\ \times (\tan^{-1} \xi_c - \tan^{-1} \xi_{d'})$$

where $a, b, c, d = \xi_+, \xi_-$ or ξ_0 (any of these); and the corresponding $a', b', c', d' = \xi_-, \xi_+$ or ξ_0 respectively. This result is obtained when one of the local electrons (say spin σ) changes potential from ξ_a to ξ_b at the flip i and from ξ_c to ξ_d at j , and the opposite spin, from ξ_a to $\xi_{b'}$ at i at ξ_c to $\xi_{d'}$ at j .

Thus there are four kinds of exponents; $(2 - \varepsilon_1), \dots, (2 - \varepsilon_4)$, three τ 's corresponding to the three kinds of hops ($\xi_+ \nrightarrow \xi_-$, $\xi_+ \nrightarrow \xi_0$, $\xi_- \nrightarrow \xi_0$), and three corresponding J 's. One can write scaling equations involving all these parameters, following Anderson and Yuval's method. We assume that it is possible to vary τ 's in such a way that all the ε_i 's ($i = 1, \dots, 4$) reach the value of unity simultaneously. Even then, we are left with three J_{\perp} 's, or, in the resonant level type of models, three kinds of mixing. These three kinds

of mixing could be taken to denote either (i) mixing between the conduction electrons and either of two resonant levels and between the two resonant levels themselves; or (ii) mixing between the conduction electrons and either of three resonant levels.

Unfortunately, solutions to such two and three resonant level models are not known. Therefore we do not go into the details of scaling and the parameters.

CHAPTER V

BEYOND THE HFA - THE QUASIPARTICLE METHOD

Section 1: INTRODUCTION

In Chapter IV we applied to the nondegenerate Anderson model with $C = 0$, the path-integral method starting from the H-F solutions. The results gave a strong indication that as $\epsilon_d \rightarrow 0$, we have just a strong-coupled, Kondo system. However, traditional methods of treating a Kondo model, such as perturbation in coupling constant J , or scaling methods (again in powers of J) became more and more unreliable as J approaches unity. Therefore, the path-integral method is not very useful for obtaining quantitative results for physical quantities as $\epsilon_d \rightarrow 0$. Moreover, as we briefly showed, the $C \neq 0$ case becomes, in the method, quite intractable. For similar reasons, more realistic or complicated local-electron level schemes (e.g., degenerate orbitals, Hund's rule, CF splitting) became difficult to treat. It is also not clear how a lattice of impurities can be dealt with within this treatment.

The method used in this chapter to consider these problems is an interesting formulation of many body theory. DeDominicis et al.^{25,26} showed quite generally that the partition function Z of a large interacting system can be written as the product of the Z of a noninteracting system and that of a system consisting of noninteracting "quasiparticles" with

discrete real energy levels. The energy levels depend upon the interactions, and the operational part of the method is a prescription for calculating these energy levels, basically perturbatively, as a function of interaction strength. The method has been applied to a variety of systems, mostly electrons scattered from localized impurities^{27,31}. Applying it to nondegenerate Anderson model for small values of $|\epsilon_d|$, we find that it gives good results for magnetic susceptibility, valence fraction etc., as functions of temperature. Preliminary work on $C \neq 0$ case, and on more than one impurity case show promise. This method has the advantage of treating Kondo effect properly, as well as the two-impurity problem discussed in Chapter II. We therefore hope that, when extended, this method can overcome most of the difficulties encountered in earlier efforts and produce quantitative results for one as well as many impurities.

In this chapter we first briefly outline the formalism and then its application to the nondegenerate d-orbital Anderson model with $U = \infty$. We then discuss the calculation of quasiparticle energies, susceptibility, specific heat, valence fraction etc. In the last section the question of interacting impurities is taken up. One is now in a position to discuss the competition between Kondo effect, ferro- or antiferromagnetic ordering, and coherent or incoherent mixed valence ordering.

Section 2 : FORMALISM

Section 2(a) : THE GENERAL QUASIPARTICLE FORMALISM

Bloch and De Dominicis start from the perturbation expression for the partition function -

$$\begin{aligned} \frac{Z}{Z_0} &= 1 + \sum_{n=1}^{\infty} \text{Tr} \int_0^{\beta} d\tau_n \dots \int_0^{\tau_2} d\tau_1 e^{-\beta H_0} V(\tau_n) \dots V(\tau_1) \\ &= 1 + \sum_n \text{Tr} \int_0^{\beta} d\tau_n \dots \int_0^{\tau_2} d\tau_1 e^{-\beta H_0} e^{H_0 \tau_n} V e^{-H_0(\tau_n - \tau_{n-1})} \\ &\quad V e^{-H_0(\tau_2 - \tau_1)} V e^{-H_0 \tau_1} \dots \quad (1) \end{aligned}$$

In expression (1), $(\tau_i - \tau_{i-1})$ denote the i th time interval between two successive V 's during which the system is in an excited state of the Hamiltonian H_0 . Let us denote the energy of this state, over that of the initial state, by ε_i . Then the exponential operators in (1) become factors of the kind $\exp(\varepsilon_i(\tau_i - \tau_{i-1}))$. These time intervals can be easily integrated over and we obtain,

$$\frac{Z}{Z_0} = 1 + \sum_{n=1}^{\infty} \sum_{\substack{\text{all dia.} \\ \text{of } O(n)}} (-1)^c N \times M \frac{1}{2\pi i} \int dz \frac{e^{-\beta z}}{z} \prod_{i=1}^{2n-1} \frac{1}{z - \varepsilon_i} \dots \quad (2)$$

where N is the statistical factor (occupation probability) associated with the initial state, and M is the product of matrix elements of V , $V_{i,j-1}$.

Regrouping $\prod \frac{1}{z - \varepsilon_i}$ in (2) into products of irreducible parts - those separated by a denominator z , or intermediate energy zero, or initial state -- it can again be shown that

$$\frac{Z}{Z_0} - 1 = \sum_i (-\beta) n_i \sum_{\alpha_0=1}^{\infty} \frac{1}{\alpha_0!} \frac{\partial^{\alpha_0-1}}{\partial \varepsilon^{\alpha_0-1}} \{ e^{-\beta \varepsilon} [r_i(\varepsilon)]^{\alpha_0} \}_{\varepsilon=0} \dots \quad (3)$$

where n_i is the statistical weight of initial state i and Γ_i is the sum of all irreducible diagrams (each of which contribute $\prod_i \frac{1}{\epsilon - \epsilon_i}$) with initial state i . Now Lagrange's theorem³², can be applied to (3) and we have

$$Z/Z_0 = \sum_i n_i e^{-\beta E_i} \quad \dots (4)$$

where E_i is determined from the self-consistent equation

$$E_i = \Gamma_i(E_i) \quad \dots (5)$$

The energies E_i are termed quasiparticle energies. Now we describe a scheme for deriving Γ_i , E_i for the $U = \infty$ Anderson model.

Section 2(b) : DERIVING THE SELF-CONSISTENT QUASIPARTICLE EQUATION

The Anderson Hamiltonian,

$$H = \sum_{k\sigma} \epsilon_{k\sigma} n_{k\sigma} + \sum_{\sigma} \epsilon_{d\sigma} n_{d\sigma} + \frac{U}{2} \sum_{\sigma} n_{d\sigma} n_{d-\sigma} + V \sum_{k\sigma} (c_{k\sigma}^+ c_{d\sigma} + c_{d\sigma}^+ c_{k\sigma})$$

can be broken into,

$$H_0 = \sum_{k\sigma} \epsilon_{k\sigma} n_{k\sigma} + \sum_{\sigma} \epsilon_{d\sigma} n_{d\sigma} + \frac{U}{2} \sum_{\sigma} n_{d\sigma} n_{d-\sigma} \quad \dots (6)$$

$$\text{and } H' = V \sum_{k,\sigma} (c_{k\sigma}^+ c_{d\sigma} + c_{d\sigma}^+ c_{k\sigma}) \quad \dots (7)$$

H_0 above has four initial states according as the d-level is singly occupied by either spin (denoted by the subscript σ), is unoccupied (denoted by subscript 0), or occupied by two electrons of both spins. This last state is excluded if $U = \infty$

$$T_G = \text{diagram 1} + \text{diagram 2} + \text{diagram 3} + \dots$$

Diagram 1: A horizontal dashed line with an incoming arrow from the left and an outgoing arrow to the right. A curved arrow labeled σ, k connects the incoming and outgoing lines.

Diagram 2: A horizontal dashed line with an incoming arrow from the left and an outgoing arrow to the right. A curved arrow labeled σ, k connects the incoming and outgoing lines. Below the line, there is a loop labeled σ, k' .

Diagram 3: A horizontal dashed line with an incoming arrow from the left and an outgoing arrow to the right. A curved arrow labeled σ, k connects the incoming and outgoing lines. Below the line, there are two loops labeled σ', k' and σ'', k'' .

$$+ \text{diagram 4} + \text{diagram 5} + \dots$$

Diagram 4: A horizontal dashed line with an incoming arrow from the left and an outgoing arrow to the right. A curved arrow labeled σ, k connects the incoming and outgoing lines. Below the line, there is a loop labeled σ', k' and another loop labeled σ', k'' .

Diagram 5: A horizontal dashed line with an incoming arrow from the left and an outgoing arrow to the right. A curved arrow labeled σ, k connects the incoming and outgoing lines. Below the line, there is a loop labeled σ, k' .

$$+ \text{diagram 6} + \text{diagram 7} + \dots$$

Diagram 6: A horizontal dashed line with an incoming arrow from the left and an outgoing arrow to the right. A curved arrow labeled σ, k connects the incoming and outgoing lines. Below the line, there is a loop labeled σ, k' .

Diagram 7: A horizontal dashed line with an incoming arrow from the left and an outgoing arrow to the right. A curved arrow labeled σ, k connects the incoming and outgoing lines. Below the line, there is a loop labeled σ, k' .

$$T_0 = \text{diagram 8} + \text{diagram 9} + \text{diagram 10} + \dots$$

Diagram 8: A horizontal dashed line with an incoming arrow from the left and an outgoing arrow to the right. A curved arrow labeled σ, k connects the incoming and outgoing lines. Below the line, there is a loop labeled σ, k' .

Diagram 9: A horizontal dashed line with an incoming arrow from the left and an outgoing arrow to the right. A curved arrow labeled σ, k connects the incoming and outgoing lines. Below the line, there is a loop labeled σ, k' .

Diagram 10: A horizontal dashed line with an incoming arrow from the left and an outgoing arrow to the right. A curved arrow labeled σ, k connects the incoming and outgoing lines. Below the line, there are three loops labeled σ', k' , σ'', k'' , and σ''', k''' .

$$+ \text{diagram 11} + \text{diagram 12} + \dots$$

Diagram 11: A horizontal dashed line with an incoming arrow from the left and an outgoing arrow to the right. A curved arrow labeled σ, k connects the incoming and outgoing lines. Below the line, there is a loop labeled σ, k' .

Diagram 12: A horizontal dashed line with an incoming arrow from the left and an outgoing arrow to the right. A curved arrow labeled σ, k connects the incoming and outgoing lines. Below the line, there is a loop labeled σ, k' .

Fig 13. Irreducible diagram contributing to T_G and T_0

since it then acquires infinitely high energy. The d-electrons in the three states have energies $\epsilon_{d\sigma}$ and 0 respectively.

The time sequence of the system (explained after eq. (1)) can be expressed in terms of diagrams. In fig. 13, some of the irreducible diagram contributing to Γ_{σ} and Γ_0 are shown.

In above diagrams, the dotted lines denote occupied d-electron states, spin being indicated on the diagram. The solid lines denote electrons or holes according as the arrow is pointing forward or backwards. The joining point between a solid and a dotted line contributes a factor of V . The intermediate state energy between two such successive points is determined as follows -- Draw a vertical line between the two points. Add the energies of all the lines pointing right and subtract energies of those pointing left. In the diagrams for Γ_{σ} , if this vertical line cuts a dotted line, there is no contribution from this line; if it passes through a gap in the dotted line, a contribution of $-\epsilon_{d\sigma}$. In the diagrams for Γ_0 , this rule should be reversed. The statistical factor associated with each electron or hole line must be written down, and finally summed.

Following the above rules, we first write down the contribution from a few diagrams and then expression for Γ_{σ} and Γ_0 in some approximation. The first diagram in eq. (8) fig. 13 will contribute,

$$r_{\sigma}^{(1)}(\epsilon) = V^2 \sum_k \frac{1 - f(\epsilon_{k\sigma})}{\epsilon - (\epsilon_{k\sigma} - \epsilon_{d\sigma})} = \frac{\Delta}{\pi} \int_{-D}^D \frac{1 - f(\epsilon_{k\sigma})}{\epsilon + \epsilon_{d\sigma} - \epsilon_{k\sigma}} d\epsilon_{d\sigma}$$

Similarly, the second diagram contributes

$$r_{\sigma}^{(2)}(\varepsilon) = \left(\frac{\Delta}{\pi}\right)^2 \int_{-D}^D \frac{1-f(\varepsilon_{k\sigma})}{(\varepsilon+\varepsilon_{d\sigma}-\varepsilon_{k\sigma})^2} \left[\sum_{\sigma'} \int_{-D}^D \frac{f(\varepsilon_{k'\sigma'}) d\varepsilon_{k'\sigma'}}{\varepsilon+\varepsilon_{k'\sigma'}-\varepsilon_{k\sigma}} \right] d\varepsilon_{k\sigma}$$

If we sum all the diagrams in the first row of (8), we get

$$\begin{aligned} \frac{\Delta}{\pi} \int_{-D}^D d\varepsilon_{k\sigma} \frac{1-f(\varepsilon_{k\sigma})}{(\varepsilon+\varepsilon_{d\sigma}-\varepsilon_{k\sigma})^2} \left[1 + \sum_{n=1}^{\infty} \left\{ \frac{\Delta}{\pi} I(\varepsilon, \varepsilon_{k\sigma}) / (\varepsilon+\varepsilon_{d\sigma}-\varepsilon_{k\sigma}) \right\}^n \right] \\ = \frac{\Delta}{D} \int d\varepsilon_{k\sigma} [1-f(\varepsilon_{k\sigma})] / [\varepsilon+\varepsilon_{d\sigma}-\varepsilon_{k\sigma} - \frac{\Delta}{\pi} I(\varepsilon, \varepsilon_{k\sigma})] \quad \dots (10) \end{aligned}$$

with $I(\varepsilon, \varepsilon_{k\sigma}) = \sum_{\sigma'} \int d\varepsilon_{k'\sigma'} f(\varepsilon_{k'\sigma'}) / (\varepsilon+\varepsilon_{k'\sigma'}-\varepsilon_{k\sigma})$.

Looking at the second row of diagrams we notice that their effect is to dress all the internal d-lines (those occurring between the first and the last dot) in the same way as for r_{σ} , but that now the initial energy for each of these lines is not ε , but $\varepsilon + \varepsilon_{k'\sigma'} - \varepsilon_{k\sigma}$. So these taken into account will modify expression (10) as,

$$\begin{aligned} r_{\sigma}(\varepsilon) = \frac{\Delta}{\pi} \int_{-D}^D d\varepsilon_{k\sigma} (1-f(\varepsilon_{k\sigma})) / [\varepsilon+\varepsilon_{d\sigma}-\varepsilon_{k\sigma} \\ - \frac{\Delta}{\pi} \sum_{\sigma'} \int \frac{f(\varepsilon_{k'\sigma'}) d\varepsilon_{k'\sigma'}}{\varepsilon+\varepsilon_{k'\sigma'}-\varepsilon_{k\sigma} + r_{\sigma'}(\varepsilon+\varepsilon_{k'\sigma'}-\varepsilon_{k\sigma})}] \quad \dots (11) \end{aligned}$$

There remains the third row of diagrams in (8) which we shall not take into account since the corresponding expressions are quite complicated and no suitable way was found to take them into account. Keiter and Kimball's expression is the same as (11), since they use the same approximation. It must however be noted, that these could contribute important logarithmic terms,

as they correspond, in the large $|\varepsilon_d|$ limit, to some of Nozières. De-Dominicis diagrams²³ for the Kondo Hamiltonian. Following Toulouse²⁹ it can be easily shown that in this limit what we have accounted for, is Kondo model diagrams of the type shown in fig. 14(a). And what we have not accounted for, is diagrams of the type shown in fig. 14(b). (Here the double line denotes the impurity spin; the dots; either J or J_z ; the conduction electron or holes, denoted by single solid lines, have spins according as the scattering is J_z or J).

For Γ_0 we make exactly the same approximation and obtain the expression,

$$\Gamma_0(\varepsilon) = \frac{\Delta}{\pi} \sum_{\sigma} \int_{-D}^D d\varepsilon_{k\sigma} f(\varepsilon_{k\sigma}) / [\varepsilon - \varepsilon_{d\sigma} + \varepsilon_{k\sigma} - \frac{\Delta}{\pi} \int_{-D}^D d\varepsilon_{k'\sigma'} \frac{1 - f(\varepsilon_{k'\sigma'})}{\varepsilon - \varepsilon_{k'\sigma'} + \varepsilon_{k\sigma} - \Gamma_0(\varepsilon - \varepsilon_{k'\sigma'} + \varepsilon_{k\sigma})} \dots \quad (12)$$

Comparing (11) and (12) we find that the integral expressions in the denominators are nothing but Γ_0 and Γ_{σ} respectively. Thus (11) and (12) become,

$$\Gamma_{\sigma}(\varepsilon) = \frac{\Delta}{\pi} \int_{-D}^D d\varepsilon_{k\sigma} \frac{1 - f(\varepsilon_{k\sigma})}{\varepsilon + \varepsilon_{d\sigma} - \varepsilon_{k\sigma} - \Gamma_{\sigma}(\varepsilon + \varepsilon_{d\sigma} - \varepsilon_{k\sigma})} \dots \quad (13)$$

$$\Gamma_0(\varepsilon) = \frac{\Delta}{\pi} \sum_{\sigma} \int_{-D}^D d\varepsilon_{k\sigma} \frac{f(\varepsilon_{k\sigma})}{\varepsilon - \varepsilon_{d\sigma} + \varepsilon_{k\sigma} - \Gamma_0(\varepsilon - \varepsilon_{d\sigma} + \varepsilon_{k\sigma})} \dots \quad (14)$$

These equations are the same as those obtained by Bringer and Lusfeld³⁰.

To determine quasiparticle energies, we must solve the

self-consistent equations

$$E_{\sigma} = \frac{\Delta}{\pi} \int d\epsilon_{k\sigma} \frac{1 - f(\epsilon_{k\sigma})}{E_{\sigma} + \epsilon_{d\sigma} - \epsilon_{k\sigma} - \Gamma_{\sigma}(E_{\sigma} + \epsilon_{d\sigma} - \epsilon_{k\sigma})} \quad \dots (15)$$

$$E_0 = \frac{\Delta}{\pi} \sum_{\sigma} \int d\epsilon_{k\sigma} \frac{f(\epsilon_{k\sigma})}{E_0 - \epsilon_{d\sigma} + \epsilon_{k\sigma} - \Gamma_{\sigma}(E_0 - \epsilon_{d\sigma} + \epsilon_{k\sigma})} \quad \dots (16)$$

Section 2(c) : THE QUASIPARTICLE ENERGIES AT DIFFERENT TEMPERATURE

2(c)(i) - ANALYTICAL FORMS FOR QUASIPARTICLE ENERGY .

The self consistent equations (15) and (16) are difficult to solve and we must make workable approximations. With this aim in mind we first look at the lowest order approximation to these equations, i.e.,

$$E_{\sigma} = \frac{\Delta}{\pi} \int_{-D}^D \frac{1 - f(\epsilon_{k\sigma})}{E_{\sigma} + \epsilon_{d\sigma} - \epsilon_{k\sigma}} d\epsilon_{k\sigma} \quad \dots (17)$$

$$E_0 = \frac{\Delta}{\pi} \sum_{\sigma} \int_{-D}^D \frac{f(\epsilon_{k\sigma})}{E_0 - \epsilon_{d\sigma} + \epsilon_{k\sigma}} d\epsilon_{k\sigma} \quad \dots (18)$$

At $T = 0$, f_k is a step function and we can perform these integrals right away, and obtain, in the absence of a magnetic field,

$$E_{\sigma} = \frac{\Delta}{\pi} \ln \{ |E_{\sigma} + \epsilon_d|/D \} \quad \dots (19)$$

$$E_0 = \frac{2\Delta}{\pi} \ln \{ |E_0 - \epsilon_d|/D \} \quad \dots (20)$$

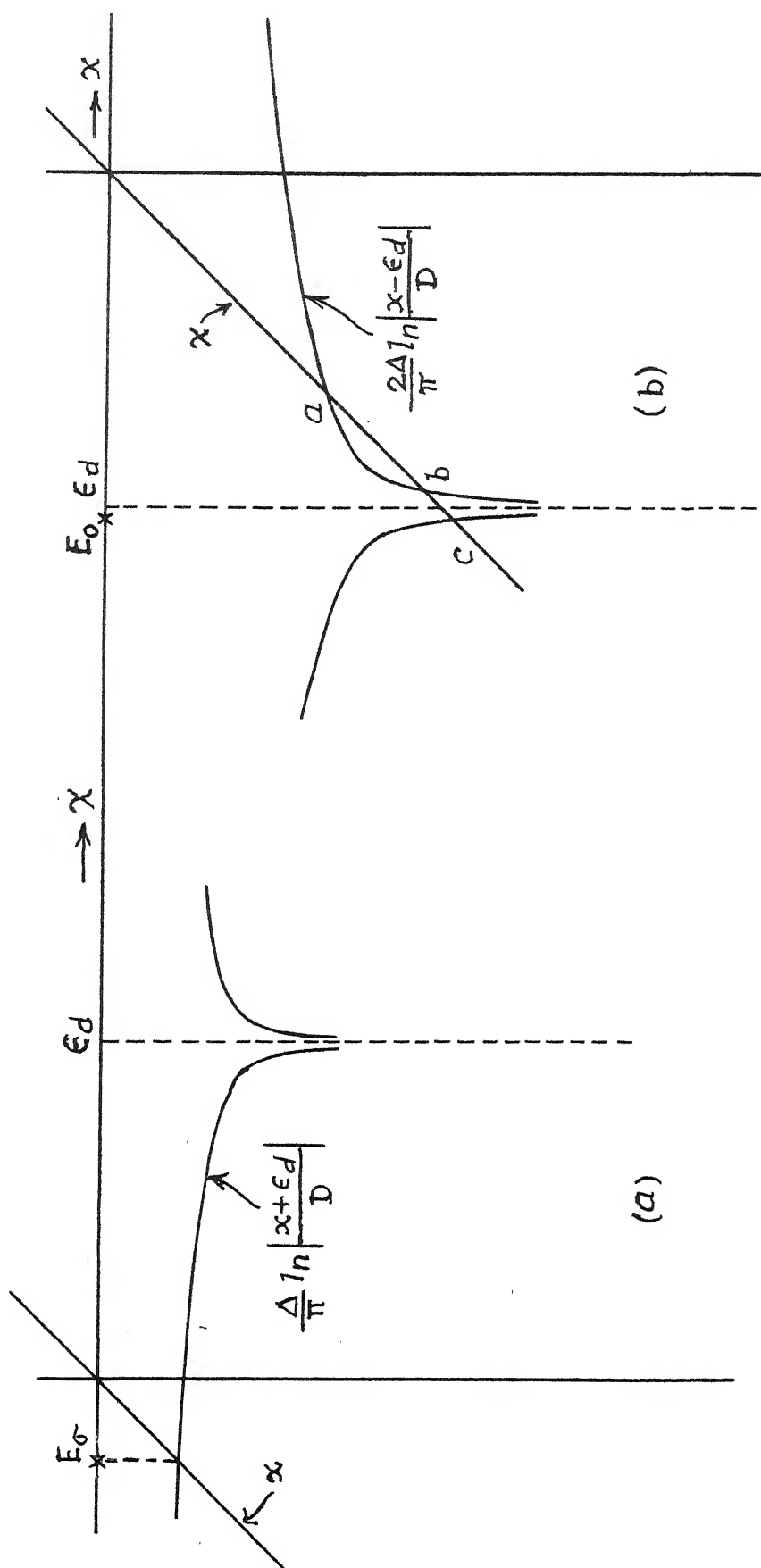


FIG. 15- Graphical solution to lowest order quasiparticle equations at zero temperature.

The graphical solutions to (19) and (20) are shown in fig. 15.

For ε_d -ve and $|\varepsilon_d| \gg \Delta$, these solutions are approximately as follows:-

From fig. V. 1, we have only one soln. given by

$$E_\sigma \approx \frac{\Delta}{\pi} \ln \frac{|\varepsilon_d + (\Delta/\pi) \ln (|\varepsilon_d|/D)|}{D} \quad \dots (21)$$

From fig. 15 we have three solutions corresponding to points a, b and c

$$E_0 = \frac{2\Delta}{\pi} \ln \frac{|\varepsilon_d + (2\Delta/\pi) \ln (|\varepsilon_d|/D)|}{D}, \quad \varepsilon_d \pm D e^{\frac{\pi\varepsilon_d}{2}} \quad \dots (22)$$

Out of the three roots (22), we choose the last one (c)

$$E_0 = \varepsilon_d - D \exp(\pi\varepsilon_d/2\Delta)$$

This is because at high temperature only this root continues (the other two become imaginary). Besides, the integrals (17) and (18) should strictly be $\ln \left(\frac{E_\sigma + \varepsilon_d}{D} \right)$ etc. whose only real branch is the left one in fig 15(a) or 15(b). Thus 'c' will be the only real root. This root represents a physical bound state. The nature of this bound state becomes clear from explicit ground state wave function of Varma and Yafet³³, since their ground state also turns out to be non-magnetic with energy $\varepsilon_d - D \exp(\pi\varepsilon_d/2\Delta)$. Actually we find above that at $T = 0$, $\varepsilon_d + E_\sigma < E_0$. But we will show in what follows immediately that the non-magnetic state is indeed lower in energy

if we make better approximations for ϵ_{σ} and E_0 .

To make approximations further than (19) and (20) we note that $r_{\sigma}(E_0 - \epsilon_{d\sigma} + \epsilon_{k\sigma})$ can be written as

$$r_{\sigma}(E_{\sigma}) + (E_0 - \epsilon_{d\sigma} + \epsilon_{k\sigma} - E_{\sigma}) r'_{\sigma}(E_{\sigma}) + \dots \quad \dots (23)$$

If we substitute this in (16) then for relevant values of $\epsilon_{k\sigma}$ (-ve at $T = 0$) and for E_0 and E_{σ} found above, the first term in (23) dominates. So we approximate

$$E_0 = \int_{\sigma} \frac{\Delta}{\pi} \int_{-D}^D \frac{f(\epsilon_{k\sigma}) d\epsilon_{k\sigma}}{E_0 - \epsilon_{d\sigma} + \epsilon_{k\sigma} - E_{\sigma}} \quad \dots (24)$$

But a similar replacement cannot be done in (15) since at E_0 , $r_{\sigma}(E)$ varies quite rapidly. So we leave this equation at its lowest approximation as in (17) i.e.,

$$E_{\sigma} = \frac{\Delta}{\pi} \int_{-D}^D \frac{1-f(\epsilon_{k\sigma})}{E_{\sigma} + \epsilon_{d\sigma} - \epsilon_{k\sigma}} \quad \dots (25)$$

Bringer and Lustfeld also started with the same expressions (13) and (14) for E_0 and E_{σ} . But their results are poor for good moment (low T_k) because of this self-energy addition in the sensitive denominator.

These approximations to quasiparticle equations were derived starting from the solutions to their lowest order approximation at $T = 0$. At high (high to be clarified later)



(a)



(b)

Fig 16

temperatures, we can make another kind of simplification. For this we truncate the quasiparticle equation (11) at

$$E_{\sigma} = \frac{\Delta}{\pi} \int d\varepsilon_{k\sigma} (1-f(\varepsilon_{k\sigma}))/[E_{\sigma} + \varepsilon_{d\sigma} - \varepsilon_{k\sigma}] \\ - \frac{\Delta}{\pi} \sum_{\sigma'} \int d\varepsilon_{k'\sigma'} f(\varepsilon_{k'\sigma'})/(E_{\sigma} + \varepsilon_{k'\sigma'} - \varepsilon_{k\sigma})] \quad \dots (26)$$

This corresponds to diagrams of the class shown in fig. 16(a). Toulouse²⁹ has shown that for large $|\varepsilon_d|$ this corresponds to the diagrams of fig. 16(b) in the Kondo model. In 16(b) double line represents the Kondo spin. Noziere's and De-Dominicis²³ have shown for the Kondo Model that these are the diagrams contributing most divergent logarithmic terms. So the approximate form (26) can be said to be accurate upto this order.

We similarly truncate (12) at

$$E_0 = \sum_{\sigma} \frac{\Delta}{\pi} \int d\varepsilon_{k\sigma} f(\varepsilon_{k\sigma})/[E_0 - \varepsilon_{d\sigma} + \varepsilon_{k\sigma}] \\ - \frac{\Delta}{\pi} \int d\varepsilon_{k'\sigma'} (1-f(\varepsilon_{k'\sigma'}))/(E_0 - \varepsilon_{k'\sigma'} + \varepsilon_{k\sigma})] \quad \dots (27)$$

We now calculate E_C , E_{σ} etc. from the equations (24, 25, 26, 27) which involve integrals of the form,

$$I(a) = \int_{-D}^D \frac{f(x) dx}{x + a}$$

This integral has been evaluated in appendix VI and we quote the result here

$$I(a) = \ln \frac{|a|}{D} + R_e [\ln (\pi/2i\beta a) + 2\psi(i\beta a/\pi) - \psi(i\beta a/2\pi)]$$

The low and high temperature expansions of this are as follows:-

$$I(a) = \ln \frac{|a|}{D} - \frac{1}{6} \left(\frac{\pi T}{a} \right)^2, \quad \pi T \ll a$$

$$I(a) \simeq \ln \left(q \frac{T}{D} \right) + \frac{7}{4} \zeta(3) \left(\frac{a}{\pi T} \right)^2, \quad \pi T \gg a$$

$$\text{where } q = \frac{\pi}{2} e^{(1-r)},$$

Sec. 2(c)(ii) : LOW TEMPERATURE LIMIT

We now look at quasiparticle energies in the low temperature limit, first E_σ and then E_0 - Equations (24) and (25) are,

$$E_\sigma = \frac{\Delta}{\pi} \int_{-D}^D \frac{f(\varepsilon) d\varepsilon}{\varepsilon + \varepsilon_d + E_\sigma} = \frac{\Delta}{\pi} I(\varepsilon_d + E_\sigma) \quad \dots (24)$$

$$E_0 = \frac{2\Delta}{\pi} \int_{-D}^D \frac{f(\varepsilon) d\varepsilon}{\varepsilon + E_0 - \varepsilon_d - E_\sigma} = \frac{2\Delta}{\pi} I(E_0 - \varepsilon_d - E_\sigma) \quad \dots (25)$$

in the absence of a magnetic field.

At zero temperature we know these integrals to be of logarithmic form, i.e.,

$$E_\sigma = \frac{\Delta}{\pi} \ln \frac{|\varepsilon_d + E_\sigma|}{D}$$

$$E_0 = \frac{2\Delta}{\pi} \ln \frac{|E_0 - \varepsilon_d - E_\sigma|}{D}$$

The solutions to these are,

$$E_\sigma \simeq \frac{\Delta}{\pi} \ln \frac{|\varepsilon_d + \frac{\Delta}{\pi} \ln |\varepsilon_d|/D|}{D} \quad \dots (26)$$

$$E_0 \simeq \varepsilon_d + E_\sigma - D \exp(\pi E_0/2\Delta) \simeq \varepsilon_d + E_\sigma - \sqrt{D|\varepsilon_d|} \exp(\pi \varepsilon_d/2\Delta) \quad \dots (27)$$

The reason for choosing only the root mentioned in (27) is the same as explained in sec. 2(c)(i). The quasiparticle energies are, E_0 and $E_d + E_\sigma$ ($\equiv \bar{E}_\sigma$) for the nonmagnetic and magnetic states respectively. So from (27) we have

$$\mathcal{E} \equiv E_0 - \bar{E}_\sigma = -\sqrt{D|\varepsilon_d|} \exp(\pi\varepsilon_d/2\Delta) \quad \dots (28)$$

Thus the nonmagnetic quasiparticle level does indeed lie below the magnetic one, by an amount that we shall later identify with T_K , the Kondo temperature.

Now, in order to see how E_0 and E_σ and in particular the gap \mathcal{E} , change at finite but low temperatures, we differentiate equations (24) and (25) -

$$\begin{aligned} \frac{dE_\sigma}{dT} &= \frac{\Delta}{\pi} \frac{d}{dT} \int_{-D}^D \frac{f(\varepsilon) d\varepsilon}{\varepsilon + \varepsilon_d + E_\sigma} \\ &= -\frac{1}{3} \frac{\Delta}{\pi} \left(\frac{\pi}{\varepsilon_d + E_\sigma} \right)^2 T / [1 - \Delta/\pi(\varepsilon_d + E_\sigma)] \quad \dots (28) \end{aligned}$$

$$\approx -\frac{1}{3} \frac{\Delta}{\pi} (\pi/\varepsilon_d)^2 T \quad \dots (29)$$

$$\frac{dE_0}{dT} = \frac{2\Delta}{\pi} \frac{d}{dT} \int d\varepsilon f(\varepsilon) / (\varepsilon + E_0 - \varepsilon_d - E_\sigma) \approx -\frac{\pi^2}{3} \frac{T}{T_K}$$

neglecting $\Delta/\varepsilon_d = T_K/\Delta$ in comparison with (1), is the limit of zero temperature. Here we have used the standard relations,

$$\frac{\partial f(\varepsilon)}{\partial T} = -\frac{\varepsilon}{T} \frac{\partial f(\varepsilon)}{\partial \varepsilon} \quad \dots (30)$$

$$\text{and } \int_{-\infty}^{\infty} \phi(\varepsilon) \frac{\partial f}{\partial \varepsilon} d\varepsilon = -\phi(0) - \frac{\pi^2}{6} T^2 \frac{\partial^2 \phi}{\partial \varepsilon^2} \Big|_{\varepsilon=0}, \quad T \rightarrow 0 \quad \dots (31)$$

Same results are obtained from the low temperature expansion of $I(a)$ given in appendix VI.

From (28) and (29) we see that as temperature starts increasing from zero, the magnitude of the energy gap $E_0 - \bar{E}_\sigma$ ($\equiv \mathcal{E}$) increases. But as has been shown graphically in fig. 17 after some temperature it decreases, becomes zero, and ultimately becomes positive, i.e., nonmagnitude quasi-particle state lies above the magnetic quasiparticle state. To see this, take up the equation

$$E_0 = \frac{2\Delta}{\pi} I(E_0 - \bar{E}_\sigma)$$

The graphical solutions to this are shown in fig. 17 for different temperatures.

The curves are plots of $\frac{2\Delta}{\pi} I(E_0 - \bar{E}_\sigma)$, $T_1 < T_2$

From this we can also obtain the value of T at which the gap closes, i.e., the nonmagnetic and the magnetic quasiparticles have the same energy. This will happen when the straight line in fig. 17 cuts the curve at \bar{E}_σ , i.e.,

$$\bar{E}_\sigma = \frac{2\Delta}{\pi} I(0)$$

But we know that $I(0) = \ln(q \frac{T}{D})$ (see high temperature expression of $I(a)$). The required temperature will thus be given by,

$$\bar{E}_\sigma = \frac{2\Delta}{\pi} \ln(q \frac{T}{D})$$

$$\text{or } T = \frac{1}{q} D \exp[\pi(E_\sigma + \varepsilon_d)/2\Delta] \simeq \frac{1}{q} \sqrt{D|\varepsilon_d|} e^{\pi\varepsilon_d/2\Delta} \dots (32)$$

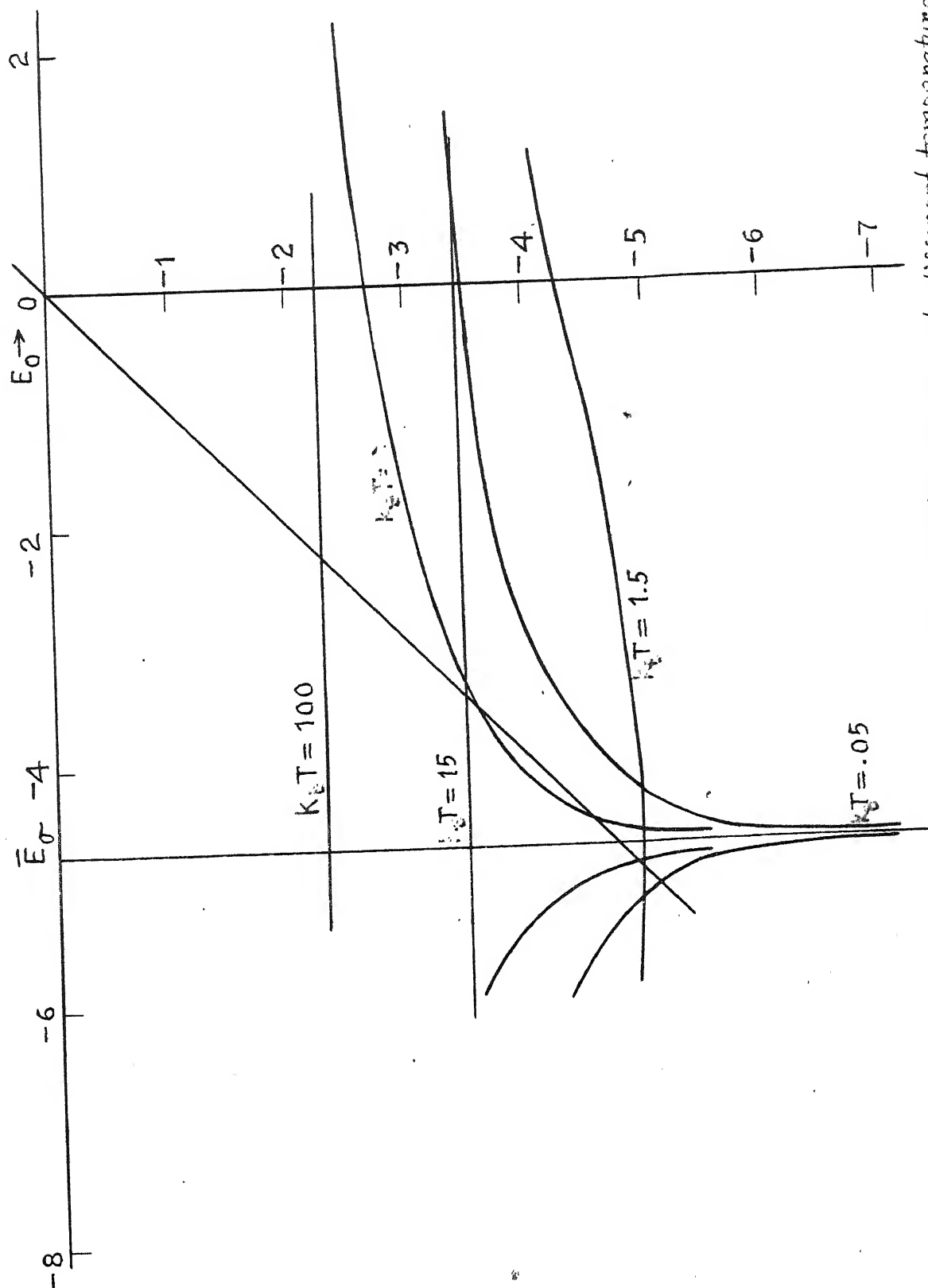


FIG. 17- Graphical solution to quasiparticle equation for E_0 at different temperatures ($\bar{E}_\sigma = -4.75$)
 The curves show $I(a)$ at different temperatures.
 Energies are in units of \hbar .

since E_σ does not change much over this temperature range ($\sim T_K$).

Thus we have shown that at zero temperature, the ground state is that of the nonmagnetic quasiparticle which lies below the magnetic quasiparticle levels by an amount T_K . This state is a mixture of $n_d = 0$ and equal amounts of the two $n_d^\sigma = 1$ states with more of the latter, as is made clear from the valence fraction obtained (sec. 4). The difference between the magnetic and nonmagnetic quasiparticle levels vanishes at a temp $\sim \frac{T_K}{q}$, at temperature above which, the magnetic state is the ground state. At temperature much higher than this, as we will show below, this difference is $O(|\epsilon_d|)$.

Section 2(c)(iii) - QUASIPARTICLE ENERGIES AT HIGH TEMPERATURES

We now turn to the high temperature equations (26) and (27).

$$E_\sigma = \frac{\Delta}{\pi} \int_{-D}^D \frac{f(\epsilon_k) d\epsilon_k}{\epsilon_k + E_\sigma + \epsilon_d - \frac{2\Delta}{\pi} I(E_\sigma - \epsilon_k)} \quad \dots (26)$$

If for $I(E_\sigma - \epsilon_k)$ in the integrand we simply put the first term of high temperature expansion, then we get,

$$E_\sigma \approx \frac{\Delta}{\pi} I(E_\sigma + \epsilon_d - \frac{2\Delta}{\pi} \ln(q \frac{T}{D})) \quad \dots (33)$$

And again applying the high temperature expansion,

$$E_\sigma \approx \frac{\Delta}{\pi} \ln(q \frac{T}{D}) + \frac{7}{4} \zeta(3) \left(\frac{E_\sigma + \epsilon_d - \frac{2\Delta}{\pi} \ln(q \frac{T}{D})}{\pi T} \right)^2$$

$$\approx \frac{\Delta}{\pi} \ln(q \frac{T}{D}) + \frac{7}{4} \zeta(3) \left\{ \left(\epsilon_d - \frac{\Delta}{\pi} \ln(q \frac{T}{D}) \right) / \pi T \right\}^2 \quad \dots (34)$$

Similarly, for E_0 , from equation (27),

$$E_0 \approx \frac{2\Delta}{\pi} \ln \frac{qT}{D} + \frac{7}{4} \zeta(3) \left\{ \left(\epsilon_d - \frac{\Delta}{\pi} \ln \frac{qT}{D} \right) / \pi T \right\}^2 \quad \dots (35)$$

The assumptions going into (33), (34) and (35) are,

$$T \gg E_\sigma, \quad T \gg \frac{2\Delta}{\pi} \ln \left(q \frac{T}{T_k} \right)$$

These are satisfied for $T \gg \Delta$

From above relations we find that

$$\epsilon_d \approx \frac{\Delta}{\pi} \ln \frac{qT}{D} - \epsilon_d \approx \frac{\Delta}{\pi} \ln \left(q \frac{T}{T_k} \right) \left| \epsilon_d \right| / T_k^2$$

This shows that the difference between the magnetic and non-magnetic quasiparticle levels starts diminishing as the temperature is lowered. This is consistent with the low temperature results.

Section 3. THE MAGNETIC SUSCEPTIBILITY

We have seen that the partition function of the system resembles that of a system with three discrete levels with magnetic moments corresponding to ± 1 or 0 spin states. Therefore we expect a Van-Vleck like susceptibility where the levels shift with temperature -- one in which low temperature susceptibility shows zero moment (that of the ground state) and high temperature susceptibility shows local moment. Moreover, the magnetic moments of the quasiparticles, or spinlike states do not remain constant and vary with temperature. Therefore we

obtain the static susceptibility directly by considering the system in a magnetic field. The partition function is,

$$Z = \sum_{\sigma} \exp [-\beta(\epsilon_{d\sigma} + E_{\sigma})] + \exp (-\beta E_0) \quad \dots (36)$$

where $\epsilon_{d\sigma} = \epsilon_d + \mu_d \sigma H$, and $\epsilon_{d\sigma} + E_{\sigma}$ and E_0 are the quasiparticle energies in the presence of a magnetic field H . The static susceptibility is given by the expression,

$$\chi = \frac{1}{\beta} \frac{\partial^2 \ln Z}{\partial H^2}$$

For the partition function of (36), we get,

$$\chi = 2 \{ \beta (\sigma \mu_d - E'_{\sigma})^2 - E''_{\sigma} \} \frac{e^{-\beta(\epsilon_d + E_{\sigma})}}{Z} - E''_0 \frac{e^{-\beta E_0}}{Z} \quad \dots (37)$$

where primes and double primes denote first and second derivatives, respectively, w.r.t. H . In (37) we have put $E_0' = 0$ which will be shown below.

Section 3(a) : ZERO-TEMPERATURE SUSCEPTIBILITY

To find the field derivatives of E_0 and E_{σ} we again take up their low and high temperature expressions separately. From the low temperature quasiparticle equations (24) and (25) we have

$$\begin{aligned} E &= \frac{\Delta}{\pi} \int_{-D}^D \frac{\{1 - f(\epsilon_{k\sigma})\} d\epsilon_{k\sigma}}{E_{\sigma} - \epsilon_{d\sigma} - \epsilon_{k\sigma}} = \frac{\Delta}{\pi} \int_{-D}^D \frac{(1 - f(\epsilon_k)) d\epsilon_k}{E_{\sigma} + \epsilon_d - \sigma \mu_d H - \epsilon_k} \\ &= \frac{\Delta}{\pi} I (E_{\sigma} - \epsilon_d - \sigma \mu_d H) \quad \dots (38) \end{aligned}$$

$$E_0 = \frac{\Delta}{\pi} \sum_{\sigma} \int_{-D}^D \frac{f(\varepsilon_{k\sigma}) d\varepsilon_k}{E_0 - \varepsilon_{d\sigma} + \varepsilon_{k\sigma} - \bar{E}_{\sigma}} = \frac{\Delta}{\pi} \int_{-D}^D \frac{f(\varepsilon_k) d\varepsilon_k}{E_0 - \varepsilon_d + \sigma\mu_d H + \varepsilon_k - \bar{E}_{\sigma}}$$

$$= \frac{\Delta}{\pi} \sum_{\sigma} I(E_0 - \bar{E}_{\sigma} - \varepsilon_d + \sigma\mu_d H) \quad \dots (39)$$

where we have put $\varepsilon_{k\sigma} = \varepsilon_k - \sigma\mu_c H$ and transformed the integration variable to $\varepsilon_{k\sigma}$ which introduces H -dependence at the band edges which can be neglected. μ_c and μ_d are the magnetic moments of bare conduction and d -electrons respectively.

Differentiating above equations for E_{σ} and E_0 , we find,

$$E'_{\sigma} = \frac{\Delta}{\pi} (E'_{\sigma} - \sigma\mu_d) I'(E_{\sigma} + \varepsilon_d - \sigma\mu_d H) \quad \dots (40)$$

$$E_0 = \frac{\Delta}{\pi} \sum_{\sigma} (E'_0 - E'_{\sigma} + \sigma\mu_d) I'(E_0 - E_{\sigma} - \varepsilon_d + \sigma\mu_d H) \quad \dots (41)$$

where $I'(a) = \frac{d}{da} I(a)$

From (40) and (41) we find that as $H \rightarrow 0$

$$E'_{\sigma} = -\sigma\mu_d \frac{\Delta I'(\bar{E}_{\sigma})/\pi}{1 - \Delta I'(\bar{E}_{\sigma})/\pi} \quad \dots (42)$$

and $E_0 = 0$

where $\bar{E}_{\sigma} = \varepsilon_d + E_{\sigma}$

Differentiating (40) and (41) once more, we get

$$E''_{\sigma} = \frac{\Delta}{\pi} (E'_{\sigma} - \sigma\mu_d)^2 I''(\bar{E}_{\sigma}) + \frac{\Delta}{\pi} E''_{\sigma} I'(\bar{E}_{\sigma}) \quad \dots (43)$$

$$E''_0 = \frac{\Delta}{\pi} \sum_{\sigma} \{ (E'_{\sigma} - \sigma\mu_d)^2 I''(E_0 - \bar{E}_{\sigma}) + (E''_0 - E''_{\sigma}) I'(E_0 - \bar{E}_{\sigma}) \} \quad \dots (44)$$

Substituting from (42) into these and rearranging, we find,

$$E''_{\sigma} = \mu_d^2 \frac{\Delta}{\pi} \frac{I''(\bar{E}_{\sigma})}{\{1 - \frac{\Delta}{\pi} I'(\bar{E}_{\sigma})\}^2} \quad \dots (45)$$

$$E''_0 = \frac{\mu_d^2 \Delta / \pi}{\{1 - \frac{2\Delta}{\pi} I'(\bar{E}_0 - \bar{E}_{\sigma})\} \{1 - \frac{\Delta}{\pi} I'(\bar{E}_{\sigma})\}^2} \left[2I''(\bar{E}_0 - \bar{E}_{\sigma}) - \frac{\Delta}{\pi} \frac{I'(\bar{E}_0 - \bar{E}_{\sigma}) I''(\bar{E}_{\sigma})}{1 - \frac{\Delta}{\pi} I'(\bar{E}_{\sigma})} \right] \quad \dots (46)$$

Substituting (42), (44) and (45) in (37), the susceptibility can be found.

We first find χ at zero temperature. For large $|\varepsilon_d|$ at zero temperature we found that

$$\bar{E}_{\sigma} \simeq \varepsilon_d + \frac{\Delta}{\pi} \ln \frac{|\varepsilon_d|}{D}$$

$$\text{and } E_0 - \bar{E}_{\sigma} = -\sqrt{D|\varepsilon_d|} \exp(\pi\varepsilon_d/2\Delta)$$

$$\text{Also, at } T = 0, I(a) \simeq \ln(|a|/D)$$

Therefore at this temperature,

$$I'(a) = \frac{1}{a} \quad \text{and } I''(a) = -\frac{1}{a^2}$$

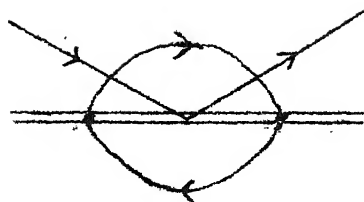
Since at $T = 0$ only the nonmagnetic state is occupied, from (37) and (46) we have

$$\chi = -E_0'' = -\frac{\mu_d^2}{(E_0 - \bar{E}_{\sigma})} \quad \dots (47)$$

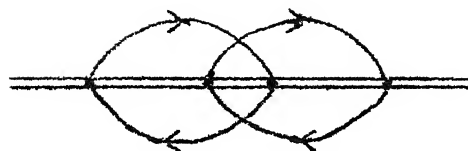
where we have neglected terms $O(\Delta/\pi|\varepsilon_d|)$ and $O(T_K/\Delta)$ in comparison with unity. Thus we have,

$$\chi(T = 0) = \frac{\mu_d^2}{\sqrt{D|\varepsilon_d|} \exp(\pi\varepsilon_d/2\Delta)} \quad \dots (47')$$

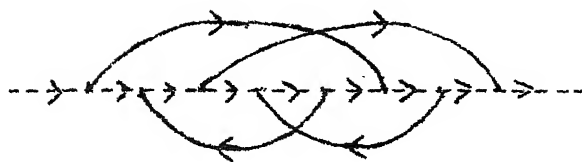
We can now identify the denominator in (47') with the Kondo



(a)



(b)



(c)

Fig 18

temperature T_K since the result (47') is standard and is, in form and upto numerical factors, obtained by all methods applicable to the Kondo problem at low temperatures -- scaling applied to the asymptotic (long time) approximation³⁴, numerical calculations applying renormalization group methods³⁵, etc. Thus we have,

$$T_K = \sqrt{D|\epsilon_d|} \exp(\pi\epsilon_d/2\Delta) \dots (48)$$

$$\equiv \frac{1}{\tau_0} \exp(-1/J\rho)$$

(This latter is the standard Kondo expression).

Thus, for the good moment ($|\epsilon_d| \gg \Delta$) case we identify the effective exchange coupling, J , as,

$$J = - \frac{2\Delta}{\pi|\epsilon_d|}$$

This is the same as obtained by KWW.

Haldane has pointed out that ~~xxxx~~ τ_0^{-1} should be $\sqrt{4D}$ for a $U = \infty$ model rather than $\sqrt{D|\epsilon_d|}$ which is obtained by us. Thus our expression is deficient by a factor $\sqrt{\frac{\Delta}{|\epsilon_d|}} \sim \sqrt{|J|\rho}$. Armytage³⁴ has shown in the scaling approach for the Kondo model that the contribution comes about from III order scatterings of the type shown in fig. 18(a), which will contribute to Z diagrams of the type shown in fig. 18(b). In the Anderson model, in our formalism, this corresponds to the diagram in fig. 18(c). As mentioned in sec. 2, we have not taken such processes into account, and hence the missing factor of $\sqrt{|J|\rho}$.

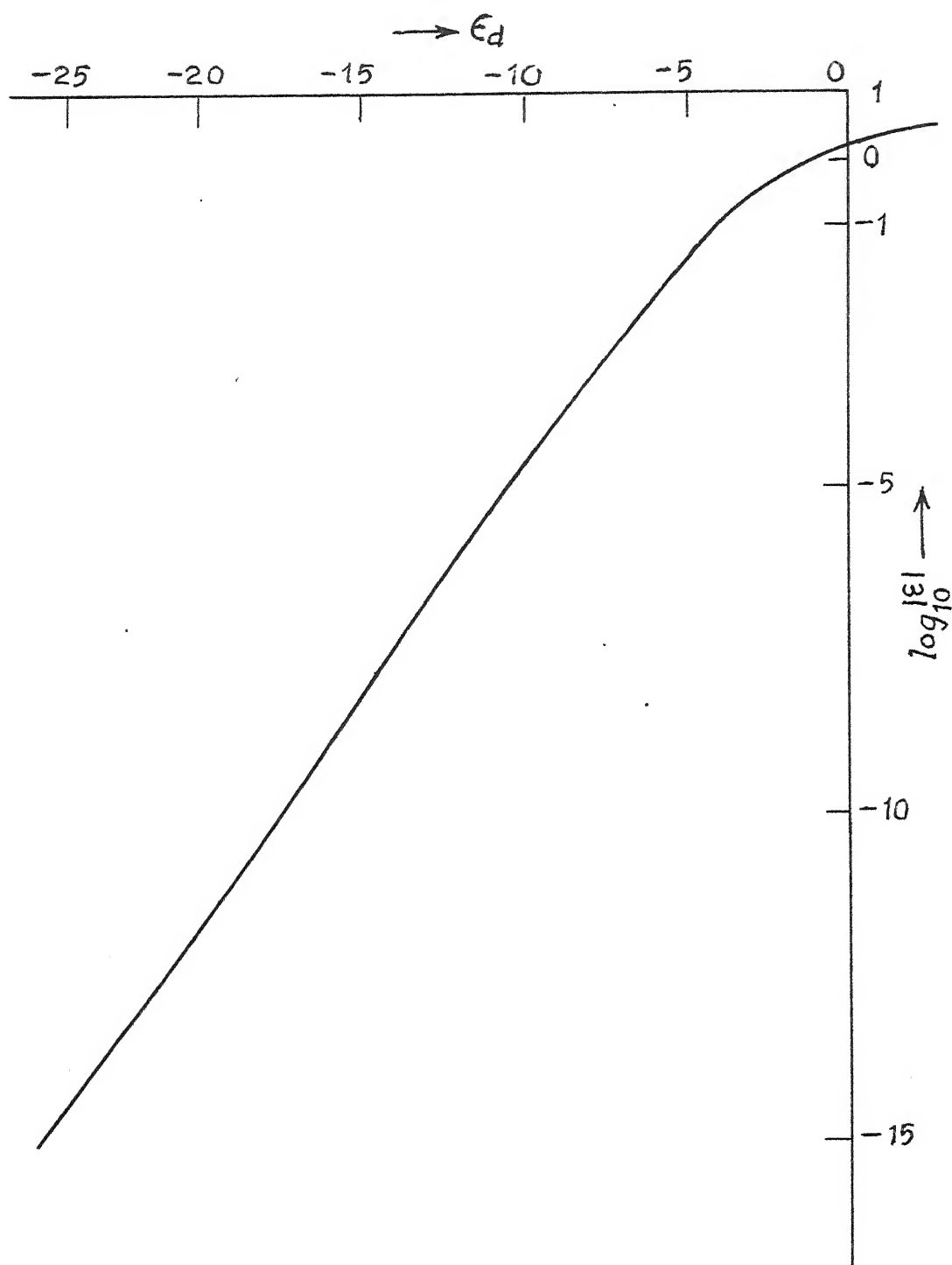


FIG. 19— Variation of ϵ with d -energy
 $\epsilon = E_0 - \bar{E}_\sigma$

The above expressions have been derived only for $|\varepsilon_d| \gg \Delta$. But the identification with T_K tells us that we have already taken into account the most important diagrams (except those already mentioned). So the same kind of diagrams should give correct results for $|\varepsilon_d| \lesssim \Delta$, although in this case the expressions are no longer so compact (all relevant energies being of the same order, $\sim O(\Delta)$), and we have to resort to numerical calculations.

Section 3(b) : THE MAGNETIC SUSCEPTIBILITY AT HIGH TEMPERATURES

To obtain an expression for χ at high temperatures, we likewise start with the high temperature quasiparticle equations. Before that, we note that the nonmagnetic quasiparticle level is much above ($\sim |\varepsilon_d|$) the magnetic quasiparticle levels, for $|\varepsilon_d| \gg \Delta$. So its occupation, and therefore contribution to Z or χ can be neglected and we may write

$$Z \simeq \sum_{\sigma} e^{-\beta \bar{E}_{\sigma}} \quad \dots (49)$$

So we need to know only the magnetic quasiparticle energy which is given at high temperatures by

$$E_{\sigma} = \frac{\Delta}{\pi} \int_{-D}^D \frac{(1 - f_k) d\varepsilon_k}{E_{\sigma} + \varepsilon_d - \sigma \mu_d H - \frac{2\Delta}{\pi} \ln \left(\frac{qT}{D} \right) - \varepsilon_k} \equiv \frac{\Delta}{\pi} I(E_{\sigma} + \varepsilon_d - \sigma \mu_d H - \frac{2\Delta}{\pi} \ln \frac{qT}{D}) \quad \dots (50)$$

where we have eliminated μ_C in the same way as for zero temperature case.

From (49) we obtain the expression for x as,

$$\begin{aligned} x &= -\frac{1}{Z} \sum_{\sigma} \{E_{\sigma}'' - \beta(\sigma\mu_d - E_{\sigma}')^2\} e^{-\beta\bar{E}_{\sigma}} \\ &= -E_{\sigma}'' + \beta(\sigma\mu_d - E_{\sigma}')^2 \end{aligned} \quad \dots (51)$$

Differentiating (50) twice, in the limit $H = 0$, we obtain,

$$E_{\sigma}' = -\sigma\mu_d \frac{\frac{\Delta}{\pi} I'(\bar{E}_{\sigma} - \frac{2\Delta}{\pi} \ln \frac{qT}{D})}{1 - \frac{\Delta}{\pi} I'(\bar{E}_{\sigma} - \frac{2\Delta}{\pi} \ln \frac{qT}{D})} \quad \dots (52)$$

and

$$\begin{aligned} E_{\sigma}'' &= \mu_d^2 \left[\frac{\Delta}{\pi} \frac{I''(\bar{E}_{\sigma} - \frac{2\Delta}{\pi} \ln \frac{qT}{D})}{\{1 - \frac{\Delta}{\pi} I'(\bar{E}_{\sigma} - \frac{2\Delta}{\pi} \ln \frac{qT}{D})\}^2} \right. \\ &\quad \left. + \left(\frac{\Delta}{\pi}\right)^2 \frac{I'(\bar{E}_{\sigma} - \frac{2\Delta}{\pi} \ln \frac{qT}{D}) I''(\bar{E}_{\sigma} - \frac{2\Delta}{\pi} \ln \frac{qT}{D})}{\{1 - \frac{\Delta}{\pi} I'(\bar{E}_{\sigma} - \frac{2\Delta}{\pi} \ln \frac{qT}{D})\}^3} \right] \end{aligned} \quad \dots (53)$$

At sufficiently high temperature, but $T \ll |\varepsilon_d|$, (50) can be written as,

$$E_{\sigma} = \frac{\Delta}{\pi} \ln \frac{|\varepsilon_d + E_{\sigma} - \frac{2\Delta}{\pi} \ln \frac{qT}{D}|}{D}$$

So that

$$\bar{E}_{\sigma}' \approx -\sigma\mu_d \left[1 + \frac{\Delta/\pi}{\varepsilon_d + \frac{\Delta}{\pi} \ln \frac{|\varepsilon_d|}{D} - \frac{2\Delta}{\pi} \ln \frac{qT}{D}} \right]$$

and

$$E_{\sigma}'' \approx -\mu_d^2 \frac{\Delta/\pi}{(\varepsilon_d + \frac{\Delta}{\pi} \ln \frac{|\varepsilon_d|}{D} - \frac{2\Delta}{\pi} \ln \frac{qT}{D})^2}$$

neglecting terms $O(\Delta/|\varepsilon_d|)$.

Putting these in (51) we get the result,

$$\chi \simeq \beta \mu_d^2 \left[1 + \frac{2\Delta/\pi\epsilon_d}{1 + \frac{\Delta}{\pi\epsilon_d} \ln \frac{|\epsilon_d|}{D} - \frac{2\Delta}{\pi\epsilon_d} \ln \frac{qT}{D}} \right]$$

This is the standard high temperature result for a Kondo system with J_p replace by the value $2\Delta/\pi\epsilon_d$. The expression (54) blows up at

$$T = \frac{E_F}{q}$$

where $T_K = \sqrt{D|\epsilon_d|} e^{\pi\epsilon_d/2\Delta}$, identified in the previous section. We have $1/q = .882$, whereas Nziere has pointed out that this factor should be .303.

3(c) - NUMERICAL RESULTS

We have discussed above analytically the susceptibility for high and low temperature, especially for the good moment case (ϵ_d -ve, $|\epsilon_d| \gg \Delta$). In addition we find $\chi(T=0)$ for all ϵ_d . In the general case, i.e., for all temperatures and ϵ_d , $\chi(T)$ has been calculated numerically by solving self consistently for the quasiparticle energies E_σ and E_σ (separately at each temperature and for each value of ϵ_d), and obtaining their field derivatives. We exhibit the results of some numerical computations in fig. 20.

On comparing these with KWW we find that our susceptibility results are qualitatively correct, but higher by a factor of about 4. Also, nonmonotonicity is more pronounced in the $\epsilon_d = 0$ case. Our model is also somewhat different from KWW as we have

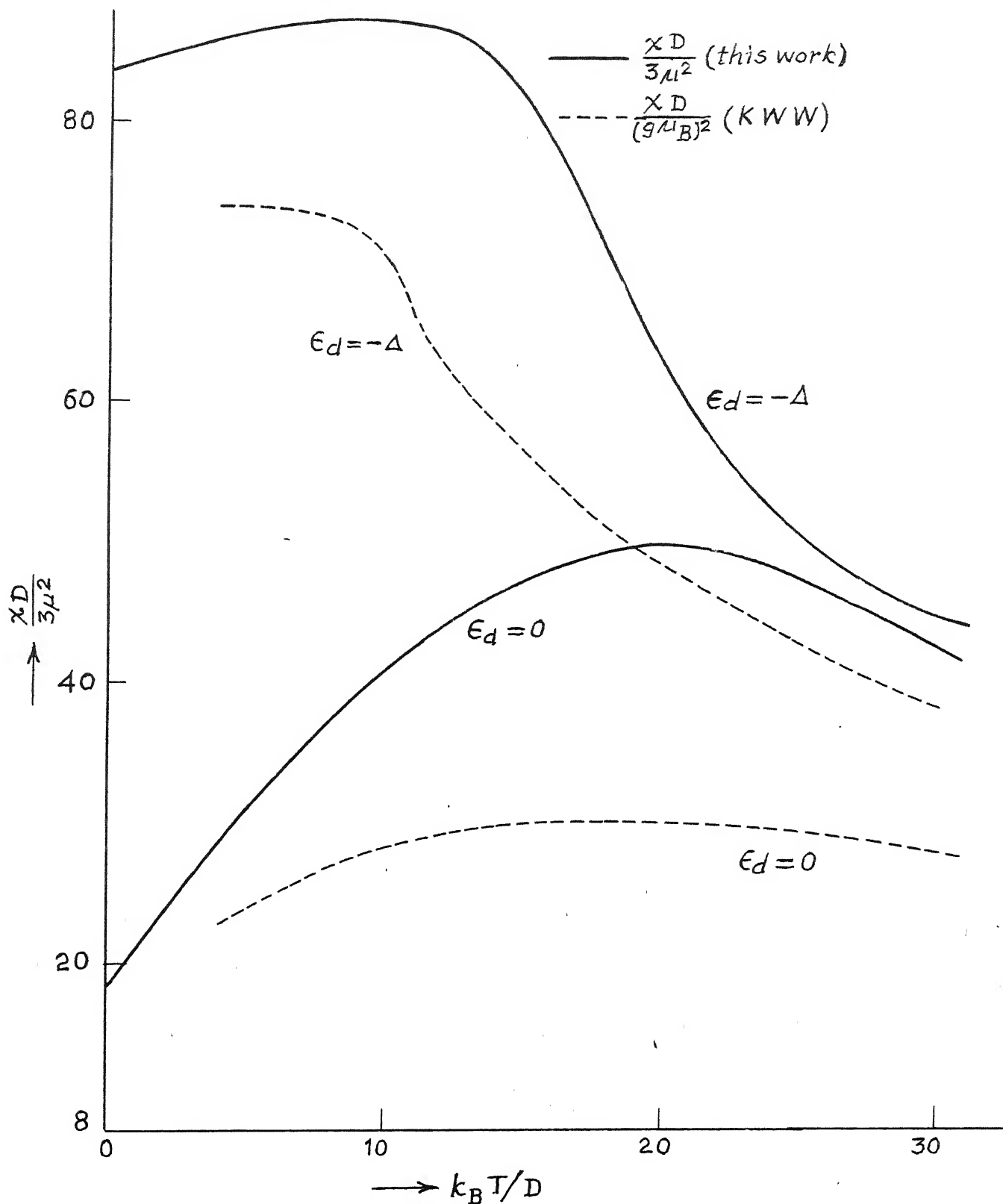


FIG. 20 - The magnetic susceptibility results for $D=1000\Delta/\pi$, $U=\infty$
(For KWW, $D=2U=1000\Delta/\pi$)

taken $U = \infty$ whereas they have taken $U = D/2$. Since the characteristics of these curves are very similar to KWW, we expect similar deviations from universality.

Section 4 : THE VALENCE FRACTION

The d-electron occupation, or, as we call it, the valence fraction is a quantity which helps us in understanding the nature of the state. It is defined as,

$$V = \sum_{\sigma} \langle n_{d\sigma} \rangle$$

Since $Z = \text{Tr} \{ \exp (-\beta [\epsilon_d \sum_{\sigma} n_{d\sigma} + \sum_{k\sigma} \epsilon_{k\sigma} n_{k\sigma} + (V_{kd} c_{k\sigma}^{\dagger} c_{d\sigma} + \text{h.c.})$

we have $\sum_{\sigma} \langle n_{d\sigma} \rangle = - \frac{1}{\beta} \frac{\partial}{\partial \epsilon_d} (\ln Z) = \frac{\partial F}{\partial \epsilon_d} + U n_{d\uparrow} n_{d\downarrow}] \}$

where F is the free energy.

At zero temperature, $F = E_0$, the energy of the nonmagnetic ground state.

$$\therefore V(T = 0) = \frac{\partial E_0}{\partial \epsilon_d}$$

From low temperature equations (24) and (25) we have,

$$E_0 = \frac{2\Delta}{\pi} I(E_0 - \epsilon_d - E_{\sigma})$$

$$E_{\sigma} = \frac{2\Delta}{\pi} I(E_{\sigma} + \epsilon_d)$$

Differentiating these w.r.t. ϵ_d , we find

$$\frac{\partial E_{\sigma}}{\partial \epsilon_d} = \frac{\Delta I'(E_{\sigma} + \epsilon_d)/\pi}{1 - \Delta I'(E_0 - \epsilon_d)/\pi}$$

$$\frac{\partial E_0}{\partial \varepsilon_d} = -\left(1 + \frac{\partial E_\sigma}{\partial \varepsilon_d}\right) \frac{2\Delta I'(E_0 - \varepsilon_d - E_\sigma)/\pi}{1 - 2\Delta I'(E_0 - \varepsilon_d - E_\sigma)/\pi} \approx \left(1 - \frac{\pi T_K}{2\Delta}\right) \left(1 + \frac{\Delta}{\pi \varepsilon_d}\right) \quad \dots (58)$$

putting $I'(a) = \frac{1}{a}$, $E_0 - E_\sigma = -T_K$, and taking lowest order in $\frac{T_K}{\Delta}$, $\frac{\Delta}{|\varepsilon_d|}$.

The expression (58) is very close to unity. We therefore conclude that the ground state almost entirely consists of d-electrons. This is confirmed by the ground-state calculation of Yafet and Varmil. Also notice that naive HFA would give

$$V \approx 1 - \frac{\Delta}{\pi(\varepsilon_d^2 + \Delta^2)^{1/2}}$$

Thus the ionic model is close to truth and the relative error is very small, $\sim 0\left(\frac{T_K}{\Delta}\right)$.

Section 5 : SUGGESTIONS ON INCLUSION OF SCREENING TERMS AND OF INTERACTIONS BETWEEN IONS

The inclusion of a screening term, $g(n_{d\uparrow} + n_{d\downarrow}) \sum_{kk', \sigma} c_{k\sigma}^+ c_{k'\sigma}$ gives rise to additional diagrams of the type shown in fig. 21a. And all combinations of such conduction electron parts inserted in all the d-lines in all diagrams for $Z \geq 1$. These are self energy insertions and have the effect of simply adding to ε_d , in second order,

$$\rho g^2 \int \frac{f_k (1 - f_{k'})}{\varepsilon_k - \varepsilon_{k'}} d\varepsilon_k d\varepsilon_{k'}$$

This has been shown to be G. In higher order the contributions are more complicated and provide logarithmic terms.

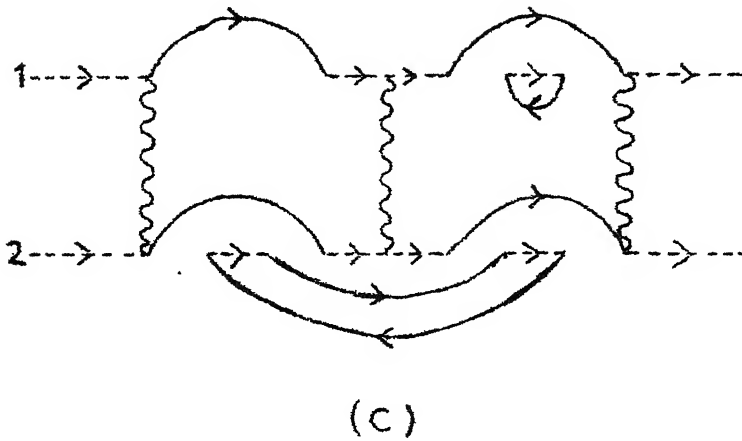
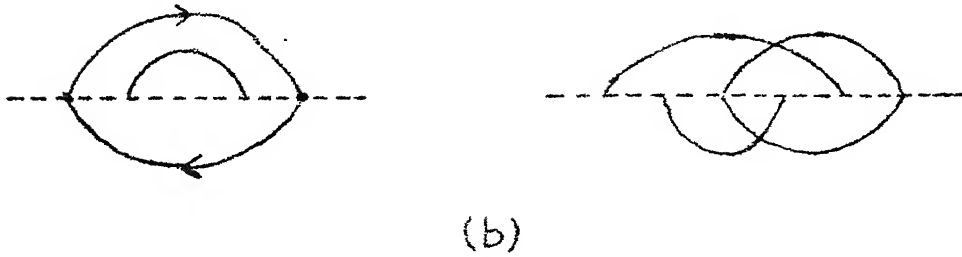
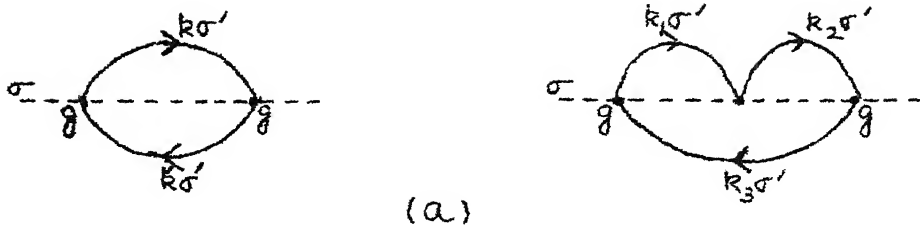


diagram for imp-imp. interaction ($q=0$) [wavy indicates λ]

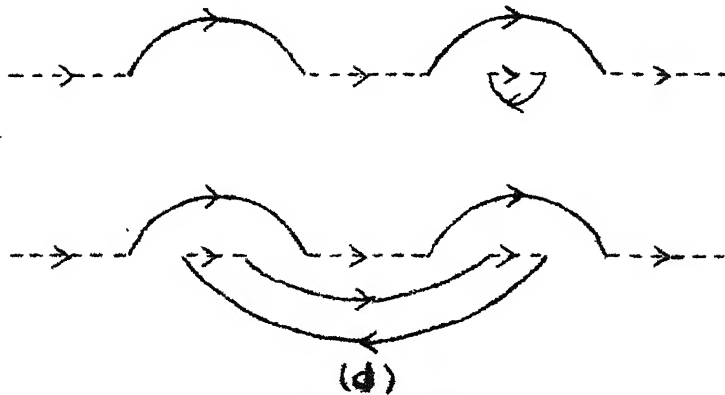


diagram for two non-interacting imp.

Fig 21

The other class of diagrams involving g are of the type that are difficult to handle for the same reasons as mentioned in section 2. These diagrams are shown in fig. 21b.

Thus, right now, we are not in a position to fully discuss the effect of a screening term. However, taking only the second order term shown above, we get the addition of C to ϵ_d which is physically plausible.

The interaction between two impurities, with an added hopping term, $\lambda c_{d1\sigma}^+ c_{d2\sigma} + \text{h.c.}$, proceeds via two mechanisms - the direct hopping and that via conduction electrons. These will give rise to diagrams of the type shown in fig. 21c, where the wavy lines denote direct hopping, λ .

As for HFA, the quasiparticles here will be of the type $|00\rangle$, $|0\sigma\rangle$, $|\sigma\sigma\rangle$ and $|\sigma-\sigma\rangle$, but their nature, obviously, is very much different from HF ones, since 0 here denotes the ground state and is not like the HF nonmagnetic state (which arises only for $C \neq 0$ case). However, once we obtain the interaction energies in the quasiparticle formalism for these product states, the pseudospin analogy can be carried over.

We do not proceed with the formalism for interacting impurities since, in this formalism, we find it difficult to show the basic relation for two noninteracting impurities (diagrams shown fig. 21d)

$$E_2 = 2E_1$$

where E_2 and E_1 are total quasiparticle energies for two and one impurities respectively.

CHAPTER VI

CONCLUSIONS

The single valence fluctuation impurity has been treated in the Hartree-Fock approximation, the path integral, and the quasiparticle formalism. They give successively sophisticated results. Only in the first of these (HFA) we have taken interaction of the impurity with conduction electron or Boson fields into account. We obtain no new qualitative results in the HFA, but our approximate analytical results are shown to be quite accurate; so that theories, which have HFA as basis (e.g. those in chapters III and IV) can get the HF energies quickly without going into detailed solutions of HF equations for a given set of parameters.

The path-integral method establishes firmly connections of the Anderson model with the Kondo model. But, as is well known (e.g. from KWW calculations showing deviations from universality), as the Anderson model parameters approach the nonmagnetic regime, at higher temperatures, the correspondence with Kondo model is not complete. The partition function obtained from the path integral method has to be scaled to a known model in order to obtain quantitative results for physical properties. Scaling becomes tedious at higher temperatures (not discussed in the thesis).

In the quasiparticle method of chapter V we believe to have found a method which will deal successfully with all temperature and parameter ranges. The results in this chapter have matched correctly with known results for relevant parameter ranges. It however remains to treat the model with realistic modifications.

The concentrated IV system has been treated only in the HFA. In the mean field approximation it shows an interesting new kind of phase, the coherent valence fluctuation phase. Because of the limitations of HFA we have not carried the treatment in chapter III beyond the mean field approximation. It however shows the pseudospin models to be realistic and easy to handle.

Thus we find the quasiparticle method of chapter V to be the most useful for solving the single IV ion problem. Once this has been done and the two-ion problem has been sorted out, the results can form the basis of a pseudospin model for the concentrated system, as in chapter III.

APPENDIX I

FREE ENERGY FOR THE ANDERSON MODEL ($C \neq 0$) IN HFA AND CONDITION FOR MINIMUM ENERGY SOLUTIONS

$$H = \sum_{k\sigma} \epsilon_{k\sigma} c_{k\sigma}^+ c_{k\sigma} + \sum_{\sigma} \epsilon_d c_{d\sigma}^+ c_{d\sigma} + V \sum_{k\sigma} (c_{k\sigma}^+ c_{d\sigma} + \text{h.c.}) + U n_d n_d - C(n_{d\uparrow} + n_{d\downarrow})^2/2 \quad (\text{AI.1})$$

The HFA consists of replacing a pair of operators AB as

$$AB \rightarrow A\langle B \rangle + B\langle A \rangle - \langle A \rangle \langle B \rangle \quad (\text{AI.2})$$

Doing this to the last two terms in (AI.1) we get

$$H_{\text{HF}}^{\text{eff}} + \frac{C}{2} (\langle n_{d\uparrow} \rangle + \langle n_{d\downarrow} \rangle)^2 - U \langle n_{d\uparrow} \rangle \langle n_{d\downarrow} \rangle \quad (\text{AI.3})$$

$$\text{where } H_{\text{HF}}^{\text{eff}} = \sum_{\sigma} \epsilon_{d\sigma}^{\text{eff}} c_{d\sigma}^+ c_{d\sigma} + \sum_{k\sigma} \epsilon_{k\sigma} c_{k\sigma}^+ c_{k\sigma} + V \sum_{k\sigma} (c_{k\sigma}^+ c_{d\sigma} + \text{h.c.}) \quad (\text{A.I.4})$$

$$\text{where } \epsilon_{d\sigma}^{\text{eff}} \equiv \epsilon_{d\sigma} + (U-C) \langle n_{d-\sigma} \rangle - C \langle n_{d\sigma} \rangle.$$

$$\text{Denote } \epsilon_{d\sigma}^{\text{eff}} \equiv x_{\sigma} \text{ where } \sigma = \pm$$

$$\text{and } \langle n_{d\sigma} \rangle \equiv n_{\sigma} \text{ and write (AI.4) as}$$

$$x_{\sigma} = \epsilon_{d\sigma} + (U-C)n_{-\sigma} - C n_{\sigma} \quad (\text{AI.4'})$$

$H_{\text{H-F}}^{\text{eff}}$ is the Hamiltonian for two d electrons of opposite spin with effective d state energy x_{\pm} and hybridizing with the conduction electrons via the last term in (AI.3). The Green's function for them will be

$$G_{d\sigma}(\omega) = G_{d\sigma}^0(\omega) + \sum_k G_{d\sigma}^0(\omega) V G_{k\sigma}(\omega) V G_{d\sigma}(\omega) = \frac{G_{d\sigma}^0(\omega)}{1 - V^2 \sum_k G_{k\sigma}(\omega)} \quad (\text{AI.5})$$

$$\text{where } G_{d\sigma}^0(\omega) = \frac{1}{\omega - \epsilon_{d\sigma}^{\text{eff}}} \text{ and } G_{k\sigma}(\omega) = \frac{1}{\omega - \epsilon_{k\sigma}}$$

In finding the sum $\sum_k G_{k\sigma}(\omega)$, we make the usual approximation of summing the δ -function part alone and obtain $\sum_k G_{k\sigma}(\omega) = i\Delta$, with $\Delta = \pi \rho V^2$. Then,

$$G_d(\omega) = \frac{1}{\omega - \epsilon_{d\sigma}^{\text{eff}} - i\Delta} \quad (\text{AI.6})$$

The density of states for such a propagator is

$$\rho_{d\sigma}(\omega) = \frac{\Delta/\pi}{(\omega - \epsilon_{d\sigma}^{\text{eff}})^2 + \Delta^2}$$

and the energy is given at zero temperature by

$$\int_{-D}^0 \rho_{d\sigma}(\omega) \cdot \omega \cdot d\omega \quad (\text{AI.7})$$

To obtain free energy of the system we must add energies for electrons of both spin and to it the remaining terms in (AI.2). So finally,

$$F_{\text{HF}} = \frac{\Delta}{\pi} \sum_{\alpha} \int_{-D}^0 \frac{\omega d\omega}{(\omega - \epsilon_{\sigma}^{\text{eff}})^2 + \Delta^2} - U n_+ n_- + \frac{C}{2} (n_+ + n_-)^2$$

$$\alpha = \pm \quad (\text{AI.8})$$

$$\begin{aligned} \frac{\Delta}{\pi} \int_{-D}^0 \frac{\omega d\omega}{(\omega - \epsilon_{\pm}^{\text{eff}})^2 + \Delta^2} &= - \int_{-D - \epsilon_{\pm}^{\text{eff}}}^{-\epsilon_{\pm}^{\text{eff}}} dz \cdot z \cdot n'(z) + \epsilon_{\pm}^{\text{eff}} n(\epsilon_{\pm}^{\text{eff}}) \\ &= - \int_{D + \epsilon_{\pm}^{\text{eff}}}^{\epsilon_{\pm}^{\text{eff}}} dz \cdot z \cdot n'(z) + \epsilon_{\pm}^{\text{eff}} n(\epsilon_{\pm}^{\text{eff}}) \end{aligned} \quad (\text{AI.9})$$

$$\text{where } n'(z) = \frac{\Delta/\pi}{z^2 + \Delta^2}$$

The free energy expression (AI.8) can then be written in the form

$$\begin{aligned}
F_{HF} = & - \sum_{\alpha} \left\{ \int_{-\infty}^{x_{\alpha}} dz \cdot z \cdot n'(z) - x_{\alpha} n(x_{\alpha}) \right\} - U n(x_{+}) n(x_{-}) + \\
& + \frac{C}{2} \{n(x_{+}) + n(x_{-})\}^2 \quad \text{where } \alpha = \pm
\end{aligned} \tag{AI.10}$$

In (AI.8) we had used the abbreviation

$$x_{\pm} = \varepsilon_d + (U-C) n(x_{\mp}) - C n(x_{\pm})$$

Putting x_{\pm} back in terms of $n(x_{\mp})$ in (AI.10)

$$\begin{aligned}
F_{HF} = & - \sum_{\alpha} \left\{ \int_{-\infty}^{x_{\alpha}} dz \cdot z \cdot n'(z) - \varepsilon_d n(x_{\alpha}) \right\} + U n(x_{+}) n(x_{-}) - \\
& - \frac{C}{2} \{n(x_{+}) + n(x_{-})\}^2, \quad \alpha = \pm
\end{aligned} \tag{AI.11}$$

This is the free energy expression obtained by Haldane.

Now differentiate (AI.11) w.r.t. x_{\pm}

$$\begin{aligned}
\frac{\partial F_{HF}}{\partial x_{+}} = & -x_{+} n'(x_{+}) + U n'(x_{+}) n(x_{+}) - C n'(x_{+}) (n(x_{+}) + n(x_{-})) + \\
& + \varepsilon_d n'(x_{+}) = n'(x_{+}) [\varepsilon_d - x_{+} + (U-C)n(x_{+}) - C n(x_{-})]
\end{aligned} \tag{AI.12}$$

Extrema of the free energy function occur when (AI.12) vanish i.e.,

$$x_{\pm} = \varepsilon_d + (U-C) n(x_{\mp}) - C n(x_{\pm})$$

These are the same as self consistency conditions obtained in equations (2) and (3) in Chapter II.

To find out the condition for these extrema to be minima, we must find the matrix of second derivatives of $F_{H.F}$, the determinant of which must be $+ve$ for solutions which are absolute

minima, i.e., stable solutions. From (AI.12)

$$\begin{aligned} \frac{\partial^2 F_{HF}}{\partial x_{\pm}^2} &= n''(x_{\pm}) [\epsilon_d - x_{\pm} + (U-C)n(x_{\mp}) - Cn(x_{\pm})] + n'(x_{\pm}) [-1 - cn'(x_{\pm})] \\ &= -n'(x_{\pm})(1 + cn'(x_{\pm})) \end{aligned} \quad (\text{AI.13})$$

at an extremum since there the quantity within the first bracket vanishes. Also from (AI.12)

$$\frac{\partial^2 F_{HF}}{\partial x_+ \partial x_-} = (U-C) n'(x_-) n'(x_+) \quad (\text{AI.14})$$

The determinant, then, is,

$$n'(x_+)n'(x_-)(1+Cn'(x_+))(1+Cn'(x_-)) - (U-C)^2 \{n'(x_-)n'(x_+)\}^2 \quad (\text{AI.15})$$

Since $n'(x_+)$, $n'(x_-)$ are both ≥ 0 , the sign of the determinant is determined by the sign of

$$\begin{aligned} &(1 + C n'(x_+)) (1 + C n'(x_-)) - (U-C)^2 n'(x_-) n'(x_+) \\ &= 1 + C(n'(x_+) + n'(x_-)) - \{(U-C)^2\} - C^2 n'(x_+) n'(x_-) \end{aligned} \quad (\text{AI.15})$$

The other condition for minimum is that the trace of the matrix of second derivatives must be positive, which gives us, from (AI.13),

$$-n'(x_+) (1 + C n'(x_+)) - n'(x_-) (1 + C n'(x_-)) \quad (\text{AI.16})$$

Thus the conditions for minimum are that the expressions in (AI.15) and (AI.16) both are positive.

APPENDIX II

TO SHOW THAT THE RANGE OF UNSTABLE SOLUTIONS TO HF EQUATIONS IS BOUNDED BY EXTREME IN ε_d .

The HF equations become just stable (or unstable) as the determinant of second derivatives becomes just equal to zero.

From equation (2') of chapter II,

$$\varepsilon_d = x_+ - (U - C) n(x_-) + C n(x_+) \quad (\text{AII.1})$$

The derivative of ε_d w.r.t. x_+ is,

$$\frac{d\varepsilon_d}{dx_+} = 1 - (U - C) n'(x_-) \frac{dx_-}{dx_+} + C n'(x_+) \quad (\text{AII.2})$$

From equation (3') of chapter II,

$$x_- = \varepsilon_d + (U - C) n(x_+) - C n(x_-)$$

differentiating which we get

$$\frac{dx_-}{dx_+} = \frac{\frac{d\varepsilon_d}{dx_+} + (U - C) n'(x_+)}{1 + C n'(x_-)} \quad (\text{AII.3})$$

Substituting this in (AII.2) we get

$$\begin{aligned} \frac{d\varepsilon_d}{dx_+} (1 + U n'(x_+)) &= \{1 + C n'(x_+)\} \{1 + C n'(x_-)\} \\ &\quad - (U - C)^2 n'(x_+) n'(x_-) \end{aligned} \quad (\text{AII.4})$$

The r.h.s. in (AII.4) is the same as the determinant of second derivatives of F_{HF} . Thus when the r.h.s. vanishes, $\frac{d\varepsilon_d}{dx_+}$ must

vanish since it does not guaranteed that the quantity within brackets on the l.h.s. does.

Also,

$$\frac{d\varepsilon_d}{dV} = \frac{d\varepsilon_d}{dx_-} \frac{dx_-}{dV}$$

From the form of V in eq. (A.4') we see that it varies monotonically with x_+ or x_- . Thus

$$\frac{d\varepsilon_d}{dx_-} = 0 \implies \frac{d\varepsilon_d}{dV} = 0$$

APPENDIX III

ENERGY OF TWO INTERACTING IONS IN HFA

The general expression for the energy of two ions is simply the sum of that for each one of them, in HFA -

$$F = \sum_{i,\sigma} \frac{\text{Im}}{\pi} \int \omega \cdot d\omega G_i^\sigma(\omega) - \sum_i U n_i^\uparrow n_i^\downarrow + \frac{c}{2} \sum_i (n_i^\uparrow + n_i^\downarrow)^2 \quad (\text{AIII.1})$$

where i denotes the ion site so that $i = 1, 2$; and $G_i^\sigma(\omega)$ is to be determined for each interacting ion in the HFA. $G_i^\sigma(\omega)$ can be determined in a straightforward manner in terms of $G_i^\sigma(\omega)$, the propagation expressions for noninteracting ions in HFA. Doing this and using the HF self consistent equations mentioned in Chapter II, we get,

$$\begin{aligned} F = \frac{\Delta}{\pi} \sum_{\sigma} \left[\int_{-D}^0 \frac{\varepsilon d\varepsilon}{\{\varepsilon - \varepsilon_d - (U-C)n^\sigma + cn^{-\sigma} + V\}^2 + \Delta^2} \right. \\ \left. + \int_{-D}^0 \frac{\varepsilon d\varepsilon}{\{\varepsilon - \varepsilon_d - (U-C)n^\sigma + cn^{-\sigma} - V\}^2 + \Delta^2} - 2(U-C)(n^\uparrow n^\downarrow + d^\uparrow d^\downarrow) \right. \\ \left. + \frac{c}{2} (n_\uparrow^2 + d_\uparrow^2 + n_\downarrow^2 + d_\downarrow^2) \right] \quad (\text{AIII.2}) \end{aligned}$$

$$\sum_{\mathbf{k}} \epsilon_{\mathbf{k}} c_{\mathbf{k}\sigma}^+ c_{\mathbf{k}\sigma} + \sum_{\sigma} \epsilon_d n_d + U n_{d\uparrow} n_{d\downarrow} - \frac{C}{2} (n_{d\uparrow} + n_{d\downarrow})^2$$

The sum of last two terms can be written as ($n_{d\sigma}$'s are still the eigenvalues),

$$\frac{U-2C}{4} (n_{d\uparrow} + n_{d\downarrow})^2 - \frac{U}{4} (n_{d\uparrow} - n_{d\downarrow})^2$$

Now the corresponding exponential factors can be replaced by Gaussian integrals in the same way as in the text so that we have d electrons of spin σ travelling in potential $iY + \sigma X$ and Gaussian factors with exponents of the form

$$-\beta \left(\frac{X^2}{U} - \frac{Y^2}{U-2C} \right)$$

So the total energy of the system, when X and Y are time independent, is the sum of resonant energies of the two d electrons plus contributions from the Gaussian factor :

$$E = \frac{\Delta}{\pi} \sum_{\sigma} \int_{-D}^0 \frac{\epsilon d\epsilon}{(\epsilon - \epsilon_d - iY - \sigma X)^2 + \Delta^2} + \frac{X^2}{U} + \frac{(iY)^2}{U-2C} \quad (\text{AIV.3})$$

Differentiation the above expression for E w.r.t. X and Y respectively, and equating to zero to find its extrema, we get

$$2X = \frac{\Delta U}{\pi} \left[\left(\frac{\pi}{2} - \tan^{-1} \frac{\epsilon_d + iY - X}{\Delta} \right) - \left(\frac{\pi}{2} - \tan^{-1} \frac{\epsilon_d + iY + X}{\Delta} \right) \right] \quad (\text{AIV.4})$$

$$2iY = \frac{\Delta(U-2C)}{\pi} \left[\left(\frac{\pi}{2} - \tan^{-1} \frac{\epsilon_d + iY - X}{\Delta} \right) + \left(\frac{\pi}{2} - \tan^{-1} \frac{\epsilon_d + iY + X}{\Delta} \right) \right] \quad (\text{AIV.5})$$

Adding and subtracting (AIV.4) and (AIV.5), and putting

$$x_{\pm} = iY \pm X,$$

we get equations identical to the HF self consistent ones -

$$x_{\pm} = (U - C) n(x_{\mp}) - C n(x_{\pm})$$

APPENDIX V

THE INTEGRALS OCCURRING IN THE SHORT RANGE TERM IN THE PATH INTEGRAL METHOD AND DETERMINATION OF τ_0

The short range term obtained in the text is,

$$\frac{1}{\pi^2} \int_{t_i}^{t_i+\tau_0} d\tau \int_{t_i}^{t_i+\tau_0} d\tau' \ln|\tau-\tau'| \frac{d\xi(\tau')}{d\tau'} \cdot \frac{d}{d\tau} \left[\frac{\xi(\tau)}{\xi^2(\tau) - \xi^2(\tau')} \ln \frac{1+\xi^2(\tau)}{1+\xi^2(\tau')} \right] \quad (V.1)$$

Integrating over τ , if ξ_+ and ξ_- are values of ξ at $t_i+\tau_0$ and t_i respectively,

$$\begin{aligned} S = & \int_{t_i}^{t_i+\tau_0} d\tau' \frac{d\xi(\tau')}{d\tau'} \left\{ \ln|t_i+\tau_0-\tau'| \left[-\frac{\xi_+}{\xi_+^2 - \xi^2(\tau')} \ln \frac{1+\xi_+^2}{1+\xi^2(\tau')} \right] \right. \\ & \left. - \ln|t_i-\tau'| \left[-\frac{\xi_-}{\xi_-^2 + \xi^2(\tau')} \ln \frac{1+\xi_-^2}{1+\xi^2(\tau')} \right] \right\} \\ & - \frac{1}{\pi^2} \int_{t_i}^{t_i+\tau_0} d\tau \int_{t_i}^{t_i+\tau_0} d\tau' \frac{d\xi(\tau')}{d\tau'} \frac{P}{\tau-\tau'} \left[\frac{\xi(\tau)}{\xi^2(\tau) - \xi^2(\tau')} \ln \frac{1+\xi^2(\tau)}{1+\xi^2(\tau')} \right], \end{aligned} \quad (V.2)$$

$$\equiv S_1 + S_2$$

where the first two terms are denoted by S_1 and the last one by S_2 .

The shape of the path $\xi(\tau)$ is shown in the diagram below; and is derived in the text.

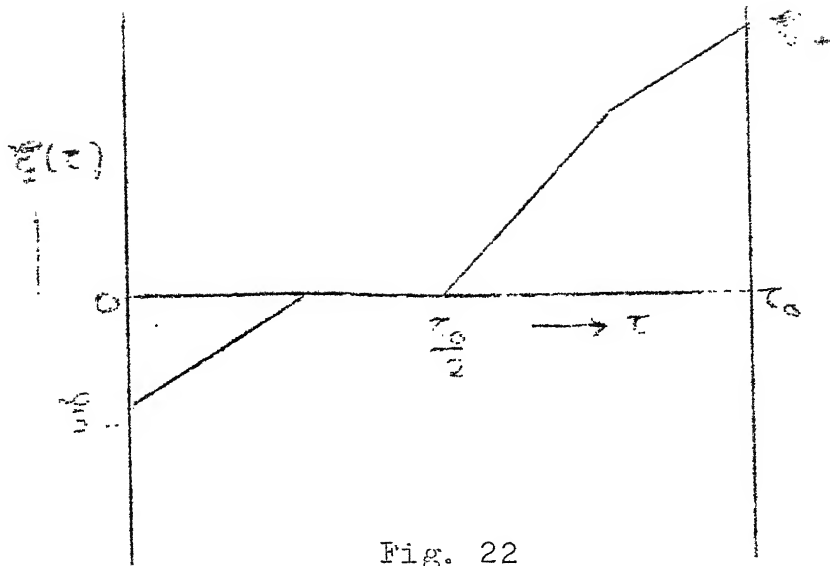


Fig. 22

From this we get, $\tau = (\xi(\tau) - \eta'_0 + \xi_0) \frac{\tau_0}{2\xi_0}$, $\xi_- < \xi < 0$

$$\tau = \frac{\tau_0}{2} + \frac{\tau_0}{4\xi_0} \xi(\tau) \quad 0 < \xi < 2\eta'_0$$

$$\tau = (\xi(\tau) - \eta'_0 + \xi_0) \frac{\tau_0}{2\xi_0} \quad 2\eta'_0 < \xi < \xi_+$$

where $\xi_{\pm} = \xi_0 \pm \eta'_0$. (V.3)

Putting (V.3) in S_1 ,

$$\begin{aligned} & - \int_{\xi_-}^0 d\xi \ln \left| \frac{\tau_0}{2\xi_0} (\xi - \eta'_0 + \xi_0) \right| \cdot (B) - \int_0^{2\eta'_0} d\xi \ln \left| \frac{\tau_0}{2} \left(1 + \frac{\xi}{2\xi_0} \right) \right| \cdot \\ & (B) - \int_{2\eta'_0}^{\xi_+} d\xi \ln \left| \frac{\tau_0}{2\xi_0} (\xi - \eta'_0 + \xi_0) \right| (B) + \int_{\xi_-}^0 d\xi \ln \left| \frac{\tau_0}{2\xi_0} |(\xi - \eta'_0 - \xi_0)| \right| \cdot \\ & (A) + \int_0^{2\eta'_0} d\xi \ln \left| \frac{\tau_0}{2} \left(-1 + \frac{\xi}{2\xi_0} \right) \right| \cdot (A) + \int_{2\eta'_0}^{\xi_+} d\xi \ln \left| \frac{\tau_0}{2\xi_0} (\xi - \eta'_0 - \xi_0) \right| (A) \end{aligned} \quad (V.4)$$

$$\text{where } A = \frac{\xi_+}{\xi_+^2 - \xi'^2} \ln \frac{1 + \xi_+^2}{1 + \xi'^2} = \frac{\eta'_0 + \xi_0}{(\eta'_0 + \xi_0)^2 - \xi'^2} \ln \frac{1 + (\eta'_0 + \xi_0)^2}{1 + \xi'^2}$$

$$\text{and } B = \frac{\xi_-}{\xi_-^2 - \xi'^2} \ln \frac{1 + \xi_-^2}{1 + \xi'^2} = \frac{\eta'_0 - \xi_0}{(\eta'_0 - \xi_0)^2 - \xi'^2} \ln \frac{1 + (\eta'_0 - \xi_0)^2}{1 + \xi'^2}$$

The term proportional to $\ln \left| \frac{\tau_0}{2} \right|$ in (V.4) is

$$\begin{aligned} & \int_{\xi_-}^0 (A-B) d\xi + \int_0^{2\eta'_0} (A-B) d\xi + \int_{2\eta'_0}^{\xi_+} (A-B) d\xi. \\ &= \int_{\xi_-}^{\xi_+} d\xi \left(\frac{\xi_+}{\xi_+ - \xi} \ln \frac{1 + \xi^2}{1 + \xi_+^2} - \frac{\xi_-}{\xi_- - \xi} \ln \frac{1 + \xi^2}{1 + \xi_-^2} \right) \quad (V.5) \end{aligned}$$

(V.5) is the same as exponent of the long time term.

The remaining terms in S_1 are,

$$\begin{aligned} & - \int_{\xi_-}^0 d\xi \ln \left| \frac{\xi - \eta'_0 + \xi_0}{\xi_0} \right| \cdot (B) - \int_0^{2\eta'_0} d\xi \ln \left| 1 + \frac{\xi}{2\xi_0} \right| \cdot (B) \\ & - \int_{2\eta'_0}^{\xi_+} d\xi \ln \left| \frac{\xi - \eta'_0 + \xi_0}{\xi_0} \right| \cdot (B) + \int_{\xi_-}^0 d\xi \ln \left| \frac{\xi - \eta'_0 - \xi_0}{\xi_0} \right| (A) + \\ & + \int_0^{2\eta'_0} d\xi \ln \left| 1 - \frac{\xi}{2\xi_0} \right| (A) + \int_{2\eta'_0}^{\xi_+} d\xi \ln \left| \frac{\xi - \eta'_0 - \xi_0}{\xi_0} \right| (A) \quad (V.6) \end{aligned}$$

Collect miracle terms in both rows in (V.6)

$$\int_0^{2\eta'_0} d\xi \ln \left| 1 - \frac{\xi}{2\xi_0} \right| (A) - \int_0^{2\eta'_0} d\xi \ln \left| 1 + \frac{\xi}{2\xi_0} \right| (B)$$

We have,

$$A = \frac{A+B}{2} + \frac{A-B}{2} \quad B = \frac{A+B}{2} - \frac{A-B}{2}.$$

So the above expression can be written as,

$$\int_0^{2\eta'_0} d\xi \frac{A-B}{2} \ln \left| 1 - \frac{\xi^2}{4\xi_0^2} \right| + \int_0^{2\eta'_0} d\xi \frac{A+B}{2} \ln \left(\frac{2\xi_0 - \xi}{2\xi_0 + \xi} \right) \quad (V.7)$$

Now take up the expression

$$\int d\tau \cdot d\tau' \frac{d\xi(\tau)}{d\tau'} \frac{P}{\tau - \tau'} \frac{\xi(\tau)}{\xi^2(\tau) - \xi^2(\tau')} \ln \frac{1 + \xi^2(\tau)}{1 + \xi^2(\tau')} .$$

Let us find the value of

$$\xi(\tau) \frac{d}{d\tau'} \xi(\tau') - \xi(\tau') \frac{d}{d\tau} \xi(\tau) \quad (V.8)$$

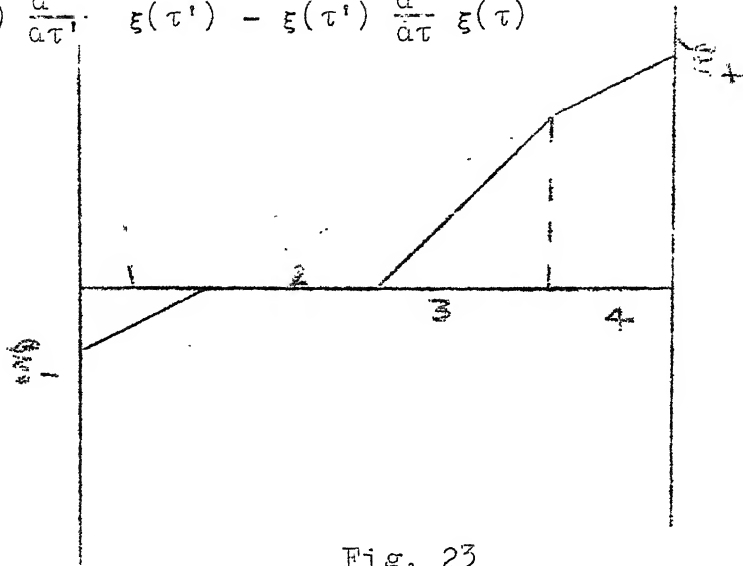


Fig. 23

Divide τ region into 4 parts 1, 2, 3, 4,

$$\xi(\tau) = \xi_i^0 + \alpha_i \tau \quad \text{and} \quad \xi(\tau') = \xi_j^0 + \alpha_j \tau' .$$

The expression (V.8) can be written as,

$$\begin{aligned} & (\xi_i^0 + \alpha_i \tau) \alpha_j - (\xi_j^0 + \alpha_j \tau') \alpha_i \\ &= \xi_i^0 \alpha_j - \xi_j^0 \alpha_i + \alpha_i \alpha_j (\tau - \tau') . \end{aligned}$$

First we check whether all the terms are independent of τ_0 .

The only doubtful case is 1-3, 3-4.

$$\xi_1^0 = \xi_- , \quad \xi_3^0 = 3\xi_- ; \quad \alpha_1 = \frac{2\xi_0}{\tau_0} , \quad \alpha_3 = \frac{4\xi_0}{\tau_0} .$$

If τ is in region 1 and τ' in region 3,

$$\tau - \tau' = \frac{\xi'(\tau) - \xi_-}{2\xi_0} \cdot \tau_0 - \frac{\xi'(\tau') - 3\xi_-}{4\xi_0} \cdot \tau_0.$$

$$\xi_1^0 \alpha_3 - \xi_3^0 \alpha_1 = \frac{\xi_- \xi_0}{\tau_0} (4-6) = -2 \frac{\xi_- \xi_0}{\tau_0}.$$

$$d\tau \cdot d\tau' = \frac{\tau_0^2}{8\xi_0^2} d\xi'(\tau) \cdot d\xi'(\tau').$$

Putting all this in above we see that τ_0 dependence cancels out. Similarly for 3-4.

Now collect all the terms and put them in two classes I and II. Class I consists of those that have τ, τ' both in same region (1, 3, 4) and class II contains those that have τ, τ' in 1-3, 1-4 or 3-4.

Terms in Class I :

(a) τ, τ' in region 1.

$$\xi(\tau) = \xi_- + \frac{2\xi_0}{\tau_0} \tau \quad \frac{d\xi(\tau)}{d\tau} = \frac{2\xi_0}{\tau_0} \therefore d\tau = \frac{\tau_0}{2\xi_0} d\xi(\tau)$$

$$\xi(\tau) = \xi_- + \frac{2\xi_0}{\tau_0} \tau' \quad \tau - \tau' = \frac{\tau_0}{2\xi_0} (\xi(\tau) - \xi(\tau')).$$

Then

$$-\pi S_2^{I(1)} = \int_{\xi_-}^0 d\xi \int_{\xi_-}^0 d\xi' \cdot \frac{P}{\xi - \xi'} \cdot \frac{\xi}{\xi^2 - \xi'^2} \ln \frac{1 + \xi^2}{1 + \xi'^2} \quad (V.9)$$

(b) Similarly,

$$-\pi S_2^{I(3)} = \int_0^{\xi_+ + \xi_-} d\xi \int_0^{\xi_+ + \xi_-} d\xi' \cdot \frac{P}{\xi - \xi'} \cdot \frac{\xi}{\xi^2 - \xi'^2} \ln \frac{1 + \xi^2}{1 + \xi'^2} \quad (V.10)$$

$$(c) \text{ And } -\pi S_2^{I(4)} = \int_{\xi_+ + \xi_-}^{\xi_+} d\xi \int_{\xi_+ + \xi_-}^{\xi_+} d\xi' \frac{P}{\xi_- \xi'} \cdot \frac{\xi}{\xi^2 - \xi'^2} \ln \frac{1 + \xi^2}{1 + \xi'^2} \quad (V.11)$$

Terms in Class II:

(a) τ, τ' in regions 1-4 and 4-1.

$$\xi'(\tau) = \xi_- + \frac{2\xi_0}{\tau_0} \tau.$$

$$\xi'(\tau') = \xi_- + \frac{2\xi_0}{\tau_0} \tau.$$

$\therefore S_2^{II(1-4)}$ integrand is exactly same as $S_2^{I(1)}$ except region of

$$\therefore S_2^{II(1-4)} + S_2^{II(4-1)} = \int_{\xi_-}^0 d\xi \int_{\xi_+ + \xi_-}^{\xi_+} d\xi' (I) + \int_{\xi_+ + \xi_-}^{\xi_+} d\xi \int_{\xi_-}^0 d\xi' (I);$$

with $I =$ integrand in (V.9).

$$= \int_{\xi_-}^0 d\xi \int_{\xi_+ + \xi_-}^{\xi_+} d\xi' \frac{1}{\xi^2 - \xi'^2} \ln \frac{1 + \xi^2}{1 + \xi'^2}.$$

(b) τ, τ' in regions 1-3 and 3-1.

$$\xi(\tau) = \xi_- + \frac{2\xi_0}{\tau_0} \tau.$$

$$\xi(\tau') = 3\xi_- + \frac{4\xi_0}{\tau_0} \tau.$$

From page ,

$$S_2^{II(1-3)} + S_2^{II(3-1)} = \frac{\tau_0^2}{8\xi_0^2} \int_{\xi_-}^0 d\xi(\tau) \int_0^{\xi_+ + \xi_-} d\xi(\tau') (\xi_- + \frac{2\xi_0}{\tau_0} \tau) \frac{4\xi_0}{\tau_0} \cdot \left(\frac{4\xi_0}{\tau_0} \right) \frac{P}{2\xi(\tau) - \xi(\tau') + \xi_-} \cdot \frac{1}{\xi(\tau)^2 - \xi(\tau')^2} \ln \frac{1 + \xi^2(\tau)}{1 + \xi^2(\tau')}$$

$$\begin{aligned}
& + \frac{\tau_0^2}{8\xi_0^2} \int_0^{\xi_+ + \xi_-} d\xi(\tau) \int_{\xi_-}^0 d\xi(\tau') \left(3\xi_- + \frac{4\xi_0}{\tau_0} \tau \right) \frac{2\xi_0}{\tau_0} \left(-\frac{4\xi_0}{\tau_0} \right) \cdot \\
& \quad \frac{P}{\xi(\tau) - 2\xi(\tau') - \xi_-} \ln \frac{1 + \xi^2(\tau)}{1 + \xi^2(\tau')} \cdot \frac{1}{\xi(\tau)^2 - \xi(\tau')^2} \\
& = \int_{\xi_-}^0 d\xi(\tau) \int_0^{\xi_+ + \xi_-} d\xi(\tau') \frac{1}{2\xi(\tau) - \xi(\tau') + \xi_-} \ln \frac{1 + \xi^2(\tau)}{1 + \xi^2(\tau')} \\
& \quad \left\{ 2\xi_- + \frac{4\xi_0}{\tau_0} \tau - 3\xi_- - \frac{4\xi_0}{\tau_0} \tau' \right\} \\
& = -\xi_- \int_{\xi_-}^0 d\xi(\tau) \int_0^{\xi_+ + \xi_-} d\xi(\tau') \frac{P}{2\xi(\tau) - \xi(\tau')\xi_-} \cdot \frac{1}{\xi^2(\tau) - \xi^2(\tau')} \\
& \quad \ln \frac{1 + \xi^2(\tau)}{1 + \xi^2(\tau')} + \int_{\xi_-}^0 d\xi(\tau) \int_0^{\xi_+ + \xi_-} d\xi(\tau') \frac{1}{\xi^2(\tau) - \xi^2(\tau')} \ln \frac{1 + \xi^2(\tau)}{1 + \xi^2(\tau')} \\
& \hspace{15em} (V.12)
\end{aligned}$$

(c) τ, τ' in regions 3-4 and 4-3.

$$\begin{aligned}
S_2^{II(3-4)} + S_2^{II(4-3)} & = \int_{\xi_+ + \xi_-}^{\xi_+} d\xi \int_0^{\xi_+ + \xi_-} d\xi' \frac{1}{\xi^2 - \xi'^2} \ln \frac{1 + \xi^2}{1 + \xi'^2} - \\
& - \xi_- \int_{\xi_+ + \xi_-}^{\xi_+} d\xi \int_0^{\xi_+ + \xi_-} d\xi' \frac{P}{2\xi - \xi' + \xi_-} \cdot \frac{1}{\xi^2 - \xi'^2} \ln \frac{1 + \xi^2}{1 + \xi'^2} \\
& \hspace{15em} (V.13)
\end{aligned}$$

And that completes the list. Now we have to evaluate them.

Most of the integrals are of the form

$$\int_a^b d\xi \int_c^d d\xi' \frac{\ln(1 + \xi^2/1 + \xi'^2)}{\xi^2 - \xi'^2} .$$

$$\text{Let } I(a) = \int d\xi \int d\xi' \frac{\ln(1 + \alpha \xi^2/1 + \alpha \xi'^2)}{\xi^2 - \xi'^2} .$$

$$\begin{aligned} \frac{dI}{d\alpha} &= \int d\xi \int d\xi' \cdot \frac{1}{\xi^2 - \xi'^2} \cdot \left(\frac{\xi^2}{1+\alpha\xi^2} - \frac{\xi'^2}{1+\alpha\xi'^2} \right) \\ &= \int_a^b \frac{d\xi}{1+\alpha\xi^2} \int_c^d \frac{d\xi'}{1+\alpha\xi'^2} = \frac{1}{\alpha} (\tan^{-1}\alpha b - \tan^{-1}\alpha a) (\tan^{-1}\alpha d - \tan^{-1}\alpha c). \end{aligned}$$

Required integral = $I(1) = I(1) - I(0)$.

$$\therefore I = \int_0^1 \frac{d\alpha}{\alpha} (\tan^{-1}\alpha b - \tan^{-1}\alpha a) (\tan^{-1}\alpha d - \tan^{-1}\alpha c).$$

We next evaluate τ_0 in terms of model parameters. The only τ_0 -dependent terms in the short-range term is $\alpha \ln |\tau_0|$. This has to be added to the contribution from the adiabatic plus Gaussian factor and then minimized.

From (page 69) $A_\sigma = -\frac{1}{\pi} \int_0^\beta d\tau \left[\frac{\pi}{2} \tan^{-1} \frac{Y'(\tau) + \sigma X(\tau)}{\Delta} + \frac{\Delta}{2(Y'(\tau) + \sigma Y(\tau))} \ln \left\{ 1 + \left(\frac{Y'(\tau) + \sigma X(\tau)}{\Delta} \right)^2 \right\} \right] \cdot Y'(\tau) + \sigma X(\tau)$

(V.14)

and the exponent of the Gaussian factor is,

$$\begin{aligned} \gamma &= -\int_0^\beta d\tau \left(\frac{X^2(\tau)}{U} + \frac{Y^2(\tau)}{U} \right) \\ &= -\int_0^\beta d\tau \left(\frac{X^2(\tau)}{U} - \frac{(Y'(\tau) - \varepsilon_d)^2}{U} \right) \end{aligned} \quad (V.15)$$

Adding these two contributions,

$$\sum_\sigma A_\sigma + \gamma = -\int_0^\beta d\tau V(X, Y'), \quad (V.16)$$

where, $V(X, Y') = \frac{X^2}{U} - \frac{(Y' - \varepsilon_d)^2}{U} + \frac{\Delta}{\pi} \sum_\sigma \int_0^\pi \frac{\varepsilon d\varepsilon}{(\varepsilon - Y' - \sigma X)^2 + \Delta^2}$ (V.17)

The time arguments in X and Y' are understood; the last integral in (V.17) is the same as RHS of (V.14). The integral in (V.16) is,

$$\begin{aligned} \int_0^\beta d\tau V(X, Y') &= \tau V(X, Y') \Big|_0^\beta - \int_0^\beta d\tau \cdot \tau \cdot \frac{dV}{d\tau} \\ &= \beta V(X_0, Y'_0) - \int_0^\beta d\tau \cdot \tau \cdot \frac{dV}{d\tau}. \end{aligned} \quad (V.18)$$

(X_0 and Y'_0 are the values of X , Y' at either minimum of free energy.) Since $\frac{dV}{d\tau}$ is nonvanishing only if $\frac{dX}{d\tau}$ or $\frac{dY'}{d\tau}$ is nonvanishing, i.e., only during hops, (V.18) is

$$\int_0^\beta d\tau V(X, Y') - \beta V_0 = -2n \int_{t_i}^{t_i + \tau_0} d\tau \cdot \tau \cdot \frac{dV}{d\tau} \quad (V.19)$$

since there are $2n$ hops, the contribution from each hop being the same. The integral on the RHS of (V.16) can also be written as

$$\int \tau dV = \frac{\tau_0}{2X_0} \int_{-X_0}^{X_0} X \cdot \frac{dV}{dX} dX, \quad (V.20)$$

substituting for time dependence of X from (V.16).

Again from (V.14) and (V.15)

$$\begin{aligned} V(X, Y') &= \frac{X^2}{U} - \frac{U}{4} + \frac{\Delta}{\pi} \int_0^{\frac{U}{2}} \int_{-\Delta}^0 \frac{\epsilon d\epsilon}{(\epsilon - \epsilon_d - \frac{U}{2} - \sigma X)^2 + \Delta^2}, \quad |X| > \epsilon_d + \frac{U}{2}. \\ &= \frac{X^2 - (X - \epsilon_d)^2}{U} + \frac{\Delta}{\pi} \int_{-\Delta}^0 \frac{\epsilon d\epsilon}{\epsilon^2 + \Delta^2} + \frac{\Delta}{\pi} \int_{-\Delta}^0 \frac{\epsilon d\epsilon}{(\epsilon - 2X)^2 + \Delta^2}, \quad |X| < \epsilon_d + \frac{U}{2}. \end{aligned} \quad (V.21)$$

So that

$$\begin{aligned} \frac{dV}{dX} &= \frac{2X}{U} - \frac{1}{\pi} \left[\tan^{-1} \frac{\epsilon_d + \frac{U}{2} + X}{\Delta} - \tan^{-1} \frac{\epsilon_d + \frac{U}{2} - X}{\Delta} \right] \quad |X| > \epsilon_d + \frac{U}{2}. \\ &= \frac{2\epsilon_d}{U} + \frac{2}{\pi} \left[\frac{\pi}{2} - \tan^{-1} \frac{2X}{\Delta} \right], \quad |X| < \epsilon_d + \frac{U}{2}. \end{aligned} \quad (V.22)$$

The integral on the r.h.s. of (V.20) now becomes, since it is symmetric in X ,

$$2 \int_0^{X_0} X \frac{dV}{dX} dX = 2 \int_0^{\epsilon_d + \frac{U}{2}} X \frac{dV}{dX} dX + 2 \int_{\epsilon_d + \frac{U}{2}}^{\frac{U}{2}} X \frac{dV}{dX} dX. \quad (V.23)$$

From (V.21) and (V.22), the first integral in (V.23) is,

$$\begin{aligned} \int_0^{\epsilon_d + \frac{U}{2}} X \frac{dV}{dX} dX &= \int_0^{\epsilon_d + \frac{U}{2}} \left\{ \left(1 + \frac{2\epsilon_d}{U}\right) X - \frac{2X}{\pi} \tan^{-1} \frac{2X}{\Delta} \right\} dX \\ &= \frac{U^2}{8} \left(1 + \frac{2\epsilon_d}{U}\right)^2 + \frac{\Delta(\epsilon_d + \frac{U}{2})}{\pi} - \frac{1}{\pi} \left\{ \left(\epsilon_d + \frac{U}{2}\right)^2 + \frac{\Delta^2}{4} \right\} \tan^{-1} \frac{2\epsilon_d + U}{\Delta}. \end{aligned}$$

which reduces, for a highly asymmetric model ($U+2\epsilon_d \gg \Delta$),

$$\int_0^{\epsilon_d + \frac{U}{2}} \frac{1}{X} \frac{dV}{dX} dX \approx \frac{\epsilon_d U}{4} + \frac{\epsilon_d^3}{U} + \epsilon_d^2 \frac{\Delta \epsilon_d}{2\pi} + \frac{\Delta U}{4\pi} + \frac{\Delta^2}{8\pi} \quad (V.24)$$

The second integral in (V.23)

$$\begin{aligned} \int_{\epsilon_d + U/2}^{U/2} X \frac{dV}{dX} dX &= \int_{\epsilon_d + U/2}^{U/2} \left[\frac{2X^2}{U} - \frac{X}{\pi} \left\{ \tan^{-1} \frac{\epsilon_d + \frac{U}{2} + X}{\Delta} + \right. \right. \\ &\quad \left. \left. + \tan^{-1} \frac{X - \epsilon_d - \frac{U}{2}}{\Delta} \right\} \right] dX \\ &= \frac{2}{3U} |\epsilon_d| \left\{ \epsilon_d^2 - \frac{2}{3} |\epsilon_d| U + \frac{3}{4} U^2 \right\} + \frac{\Delta |\epsilon_d|}{\pi} - \frac{\Delta (\frac{U}{2} - |\epsilon_d|)}{\pi} \ln \frac{\Delta (U - |\epsilon_d|)}{4 |\epsilon_d| (\frac{U}{2} - |\epsilon_d|)} \\ &\quad + \frac{\Delta^2}{4} \end{aligned} \quad (V.25)$$

for the highly asymmetric case.

Adding (V.24) and (V.25), we get for the case $U \gg |\epsilon_d| \gg \Delta$,

$$\int X \frac{dV}{dX} dX \approx -\frac{1}{3} \frac{|\epsilon_d|^3}{U} + \frac{|\epsilon_d| U}{4} \quad (V.26)$$

Putting (V.26) into (V.23) into (V.20) into (V.16), and putting the minimum condition, we get,

$$\tau_0 \approx \frac{4}{|\epsilon_d| \left(1 - \frac{4}{3} \frac{|\epsilon_d|^2}{U^2} \right)}$$

APPENDIX VI

$$\text{THE INTEGRAL } I(\cdot) = \int_{-D}^D \frac{f(x)dx}{x+a}$$

This integral has been evaluated below with the help of contour integration. Here $f(x)$ is the Fermi function $\frac{1}{1+e^{\beta x}}$

$$I(a) = \int_{-D}^D \frac{dx}{(1+e^{\beta x})(x+a)}$$

We mean to take the principal value of $\frac{1}{x+a}$. Changing the integration variable in above,

$$\begin{aligned} I(a) &= \int_{-\beta D}^{\beta D} \frac{dx}{(1+e^x)(x+\beta a)} = \int_{-\beta D}^0 \frac{dx}{(1+e^x)(x+\beta a)} + \int_0^{\beta D} \frac{dx}{(1+e^x)(x+\beta a)} \\ &= \int_0^{\beta D} \frac{dx}{1+e^x} \left[\frac{1}{x+\beta a} - \frac{e^x}{x-\beta a} \right] = \int_0^{\beta D} \frac{dx}{x-\beta a} + \int_0^{\beta D} \frac{dx}{1+e^x} \left[\frac{1}{x+\beta a} + \frac{1}{x-\beta a} \right] \end{aligned}$$

(AVI.1)

$$\int_0^{-\beta D} \frac{dx}{x-\beta a} = \ln \frac{|a|}{D}$$

(AVI.1')

$$\int_0^{\beta D} \frac{dx}{(1+e^x)(x+\beta a)} = \int_0^{\beta D} \frac{dz}{1+e^z} P\left[\frac{1}{z+\beta a}\right]$$

(AVI.2)

where the contour for integration for z runs from origin along real axis to βD .

The contribution from above is the same as from the contour shown in the upper half plane since no singularity of the integrand falls within it. So (AVI.2) can be written as

$$\int_0^{\pi} \frac{dy}{(1+e^{iy})(y-ipa)} + \int_0^{\infty} \frac{dx}{(1-e^x)(x+i\pi+\beta a)} - \frac{\frac{1}{4}x2\pi i}{i\pi+\beta a} + O\left(\frac{e^{-\beta D}}{\beta D}\right)$$

(AVI.3)

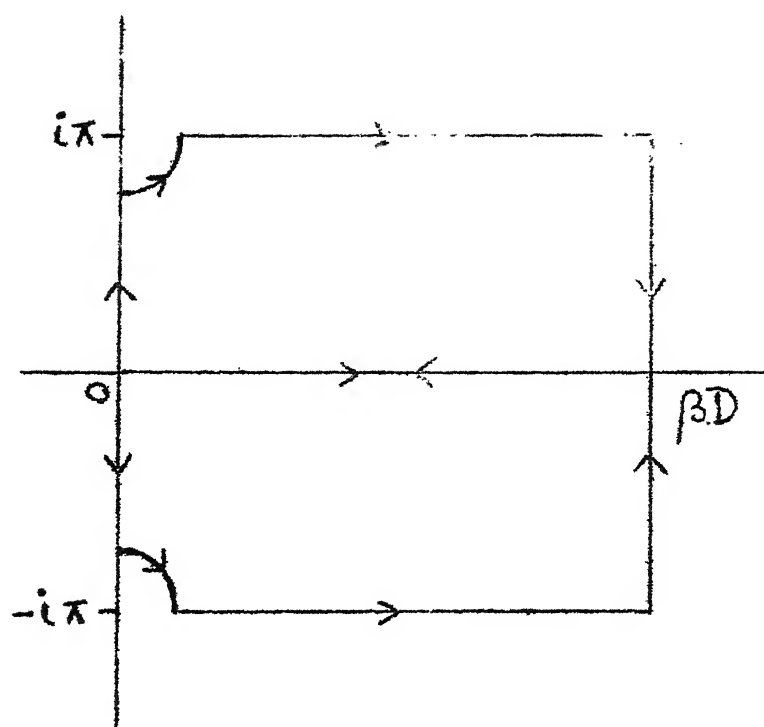


Fig 24. Contours for the integration

The third term comes from the integral around $i\pi$ and the fourth one is error due to extending the integral unto ∞ , assuming $|a| \ll D$.

In a similar way, the contribution from the last term of (AVI.1) can be shown, taking along the contour shown in the lower half plane, to be

$$\int_0^{-\pi} \frac{dy}{(1+e^{iy})(y+i\beta a)} + \int_0^{\infty} \frac{dx}{(1-e^x)(x-i\pi-\beta a)} \approx \frac{2\pi i x \frac{1}{4}}{i\pi + \beta a} + O\left(\frac{e^{-\beta D}}{\beta D}\right) \quad (\text{AVI.4})$$

Adding (AVI.3) and (AVI.4) we get

$$\int_0^{\pi} \frac{dy}{y-i\beta a} - \frac{i\pi}{i\pi+\beta a} + 2 \int_0^{\infty} \frac{x dx}{(1-e^x)\{x^2+(\pi-i\beta a)^2\}} \quad (\text{AVI.5})$$

The last integral in (AVI.5) can be expressed in terms of digamma functions 37 and we have the expression as,

$$\begin{aligned} \ln\left(\frac{i\beta a + \pi}{i\beta a}\right) - \frac{i\pi}{i\pi + \beta a} - \ln\left(\frac{1}{2} + \frac{\beta a}{2\pi i}\right) + \frac{1}{1 + \frac{\beta a}{i\pi}} + \psi\left(\frac{1}{2} + \frac{\beta a}{2\pi i}\right) \\ = \ln\left(\frac{2\pi}{i\beta a}\right) + \psi\left(\frac{1}{2} + \frac{\beta a}{2\pi i}\right) \\ = \ln\left(\frac{\pi}{2i\beta a}\right) + 2\psi\left(\frac{\beta a}{\pi i}\right) - \psi\left(\frac{\beta a}{2\pi i}\right) \end{aligned} \quad (\text{AVI.6})$$

Collecting (AVI.1') and (AVI.6), we finally have, taking real parts since only they will survive,

$$I(a) = \ln \frac{|a|}{D} + \ln \frac{\pi}{2\beta a} + 2\text{Re} \psi\left(\frac{\beta a}{i\pi}\right) - \psi\left(\frac{\beta a}{2\pi i}\right)$$

$$\text{or } I(a) = \ln \left(\frac{\pi T}{2D} \right) + 2 \operatorname{Re} \psi \left(\frac{a}{i\pi T} \right) - \operatorname{Re} \psi \left(\frac{a}{2\pi T i} \right) \quad (\text{A.VI.7})$$

where we have put $k_0 = 1$

The low and high temperature expansions of (A.VI.7) are, from small and large y expressions of $\psi(ig)$

$$I(a) \approx \ln \frac{|a|}{D} - \frac{1}{6} \left(\frac{\pi D}{a} \right)^2, \quad \pi T \ll a$$

$$I(a) \approx \ln(q \frac{T}{D}) + \frac{7}{4} (3) \left(\frac{a}{\pi T} \right)^2, \quad \pi T \gg a$$

where $q = \frac{\pi}{2e^r}$, $r = .57721\ 56649$, $(3) = 1.08232\ 32337$.

REFERENCES

1. C.M. Varma, Rev. Mod. Phys. 48, 219 (1976).
2. (c) M.B. Mapte and D. Wählleben, AIP Conf. Proc. No. 18, Magnetism and Magnetic Materials - 1973, ed. by C.D. Graham, Jr. and J.J. Rhyne, Am. Inst. of Phys., 1974, p. 447.
- (d) D. Wählleben and B.R. Coles, Magnetism Vol. V: Magnetic Properties of Metallic Alloys, ed. by H. Suhl, Academic Press, N.Y., 1973, ch. 1.
3. P.W. Anderson, Phys. Rev. 124, 41 (1961).
4. L.M. Falicov and J.C. Kimball, Phys. Rev. Lett. 22, 997 (1967).
5. F.D.M. Haldane, Thesis, Princeton Univ., 1977;
 Phys. Rev. 815, 281 (1977);
 Phys. Rev. 815, 2477 (1977).
6. S. Alexander and P.W. Anderson, Phys. Rev. A133, 1594 (1964).
7. P.W. Anderson, Phys. Rev. Lett. 18, 1049 (1967).
8. D.R. Hamann, Phys. Rev. 82, 1373 (1970).
9. G. Yuval and P.W. Anderson, Phys. Rev. 81, 1552 (1970).
10. H.R. Krishnamurthy, K.G. Wilson and J.W. Wilkins, "Valence Instabilities and Related Narrow Band Phenomena" ed. by R.D. Parks, 1976, p. 177.
11. C.M. Varma in ref. 10, p. 201.
12. A. Blandin in ref. 2(b), ch. 2.
13. P.S. Reisberough in ref. 10, p. 399.
14. P.F. DeChatel, J. Aarts and J.P. Klease, Commun. Phys. 2, 151 (1977).
15. C.M. Varma in ref. 10.
16. L.L. Hirst in ref. 10.
17. S.T. Chui and P.W. Anderson, Phys. Rev. 89, 3229 (1974).
18. S.K. Ghatak, Phys. Lett. 62A, 168 (1977).
19. A.B. Haley and P. Erlos, Phys. Rev. 85, 1106 (1972).
20. M.S.S. Brooks and T. Egami, J. Phys. C6, 531, 3719 (1973).
 J. Phys. C7, 979 (1974).

21. M. Blume, Phys. Rev. 141, 517 (1966).
22. J.R. Schrieffer and P.A. Wolff, Phys. Rev. 149, 491 (1966).
23. P. Nozières and C.T. DeDominicis, Phys. Rev. 178, 1079 (1969).
24. N.I. Muskhelishvili "Singular Integral Equations", translated by J.R.M. Radok. P. Noordhoff, Groningen, Holland, 1953.
25. C. Bloch and C.T. DeDominicis, Nucl. Phys. 7, 459 (1963).
26. A. Balian and C.T. DeDominicis, Physica. 26, 594 (1960).
27. J.M. Luttinger and Y.T. Liu, Ann. Phys. 80, (1973).
28. H. Keiter and J.C. Kimball, Intern. J. Magnetism 1, 233 (1971).
29. G. Toulouse, Phys. Rev. B2, 270 (1970).
30. A. Bringer and H. Lustfeld, Z. Physik B28, 213 (1977).
31. G. Toulouse and C.T. De Dominicis, Physica 47, 565 (1970).
32. E. Whittaker and K.M. Watson, A course on Modern Analysis. Cambridge Univ. Press.
33. C.M. Verma and Y. Yafet, Phys. Rev. B13, 2950 (1975).
34. J.R.G. Armytage, Thesis (unpublished).
35. H.R. Krishnamurthy, K.G. Wilson and J.W. Wilkins, Phys. Rev. Lett. 35, 1101 (1975).
36. F.D.M. Haldane, Phys. Rev. Lett. (1978).
37. M. Abramowitz and I.A. Stegun (Eds.) "Handbook of Mathematical Functions", Dover, N.Y., 1965.
38. T. Kasuya, K. Kojima and M. Kasuya, Ref. 10, p. 137.
39. C. M. Verma, Talk presented at the US-Japanese Seminar on Mixed Valence Compounds, Sandai, Japan (1977).
40. H. B. Maple, Valence Instabilities of Rare Earth Ions in Metals (Preprint).